TECHNICAL AND VOCATIONAL TRAINING INSTITUTE (TVTI)

School of Graduate Studies

FACULITY OF ELECTRICAL AND ELECTRONICS TECHNOLOGY AND INFORMATION AND COMMUNICATION TECHNOLOGY

(DEPARTMENT OF ELECTRICAL AND ELECTRONICS TECHNOLOGY)

Design and analysis the performance of PSO based Fuzzy-PID controller for the control of Load frequency and voltage of synchronous generator system

MSc Thesis for the partial Fulfillment of Masters of Science in Electrical Automation and Control Technology Management

By,

Yidnekachew Abebe Busho (MTR/786/13)

Supervisor,

Bisrat Gezahegn (Ph.D.)

AUGUST 2022

Addis Ababa, Ethiopia

Design and analysis the performance of PSO based Fuzzy-PID controller for the control of Load frequency and voltage of synchronous generator system

A Thesis submitted to

TECHNICAL AND VOCATIONAL TRAINING INSTITUTE (TVTI)

FACULITY OF ELECTRICAL AND ELECTRONICS TECHNOLOGY AND INFORMATION AND COMMUNICATION TECHNOLOGY (DEPARTMENT OF ELECTRICAL AND ELECTRONICS TECHNOLOGY)

In partial fulfillment for the Degree of

MASTERS OF SCIENCE IN ELECTRICAL AUTOMATION AND CONTROL TECHNOLOGY MANAGEMNET

By,

Yidnekachew Abebe Busho (MTR/786/13)

Supervisor,

Bisrat Gezehagn (Ph.D.)

DECLARATION

I hereby declare that the master's thesis "**Design and analysis of the performance of a PSO-based Fuzzy-PID controller for the control of load frequency and voltage of synchronous generator systems**" is my own original work, that it has never been submitted for a degree at this university or any other university, and that all sources used in writing this thesis have been appropriately cited.

Name: **Yidnekachew Abebe** ID No: **MTR/786/13**

Signature

Place: Addis Ababa

Date of Submission: Sep 30/2022

This thesis proposal has been submitted for examination with my approval as a TVTI advisor

Dr. Bisrat Gezahegn

Advisor's Name

Signature

30/08/2022

Date

TECHNICAL AND VOCATIONAL TRAINING INSTITUTE (TVTI)

FACULITY OF ELECTRICAL AND ELECTRONICS TECHNOLOGY AND INFORMATION AND COMMUNICATION TECHNOLOGY

(DEPARTMENT OF ELECTRICAL AND ELECTRONICS TECHNOLOGY)

Thesis on

"Design and analysis the performance of PSO based Fuzzy-PID controller for the control of Load frequency and voltage of synchronous generator system"

By,

Yidnekachew Abebe (MTR/786/13)

APPROVED BY THESIS ADVISOR COMMITTEE

Name of the Advisor	Signature	Date
Dr. Bisrat Gezahegn		30/08/2022
Name of Examiner, Internal	Signature	Date
Dr. Saravanakumar Gurusamy		01/09/22
Name of Examiner, Internal	Signature	Date
Mr. Tesfaye Nafo		Aug 30/2022
Name of Examiner, External	Signature	Date
Dr. Lebsework Negash		Aug, 30/2022
Name of chairperson	Signature	Date
Mr. Zemenu Tamir		01/09/22

ACKNOWLEDGEMENT

I am most thankful to **Almighty God** who through His countless mercy and love guided me all throughout my academic life. His love and guidance has propelled me to get this far. My most honest and heartfelt thanks go to Assistant Professor Bisrat Gezahegn(Ph.D.) , my thesis advisor, for his unreserved and well-timed help in checking, commenting, and giving constructive advice all alongside my activities.

ABSTRACT

Real power changes affect the signal's frequency most, while relative power is more susceptible to voltage magnitude changes. Changing a system's load affects its voltage and frequency. This thesis combines research on Automatic Voltage Regulator (AVR) and Automatic Generation Control (AGC) systems to manage real and reactive power and maintain a system steady state. Load frequency and voltage must be easily managed in the power system. It is challenging to keep them within the allowed limit because of unforeseen load changes. As a result, some control action must be required for this automatic generation control to manage the load frequency and voltage. Automatic generation control balances system generation with load and losses. The load frequency control (LFC) maintains the voltage profile, managing the active power flows inside the appliance, while the automatic voltage regulator keeps the bus bar voltage within acceptable limits by maintaining the synchronous generator's terminal voltage. Here, Integral Absolute Error (IAE) is considered as the objective function. PSO optimizes the Fuzzy-PID controller's gain and performance. The evaluation of frequency deviation and voltage fluctuation with time is carried out for single area systems using the MATLAB 2021a program. It is clear that the deviation of frequency response and voltage is reduced using the Fuzzy-PID controller, which is based on particle swarm optimization. In this thesis, a PID-based traditional controller and a fuzzy-PID controller are compared. The PSO-based Fuzzy-PID controller proved more effective than the old system. In comparison to PID Integral Absolute Error (IAE) values of 1.553, PSO based Fuzzy-PID Integral Absolute Error (IAE) values are 0.6793 less. As a result, PSO-based Fuzzy-PID performs better than a PID controller.

Keywords:
Automatic Generation Control (AGC); load frequency control (LFC); Automatic Voltage Regulator (AVR); PID controller, Frequency response, and PSO-Fuzzy Logic Controller (PSOFLC)

TABLE OF CONTENTS

LIST OF FIGURES

LIST OF TABLES

LIST OF SYMBOLS AND ABBREVIATION'S

Δf	Incremental change in frequency (Hz)
ΔP_L	Incremental change in load disturbance (p.u.MW)
ΔP_m	Incremental change in mechanical power (p.u.MW)
ΔP_{ref}	Incremental change in reference set power (p.u.MW)
ΔP_V	Incremental change in governor value position (p.u.MW)
ΔP_{tie}	Incremental change in tie - line power
$\Delta\delta$	Incremental change in rotor angle (rad)
AC	Alternating current
ACE	Area Control Error
AGC	Automatic Generation Control
AI	Artificial Intelligent
AVR	Automatic Voltage Controller
D	Load damping constant
DC	Direct current
$Dout$	Derivative term output
e	Error = set value - actual value
E.m.f	Electromotive force
e_{SS}	Steady state error
FIS	Fuzzy inference system
FLC	Fuzzy Logic Controller
GA	Genetic Algorithm
g_{best}	Global best of the population
Gt(s)	Transfer function (TF) of the turbine
H	Generator inertia constant
I_{out}	Integral term output
IAE	Integral Absolute Error
K1	Change in electric power for small change in stator emf
K2	Change in terminal voltage for small change in rotor angle
K3	Change in terminal voltage for small change in stator emf

KA	Amplifier gain
K_D	Derivative Gain
K_G	Generator gain constant
KI	Integral control gain
K_P	Proportional Gain
LFC	Load Frequency Control
MATLAB	Matrix laboratory
NFLC	Neuro -Fuzzy control
P.u.MW	per unit Mega Watt
P_{besti}	Personal best of particle i
PI	Proportional Integral
PID	Proportional Integral Derivatives
Pout	Proportional term output
Ps	Synchronizing power coefficient
PSS	Power system stabilizer
PSO	Particle Swarm Optimization
R	Speed regulation due to governor action (Hz.p.u.MW)
t	Instantaneous time in sec.
T	Transpose of matrix
ʈA	Amplifier time constant
ʈE	Exciter time constant
ʈF	Stabilizer time constant
ʈG	Generator time constant
t_s	Settling time
U	control signal
V_e	Error signal
$V_{e(S)}$	Error voltage signal (p.u.)
VF(s)	Exciter voltage (p.u.)
VR(s)	Amplifier voltage (p.u.)
Vref	reference voltage
$V_{Ref(s)}$	Reference input voltage

Vs(s)	Sensor voltage (p.u.)
$V_{t(s)}$	Output voltage (p.u.)
X_{tie}	Tie-line reactance
β	The weighting factor
P_e	Electrical Power
P_m	Mechanical Power
T_e	Electrical Torque
T_m	Mechanical Torque

CHAPTER ONE

INTRODUCTION

1.1. BACKGROUND

In recent years, maintaining a healthy balance in the power system has been recognised as a critical issue. It is a regarded truth that the electric power system call for and system load is not consistent however hold on changing [1]. Electricity production and supply in an interconnected system should be efficient and reliable, and power system control aims to keep voltage and frequency in steady state are within the permitted range[2].

The power system's performance depends on the generated power and load disturbance variations. In an interconnected device, each subsystem must adjust the power output of the installed generators in response to changes in system frequency and/or to set up interchange with other regions within predetermined bounds. It is known as load frequency control. The terminal voltage of a synchronous generator must also be maintained at a specific level. An Automatic Voltage Regulator (AVR) is used to accomplish this [2].

The frequency and real power are regulated by the speed governor inside the producing stations, which keeps their values within the necessary ranges. On the other hand, every generator inside the production facility is equipped with an excitation controller that can be used to set the magnitude of the voltage and the reactive power to the appropriate levels. It is possible to simultaneously control voltage and frequency [3] and separately [4],[5] due to the possibility of minimal pass coupling between the LFC block and the AVR block. The fact that the time constant of the excitation system is much smaller than the time constant of the prime mover, as well as the fact that the excitation system transient decays much more quickly and no longer affects the LFC dynamics, account for the insignificant pass coupling between the blocks.

This study's LFC and AVR loops contribute to the power system's remarkable functionality. These loops keep the synchronous generator's frequency and terminal voltage within limitations. Soundarrajan et al employed PSO-based tuning to tune a PID controller for a

LFC and AVR of a single-area power system [6]. The authors contrasted the PSO-based PID controller with conventional PID, fuzzy, and GA-based controllers.

Using modern computational techniques like fuzzy logic (FLC). Particle swarm optimization (PSO) and genetic algorithms (GA) are used to maintain synchronous generator frequency and voltage regulation [7]. In this thesis, a single area is taken into consideration where voltage and frequency are controlled using both the AVR and AGC to achieve the desired level. When PSO-based fuzzy-PID controllers are compared to traditional controllers like PID, it shows that the intelligent controller outperforms the conventional controller. To examined how the frequency changes with regard to time, the governor power of using the MATLAB software, the AVR's voltage and automatic generation control both alter over time. It is preferred that the parameters for the frequency, voltage, and power deviation be zero, including minimum overshoot, settling time, rising time, and steady-state error [8].

The outcomes received for the problem at hand provide an interesting load management situation in comparison to the traditional situation. These issues provide a better basis for researching more modern control techniques, such as fuzzy logic control. In order to obtain a better control effect, intelligent control theory and generator excitation control are increasingly being combined as control theory advances. The generator excitation adjustment technique is more challenging and inconvenient when using traditional PID control since it requires human parameter modification. Traditional PID control has a simple structure, some stability, and can create superior control effects. FLC distinguishes itself through separate control objects derived from a mathematical model, as well as an easy-to-follow, flexible design approach [9].

The approach provided in this paper allows quick and reliable control of the synchronous generator's excitation. Instead of a manual approach, an improved PSO algorithm selects the quantization and scaling factors. Rebounding improves search capability. The PSO Fuzzy PID controller has a smaller peak overshoot, faster settling time, and zero error in steady state.

1.2. Objective of the thesis

1.2.1. General Objectives

Design and analyze the performance of a PSO-based fuzzy-PID controller for the control of load frequency and voltage of synchronous generator systems.

1.2.2. Specific Objectives

The following is an itemized list of the particular objectives of this thesis:

- To adopt mathematical model for the synchronous generator systems load frequency and voltage control.
- To design and simulate control loop for voltage and frequency.
- To apply conventional PID controller for voltage and frequency.
- To apply PSO based fuzzy-PID control for voltage and frequency.
- To compare the performance of PID and PSO based fuzzy-PID controller.

1.3. Statement of the problem

Today, power system stability has been recognized as a major issue. As is common knowledge, the load on the electric power supply fluctuates rather than being constant. The power system's voltage and frequency adjust to changes in load. The real power and frequency of the system are regulated by the load frequency control (LFC) loop, whilst reactive power and voltage magnitude are regulated by the automated voltage regulator (AVR) loop. Due to flaws, conventional PID cannot meet the needs of an increasing number of commutated power systems. The traditional PID control shape is straightforward, positive, robust, and has the potential to increase control impact. The conventional PID controller, on the other hand, prefers to manually control the settings. The generator excitation system becomes more complicated and complex as a result. Furthermore, in nonlinear systems, PID controllers do not function efficiently and satisfactorily. Because of the voltage's extended upward push and settling time, it's harder to account for changes in observed values. Extended voltage push and settle time affects excitation system management. If we wish to successfully regulate the synchronous generator's load frequency and voltage, we can use a PSO-based FPID controller.

1.4. Scope and Limitation

1.4.1. Scope of the thesis

This thesis compares a PSO-based fuzzy-PID controller to a normal PID controller for regulating synchronous generator load frequency and voltages. MATLAB and Simulink ensure accuracy. The regular PID controller and the PSO-based fuzzy-PID controller (PSOFPID) differ in terms of maximum overshoot, rising time, settling time, and performance under constant input voltage and voltage fluctuations.

1.4.2. Limitation of the thesis

The usage of MATLAB/Simulink in the thesis' simulation of the machine has limitations as a means of displaying how the special additives of the machine interact with each other. This is due to the fact that the implementation of an actual machine is hard to benefit the additives. Along with it comes the added effort and expense of creating the actual prototype implementation.

1.5. Motivation

Everyone desires a steady supply of power or energy. But because the demand for active and reactive power is always fluctuating in an upward and downward direction, it is persistently impractical for a system to continue operating in its default configuration [10], [11]. The LFC and AVR concerns are key needs in today's interconnected networks, where some utilities are interconnected and electricity is shared among them using tie-lines. In order to prevent bus voltage from dropping over the acceptable threshold, the generator's excitation should be controlled to match the reactive energy demand. The generator's mechanical input power is used to regulate the output electric power's frequency and keep the power alternate between the areas operating as intended.

Manual control is not always possible in the interconnected power grid of today. As a result, every generator has automated equipment installed. The goal of the control approach is to generate and supply electricity as cheaply and dependably as possible in an interconnected power system while maintaining appropriate voltage and frequency levels. In order to get higher overall performance from any controller, its parameters want proper optimization. The

conventional/traditional techniques face a few problems to gain this purpose, consisting of complicated mathematical equations for huge systems [12]. Novel Artificial Intelligence (AI) strategies provide a few demanding situations for parameters optimization of controllers. The focus of this thesis is a PSO-based fuzzy-PID controller for synchronous generator system load frequency and voltage regulation.

1.6. Significance of the thesis

Voltage droop, electric discharge or surge and harm electric appliance is crucial problem with inside the global in addition to in our nation in the course of standard appliance. So, it must be able to use the AVR and LFC appliance to manipulate the use of fuzzy controller. The LFC maintains the voltage profile, managing the active power flows inside the appliance, while the AVR controls the reactive power flows inside the appliance. The AVR is a crucial instrument for regulating and controlling the synchronous generator's terminal voltage in power systems. Fuzzy logic-based controllers are frequently utilized to improve the AVR appliance's performance, stability, and resilience profile. Load frequency control is the term for active power-based frequency change. Preventing frequency deviation from rising as a result of ongoing load variation—often referred to as unrecognized outside load disturbance is one of LFC's key objectives.

1.7. Methodology

This thesis researches automatic generation control (AGC) using MATLAB-SIMULINK and classic controllers like PID and PSO-based Fuzzy-PID. PSO-based fuzzy-PID control is used to regulate the synchronous generator's LFC and AVR. PSO based Fuzzy PID and PID controller approaches can be utilized to determine if the AGC's dynamic responsiveness can be improved.

1.8. Thesis Organization

This thesis was divided into 6 chapters, which generally include the following: The thesis proposal is laid out in the general manner shown below.

- **Chapter 1** offers an introduction to the study, an explanation of its goals and issues, as well as information about the importance, size, and constraints of the research.

- **Chapter 2** An analysis of the literature on the creation of AI techniques for LFC and AVR structures
- **Chapter 3** Presents the modeling of the power system components such as generators, speed controllers, transmission lines (tie-lines) and electrical loads. It also discusses the models that were used to illustrate the viability of the suggested controllers throughout the thesis.
- **Chapter 4** outlines the suggested controller design.
- **Chapter 5** Presents MATLAB/SIMULINK simulation results and discussed
- **Chapter 6** Includes conclusion as well as contributions reached in the thesis. Moreover, direction for future research in this subject is also suggested.

CHAPTER TWO

LITRATURE REVIEW

2.1. INTRODUCTION

The expansion of interconnected systems has raised the necessity of voltage and frequency controllers, which has enhanced the dependability of the power system's operation. There has been numerous research [4], [13], [14] about the LFC and AVR [15] individually and simultaneously [16] i.e., a completely new integrated model for simulating the interactions between the LFC and AVR loops.

Nitesh Thapa, NiluMurmuet et al (2017), Automatic voltage regulation and automatic load frequency control are suggested in two domains of power systems. Each generator in a connected power system has a load frequency controller and an automatic voltage regulator. This means that the generators can automatically adjust their output frequency to match the load frequency, and maintain consistent voltage levels. The controller handles variations in power needs and is set up for a particular operating situation. Variations in rotor angle that affect frequency and real power. While the reactive power depends on the voltage (on the generator's excitation)[17].

Yüksel (2011), has studied Parallel Fuzzy PD Control and Fuzzy PI Control for Two-Area Power System. Automatic Generation Control. This research offers an effective approach for automatic generation control (AGC) of a two-area power system. The strategy using a modified fuzzy PI control and a parallel fuzzy control has been shown effective. In this study, typical reactions to actual power demand are represented using the latest MATLAB/SIMULINK simulation method [18].

Parveen Dabur, Naresh Kumar Yadav et al (2011), they proposed Demand Side Management and Multi Area Power Systems using AGC and AVR Matlab. By balancing machine load and losses, the AGC protects the selected frequency and energy exchange with nearby structures. Demand-side management, or DSM, is also studied. DSM is used to reduce the total load demand for energy structures between top needs to maintain machine safety [19].

T R Shyama, R Satheesh Kumarand V Shanmugasundaram (2012), in this work, the fuzzy gain scheduled proportional-integral controller (FGSPIC) characteristics for a two-location, connected power system were revealed. The LFC and AVR have specific properties. The system uses its management method to enforce the use of the MATLAB program. Additionally, it was adjusted using a conventional proportional and integral (PI) controller for the performance comparison [20].

Vinod Kumar Thota (2014), Fuzzy logic-based LFC and AVR are presented for a multi-area power system. Automatic Generation Control depends on the business's scheduled frequency and net exchange (AGC). Voltage and frequency are independently controlled because of the incompatible link between AVR and LFC. This research focuses on an LFC and AVR control technique based on fuzzy logic to rebalance load and generation [21].

Vivek Nath and D.K Sambariya (2015), Voltage regulation and automated generation control for single- and double-area power systems were done using fuzzy logic control. AGC keeps system generation stable regardless of load or losses. The synchronous generator's terminal voltage must be maintained by the AVR in order for the bus bar voltage to remain within acceptable limits. A single-area system's frequency and voltage are analyzed using MATLAB [22].

Ashok Singh, Rmeshwar Singh, and RekhaKushwah (2015) Optimal Tuning Controller PID-Based Automatic Voltage Regulator and Automatic Load Frequency Control of Electrical Power Plants. In this study, Ziegler-Nichols tuned controllers for AVR and LFC are studied along with proportional integral derivative (PID) controllers and optimal tuned without controllers (LFC). Simulation results with and without the suggested Ziegler-Nichols tuned controller are compared [23].

Chandrashekar M.J. and Dr. R. Jayapal (2015) How to set up AGC with AVR control and use PI, PID, and fuzzy logic controllers for double area systems. Also describe AGC with AVR control. The excitation of the AVR and the area control error computation of the AGC are both controlled by the fuzzy controller, which also controls the amount of additional generation that does not need to be corrected [24].

Orosun. M. M., Orosun R. O. and Adamu S. S. (2016) have modeled and simulated MPC-based automatic generation control systems. The study focused on synchronous generator

systems. In this work, actual and reactive power of a power system were controlled using an automatic generation control system to maintain the system in a steady state. The power system's overshoot/undershoot and settling time both improved significantly, indicating potential benefits [25].

Priyanka Andhare and Naveen Asati (2016), It is investigated the PID-Controlled Automatic Voltage Regulator with Load Frequency Control. Voltage changes affect reactive power, while real power changes affect system frequency. The sensitivity of reactive power to frequency variations is lower. Therefore, real power and reactive power are managed independently. Real power and frequency are regulated by LFC and AVR, whilst reactive power and voltage magnitude are regulated by AVR [26].

Amir Sharifan (2016), measured the results of the PSS and Governor's models for the power system's voltage stability. In this study, the PSS and governor's effects on the power system's voltage balance are modeled using the best electrical device dynamic model. This improves the phenomenon's portrayal. Power System Stabilizer (PSS) holds models for synchronous machines, automated voltage regulators (AVR), prime movers, and speed governors. This allows for accurate voltage analysis. Calculating the voltage balance margin (VSM) allows for the evaluation of the voltage balance [27].

Ghazanfar Shahgholian (2017), this study simulates and evaluates the LFC system used in hydroelectric power plants to reduce frequency oscillations caused by load distributions. The LFC stabilizes the electrical supply. PSS improves system damping. The small sign balancing evaluation uses Eigen value and time domain response [28].

Rajendra Fagna (2017), has researched using a Type 1 Fuzzy Logic Controller to regulate a power plant's load frequency. A type 1 fuzzy controller was created for a thermal power system's variable load frequency. Type 1 fuzzy controllers outperform PID controllers like Ziegler Nichols [29].

Modu M. Ibrahim, Jibril D. Jiya et al (2017), have discussed modeling and simulating the AVC. AVRs are becoming more common in power systems and industry. Their main goal is to ensure device stability and appropriate parameter values. Without a controller, an AVR will have delayed responses and may be unstable [30].

Manjit Bahadur Singh, Manoj Kumar Debneth, et al (2019), have offered Designing & Applications of PID-PID Dual Loop Controller for LFC. This study suggests an SMO-adjusted PID-PID dual loop controller for two-site power systems. Spider monkey optimization uses modified PID-PID dual loop controllers to outclass standard PID controllers. Faster frequency and inter-line power regulation. Spider monkey uses the algorithm [31].

Binod Kumar Sahu, and Pradeep Kumar Mohanty (2019), they built a fuzzy-PID controller with a derivative filter for a hybrid power network. The system's controller was this. This study discusses AGC of a two-area hybrid power system. When creating and installing AGC controllers for the hybrid power system, operational and design engineers encounter a significant dilemma. This research uses ordinary PID and PID controllers with derivative filters to improve the AGC system's frequency profile (PIDF). These command approaches work [32].

Deepak Kumar Lal and Ajit Kumar Barisal (2019: AGC system improvements. This article offers a load frequency and terminal voltage regulator for power systems by means of moth flame optimization algorithm that can be combined. Maintaining the system's frequency and voltage levels is difficult for engineers. For frequency and voltage control, a fractional-order proportional integral and derivative (FOPID) controller was designed to increase system performance [33].

Krishna, S, R.Ramya, Dr.K.Selvi (2011), Simple Fuzzy Synchronous Generator Excitation Control System Presented. The power system is dynamic and constantly threatened by instabilities. The power system requires a synchronous generator with an automatic voltage regulator for actual control and consistency. Increasing demand for electronic goods requires more reliable power supplies. Currently, a mathematical model can simulate and analyze a power system. Noise, lightning, load variations, and faults generate some uncertainty. Fuzzy theory has helped power system studies in recent years. Theory is better because it's easily handled and examined and flexible. It's ideal for systems with many variables. This work creates a fuzzy logic controller to emulate an automatic voltage regulator for power system analysis [34].

Bouallègue, S.Haggège, J.Ayadi, et al (2012), this paper suggests using PSO to tune PID-type fuzzy logic controllers. In order to develop additional performance and strength

properties of the proposed PID-fuzzy approach, two self-tuning mechanisms are introduced. By using a created controller PSO approach, scalability challenges in PID-type FLC setups are scientifically handled. In a real-time sketch, the situation of a DC drive standard is studied to demonstrate the usefulness and utility of PSO-based fuzzy control systems. Simulations and experiments show the usefulness and robustness of PSO-tuned PID-type FLC structures [35].

Yamille del Valle (2008), this work discussed Particle Swarm Optimization in Power Systems. Analyze PSO and its variants' core principles. It gives a full assessment of power system programs that have benefited from PSO as an optimization technique. For every application, technical information which can be required for making use of PSO, together with its types, particle formulation (answer representation), and the maximum green fitness functions also discussed [36].

S. K. Sinha, R. Prasad and R. N. Patel (2009), this paper supplied PSO Tuned Combined Optimal Fuzzy Controller for Automatic Generation Control of 2 Area Interconnected Power Systems. PSO helped optimize the fuzzy controller's parameters. The proposed controller's output performance was analyzed and compared using the combined optimal fuzzy controller. Simulation findings show that using the PSO tuned combination optimal fuzzy controller can improve overshoot and settling time [37].

2.2. SUMMARY OF LITERATURE REVIEW

The PSO-based fuzzy-PID load frequency and voltage control of synchronous generator systems was examined in this thesis by analyzing the aforementioned literature survey. Additionally, it discusses automatic generation control and the simulation's results (AGC). AVR with PSO-based Fuzzy-PID maintains synchronous generator terminal voltage and frequency at a predetermined level, Balances system generation, load, and losses, decreasing site oscillation. Automatic generation control (AGC) keeps the operating frequency and interchange power within their limits. Here's an adaptable PSO-based fuzzy-PID controller. PSO-based fuzzy-PID controllers are flexible. Fuzzy logic systems are easy to build, offer a wide range of operating circumstances, have a reduced overall production cost, and are easier to customize using natural language.

CHAPTER THREE

MODELING

This research investigates the regulation of the SG excitation/voltage and load frequency control systems utilizing a typical controller, PID, in comparison to the PSO based Fuzzy PID controller, under normal and heavy loading circumstances in order to get the synchronous generator's input output data. The fuzzy-PID PSO controller is the system's foundation. PID and fuzzy logic controllers combine (FLC). Determine how much the synchronous generator's excitation may be improved by using the AVR and LFC loops.

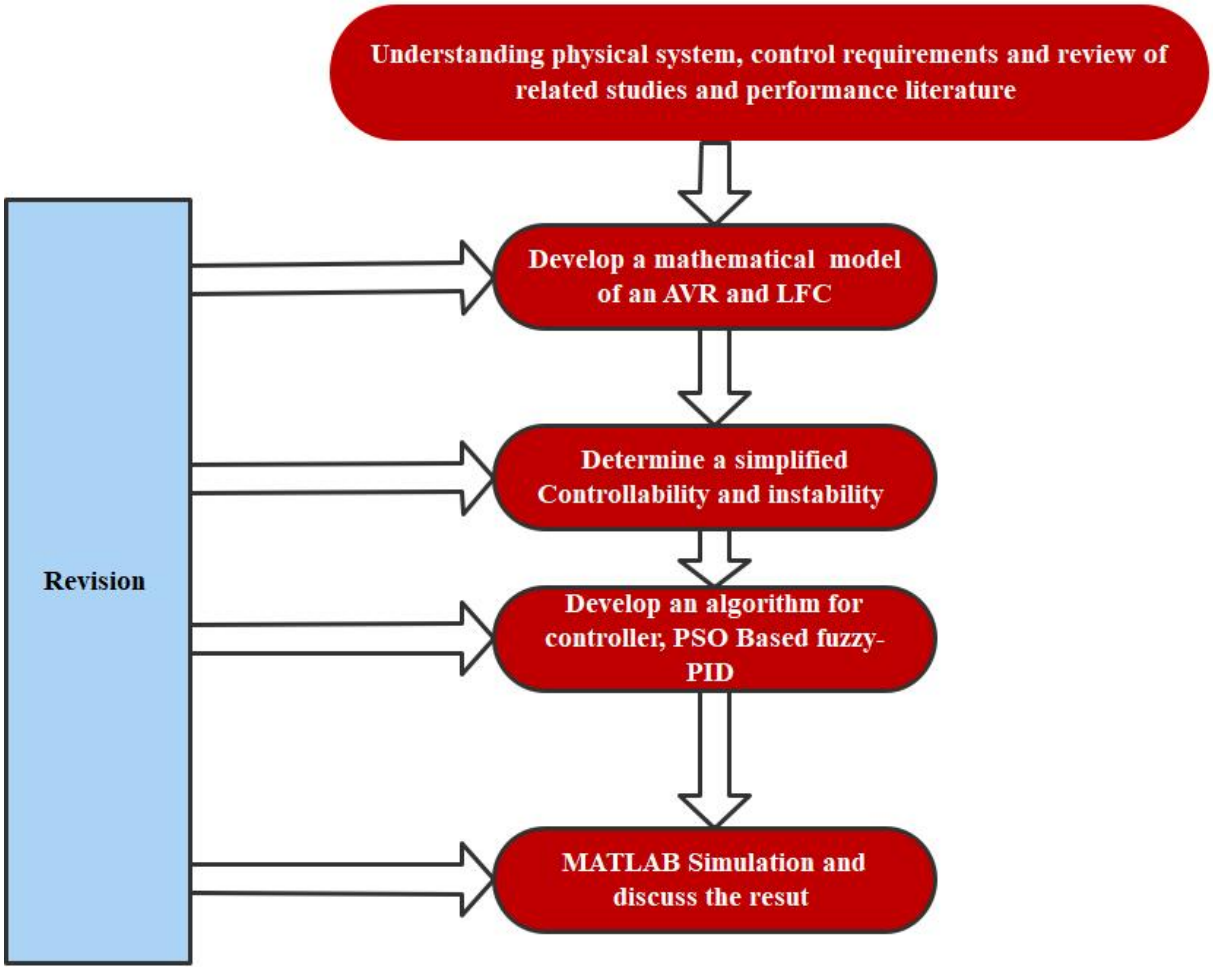

Fig. 3.1. Methodology Flowchart

3.1. MODELING OF ELECTRICAL POWER SYSTEM

3.1.1. INTRODUCTION

Currently, loads are always fluctuating [38]. When the system load increases, the turbine before the governor can change the steam intake, slows. As the system's output variation decreases, the governor's position changes to maintain constant speed. The generator AVR regulates voltage and reactive power flow. A suitable mathematical model is critical to understanding and how feedback control affects a dynamic system's performance. The dynamic study of power systems generally involves a number of system elements of the AGC loop and AVR loop. Fig. 3.2 shows load frequency control and a synchronous generator's automated voltage regulator. This Fig's source [16].

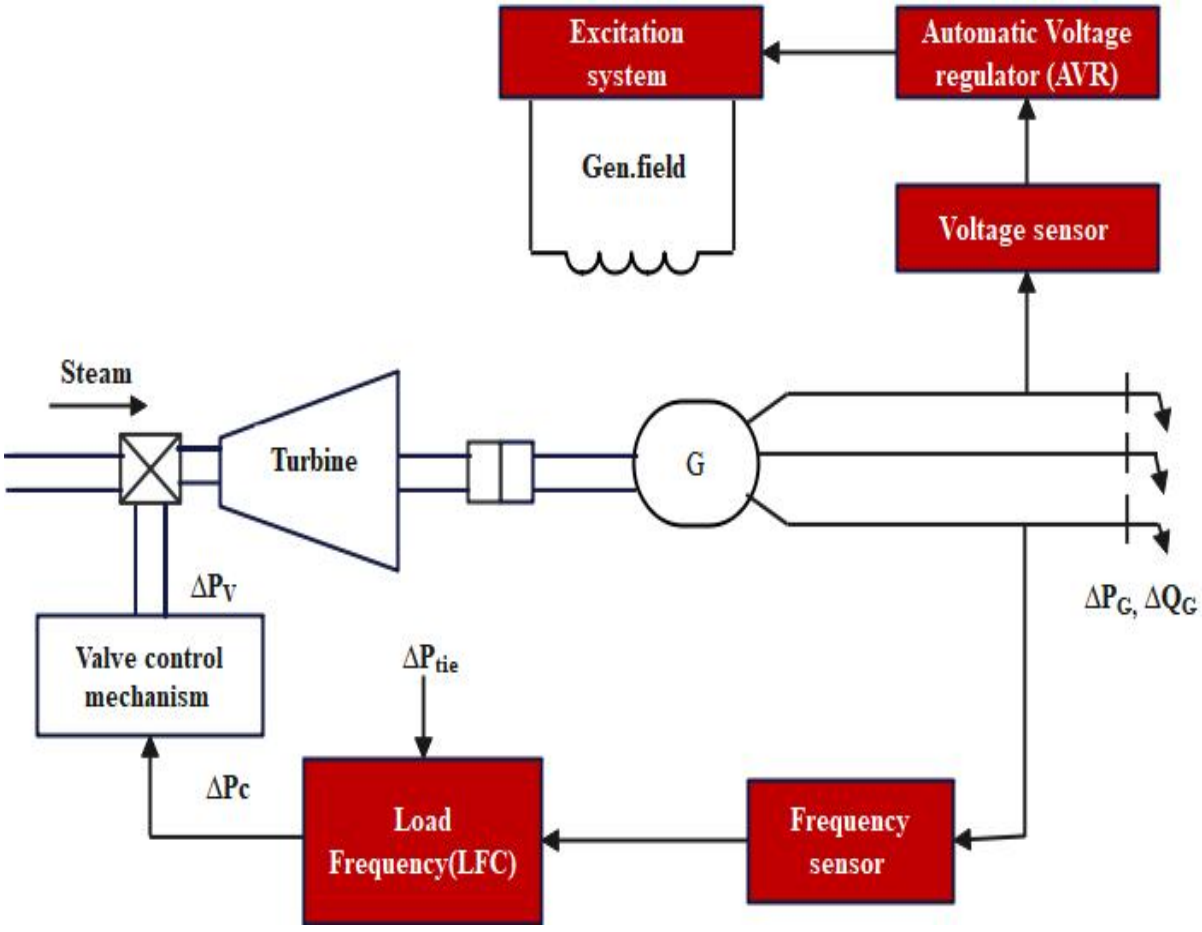

Fig. 3.2. Schematic representations of a synchronous generator's AVR and load frequency control. P symbolizes active power, Q reactive power, and Δ changes.

3.2. LFC and Modelling of Various Components

This thesis describes the transfer function model for LFC and AVR loops. This thesis explores the impact of combining LFC and AVR [2], [39].

The LFC goal is to govern the frequency deviation via a means of retaining the actual power stability inside the system. The signals, which are the tie-line deviation, can be manipulated (input) ΔP_{tie} (based on tie-line flow measurement), as well as the variation in frequency Δf (acquired via means of measuring the change in rotor angle $\Delta\delta$). These error signals Δf and ΔP_{tie} are then amplified, combined, and converted to a real power signal, which then controls the valve position. Depending on the valve position, the turbine modifies its output power to set up the actual power stability. The turbine regulates the amount of energy it produces to ensure power stability [2]. For evaluation purposes, the version for every block in Fig 3.3 is required.

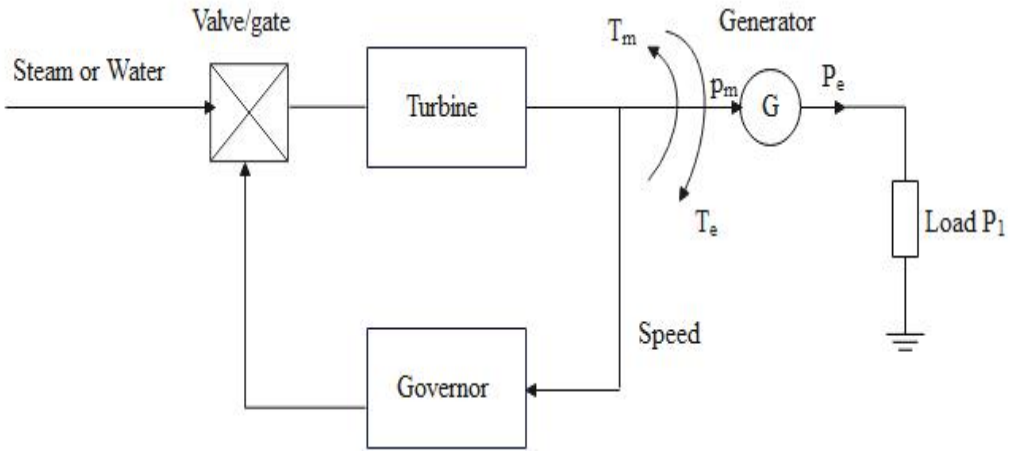

Fig. 3.3. The Schematic Representation of the LFC System

Where,

T_m: Mechanical torque

T_e: Electrical torque

P_e: Electrical power

P_m: Mechanical power

3.2.1. Generator Model

The power system is made up of the produced power and the electrical load. The generator can be represented using the swing equation [2].

$$\frac{2\mathrm{H}}{\omega_s}\frac{d^2\Delta\delta}{dt^2} = \Delta P_m - \Delta P_e \tag{3.1}$$

Where

$\Delta\delta$: is the slight variation in rotor angle that occurs throughout time (rad).

H: is a constant value for the generator's inertia.

ω_s: is the synchronous angular speed expressed in radians per second.

By calculating the speed difference in terms Pu.

$$\frac{d\Delta_\omega}{d_t} = \frac{1}{2H}(\Delta P_m - \Delta P_e) \tag{3.2}$$

This relation can be represented as shown in Fig 3.4.

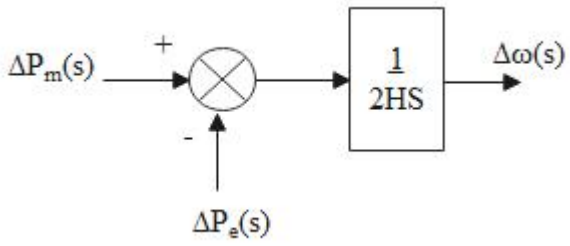

Fig. 3.4.The block diagram representation generator model.

3.2.2. Load Model

Frequency independent components are included in the load that is being applied to the system (ΔP_L) and System load includes frequency-independent components (ΔP_f). The load can be written as well as

$$\Delta P_e = \Delta P_L + \Delta P_f \tag{3.3}$$

Where,

ΔP_e : is the change in the load.

ΔP_L: is the load component that is not dependent on frequency.

ΔP_f: is Frequency-dependent load.

The motor load is sensitive to variations in frequency, and it may be analyzed using the speed load characteristic.

$$\frac{\Delta_W(s)}{\Delta P_m - \Delta P_l} = \frac{1}{2H + D} \tag{3.4}$$

$$\Delta P_f = D\Delta\omega \tag{3.5}$$

Where D or Damping constant is expressed as percent change in load divided by percent change in frequency, as a percentage change If D is 1.5 percent, every 1% variation in frequency results in a 1.5 percent increase in load. A 1% increase in frequency causes a 1.5% increase in load. Fig. 3.5 shows the generator and load working together.

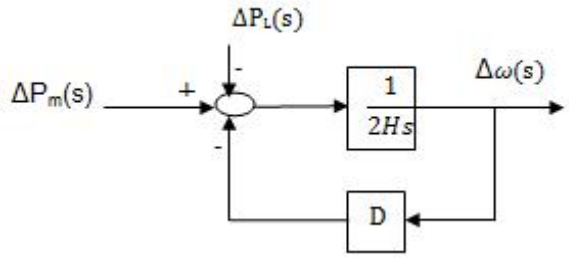

Fig. 3.5. An illustration of a generator and load

Eliminating the simple feedback loop in Fig. 3.5, results in the block diagram of Fig. 3.6.

$$\mathrm{T} = \frac{G}{1 + G_H}$$

$$\frac{\Delta\omega_S}{\Delta P_m - \Delta P_L} = \frac{\frac{1}{2H_{*S}}}{1 + \frac{1}{2H_{*S}}} D$$

$$= \frac{1}{2H * s + D}$$

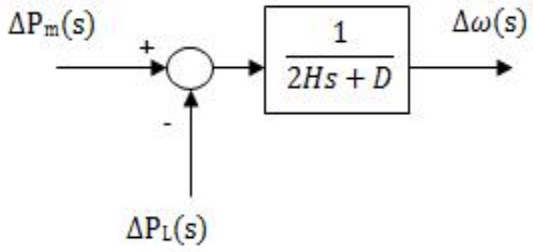

Fig. 3.6. The simplified block diagram that represents the generator and the load

3.2.3. Turbine Model

Prime movers generate mechanical power. This prime mover can be steam or water. The model of prime mover P_m correlates the change in steam valve value ΔPv to the mechanical power output, and TF is

$$\frac{\Delta P_m\,(s)}{\Delta Pv\,(s)} = \frac{1}{1 + T_t} \tag{3.6}$$

Fig. 3.7 depicts a first-order time delay turbine

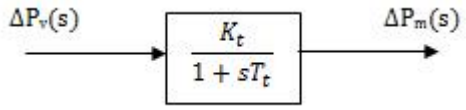

Fig. 3.7. The turbine model.

$$G_t(s) = \frac{\Delta P_m\,(s)}{\Delta P_v(s)} = \frac{K_t}{1 + sT_t} \tag{3.7}$$

Where

ΔP_V*:* Location of the governor valve varying over time (p.u.MW).

$G_t(s)$*:* is the turbine's Transfer Function (TF).

ΔP_m*:* is incremental change in mechanical power (p.u.MW).

T_t: Turbine time constant

3.2.4. Governor Model

Governor model: the command Δpg is the hydraulic amplifier helped convert and target the steam valve ΔPV. Governor's time constant,T_g and transfer function are as follows:

$$\frac{\Delta P_V\,(s)}{\Delta P_g\,(s)} = \frac{1}{1 + T_g\,s} \tag{3.8}$$

Governor can further model as proven in Fig 3.8. The governor's output is determined by:

$$\Delta P_g = \Delta P_{ref} - \frac{\Delta\omega}{R} \tag{3.9}$$

Where

ΔP_{ref}: Reference power

$\frac{\Delta\omega}{R}$: speed governor's power characteristic and: is the speed regulation.

Hydraulic amplifiers change the signal ΔP_g into valve or gate position similar to a power ΔP_V. Thus

$$\Delta P_V(s) = \left(\frac{K_g}{1+sT_g}\right)\Delta P_g(s) \tag{3.10}$$

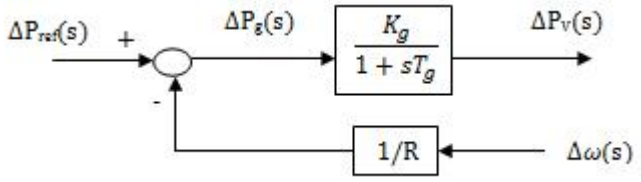

Fig. 3.8. Governor block diagram.

Fig. 3.9 shows how all the pieces can be joined to form the LFC loop.

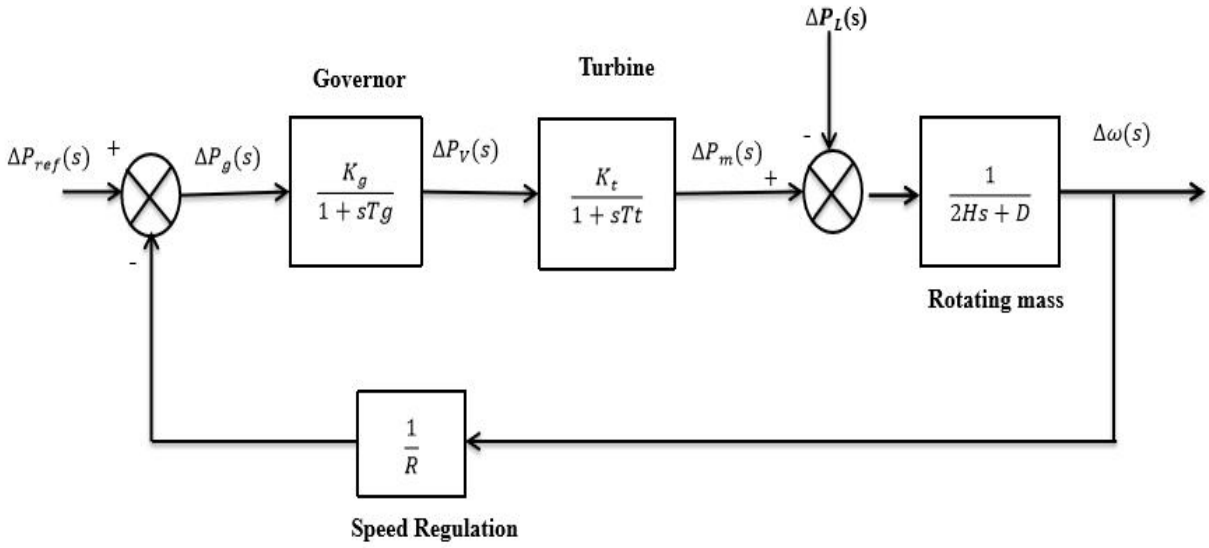

Fig. 3.9. The block diagram representation of the LFC

Change $-\Delta P_{L(s)}$ The results are displayed in Fig. 3.9 using the frequency deviation $\Delta\omega_{(s)}$ as the input and the results as the output.

The open loop transfer functions of the Fig 3.9.

$$KG_{(S)}H_{(S)} = \frac{1}{R}\frac{1}{(2H_S + D)(1+sT_g)(1+sT_t)} \tag{3.11}$$

Additionally, the closed loop transfer functions with regard to load changes ΔP_L towards the frequency deviation $\Delta\omega$ given as below

$$\frac{\Delta\omega_{(s)}}{-\Delta P_{L(s)}} = \frac{(1+sT_g)(1+sT_t)}{(2H_S+D)(1+sT_g)(1+sT_t)} + \frac{1}{R} \tag{3.12}$$

$$\Delta\omega_{(s)} = -\Delta P_{L(s)} T(s) \tag{3.13}$$

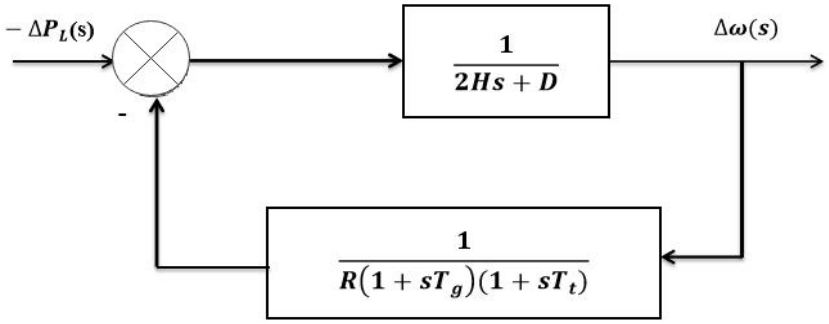

Fig. 3.10. Load frequency control block diagram with input $= -\Delta P_{L(s)}$ and output $\Delta\omega_{(s)}$

Step input is load change, i.e. $-\Delta P_{L(s)} = \Delta P_L/s$ the steady-state value can be determined using final values theory of $\Delta\omega$ is

$$\Delta\omega_{ss} = \lim_{S\to 0} S\Delta\omega(s) = (-\Delta P_L)\frac{1}{D+\frac{1}{R}} \tag{3.14}$$

When, $D = 0$, the speed regulation of the governor determines the steady-state frequency variance. Formula shows this:

$$\Delta\omega_{ss} = (-\Delta PL)R \tag{3.15}$$

When a number of generators have speed regulators $R_1 R_2$, ..., R_n the steady-state frequency variance can be calculated when the system is coupled.

$$\Delta\omega_{ss} = (-\Delta P_L)\frac{1}{D+\frac{1}{R_1}+\frac{1}{R_2}+\ldots\frac{1}{R_n}} \tag{3.16}$$

An isolated power plant needs these parameters [2].

Turbine time constant $T_t = 0.5\ sec$

Governor time constant $T_g = 0.2\ sec$

Generator time constant $H = 5\ \text{sec}$

Governor speed regulation = R per unit

D is equal to 0.8 because a 1% change in frequency causes a 0.8 % change in load. The governor's current speed restriction is R = 0.05 p.u. The turbine produces 600 MVA at 50 hertz. 192.3 MW load shift ($\Delta PL = 0.2\ \text{p.u.}$) happens [2].

The transfer function for the open loop.

$$KG_{(S)}H_{(S)} = \frac{K}{(10s + 0.8)(1 + 0.2s)(1 + 0.5s)}$$

$$= \frac{K}{s^3 + 7.08s^2 + 10.56s + 0.8}$$

Where $K = \frac{1}{R}$

$$K < 73.965$$

$$\frac{1}{R} > 73.965$$

$$R > \frac{1}{73.965}$$

The equation for the attributes is as follows:

$$1 + KG_{(S)}H(s) = 1 + \frac{K}{s^3 + 7.08s^2 + 10.56s + 0.8 + K = 0}$$

The solutions that are obtained using the characteristics polynomial equation

$$s^3 + 7.08s^2 + 10.56s + 0.8 = 0$$

Stability test

The Routh–Hurwitz array corresponding to this polynomial can thus be written as

$$\begin{array}{c|cc} S^3 & 1 & 10.56 \\ S^2 & 7.08 & 0.8 + K \\ S^1 & \frac{73.965 - K}{7.08} & 0 \\ S^0 & 0.8 + K & 0 \end{array}$$

From the S^1 row, K must be > 73.965 to ensure system stability. Also from S^0 row, $K > -0.8$. Given positive K values, the control system stability.

$$73.965 - K > 0 \wedge\ 0.8 + K > 0$$

$$K < 73.965 \wedge K < -0.8$$

$$-0.8 < K < 73.965$$

Since $R = \frac{1}{K}$ Regulate governor speed to maintain control system stability.

$$R > \frac{1}{73.965} \text{ or } R > 0.0135$$

For $K = 73.965$, the auxiliary equation S^2 row is

$$7.08s^2 + 74.765s = 0$$

Or $s = \pm j3.25$. At R=0.0135, conjugate poles on the jω axis, and the control system is marginally stable.

The loci intersects the jω axis at $s = \pm j3.25$ for $K = 73.965$. The system is marginally stable $R = \frac{1}{73.965} = 0.0135$. Use appendix A to get the root-locus.

Here's the closed-loop transfer function.

$$\frac{\Delta\omega(s)}{-\Delta PL(s)} = T(s) = \frac{(1 + 0.2s)(1 + 0.5s)}{(10s + 0.8)(1 + 0.2s)(1 + 0.5s) + \frac{1}{0.05}}$$

$$= \frac{0.1s^2 + 0.7s + 1}{s^3 + 7.8s^2 + 10.56s + 20.8}$$

To obtain the step response, use Appendix B

Step input causes a frequency fluctuation from steady state.

$$\Delta\omega_{ss} = \lim_{s \to 0} S\Delta\omega_{(S)} = \frac{1}{20.8}(-0.2) = -0.0096 \text{ pu}$$

The rapid change in 0.2 load causes the following steady-state frequency fluctuations in hertz:

$$\Delta f = (\Delta\omega_{ss})(f_0) = (-0.0096)(50) = -0.48 \text{ Hz}$$

And a new frequency is

$$f = (f_0) + (\Delta f) = 50 + (-0.48 \text{ Hz}) = 50 - 0.48 = 49.52\text{Hz}$$

Change in power deviation is

$$\frac{\Delta\omega_{ss}}{R} = \frac{-0.0096}{0.05} = 0.1923 \text{ pu} = 192.3\text{MW}$$

The generating unit supplies 792.3 MW at a new operating frequency of 49.52Hz

3.2.5. State Space Model of LFC

Fig 3.9's dynamic equations are as follows:

$$\Delta\omega = \frac{1}{D + 2Hs}(\Delta P_m - \Delta P_L)$$

$$\Delta\omega(D + 2Hs) = (\Delta P_m - \Delta P_L)$$

$$\frac{d\Delta\omega}{dt} = -\frac{D}{2H}\Delta\omega + \frac{1}{2H}\Delta P_m - \frac{1}{2H}\Delta P_L \tag{3.17}$$

$$\Delta P_m = \frac{1}{1 + Tts}\Delta P_V$$

$$\Delta P_m(1 + Tts) = \Delta P_V$$

$$\Delta P_m + Tt\frac{d\Delta P_m}{dt} = \Delta P_V$$

$$\frac{d\Delta P_m}{dt} = \frac{-1}{T_t}\Delta P_v - \frac{1}{T_t}\Delta P_m \tag{3.18}$$

$$\Delta P_V = \frac{1}{1 + Tgs}(\Delta P_{ref} - \frac{1}{R}\Delta\omega)$$

$$\Delta P_V(1 + Tgs) = (\Delta P_{ref} - \frac{1}{R}\Delta\omega)$$

$$\Delta P_V(1 + Tg\frac{d\Delta P_V}{dt}) = (\Delta P_{ref} - \frac{1}{R}\Delta\omega)$$

$$\frac{d\Delta P_V}{dt} = -\frac{1}{TgR}\Delta\omega - \frac{1}{Tg}\Delta P_V + \frac{1}{Tg}\Delta P_{ref} \tag{3.19}$$

The model defined by Equations (3.17)-(3.19) can be rewritten in the state space form as

$$\dot{\Delta_X}(t) = Ax(t) + Bu(t) + Ew(t) \tag{3.20}$$

$$\frac{d}{dt}\begin{bmatrix}\frac{\Delta\omega}{dt}\\ \frac{\Delta P_m}{dt}\\ \frac{\Delta P_v}{dt}\end{bmatrix} = \begin{bmatrix}-\frac{D}{2H} & \frac{1}{2H} & 0\\ 0 & -\frac{1}{T_t} & \frac{K_t}{T_t}\\ -\frac{K_g}{RT_g} & 0 & -\frac{1}{T_g}\end{bmatrix}\begin{bmatrix}\Delta\omega\\ \Delta P_m\\ \Delta P_v\end{bmatrix} + \begin{bmatrix}-\frac{1}{2H} & 0\\ 0 & 0\\ 0 & \frac{1}{T_g}\end{bmatrix}\begin{bmatrix}\Delta P_L\\ \Delta r_{ef}\end{bmatrix}$$

3.2.6. Automatic Generation Control in Single Area System

The main load frequency control loop will cause a steady-state frequency variation in response to a change in the system's load. Whether the governor is using velocity regulation or speed regulation will determine this divergence. To quickly lower frequency fluctuation to zero, we require a reset procedure. The reset is finished by installing an integrated controller that adjusts the speed set point in accordance with the load reference setting. By adding one to the system, KI makes the final frequency deviation zero. A secondary loop for modifying load frequency is shown in Fig. 3.11. Modify KI to achieve the desired transitory response.

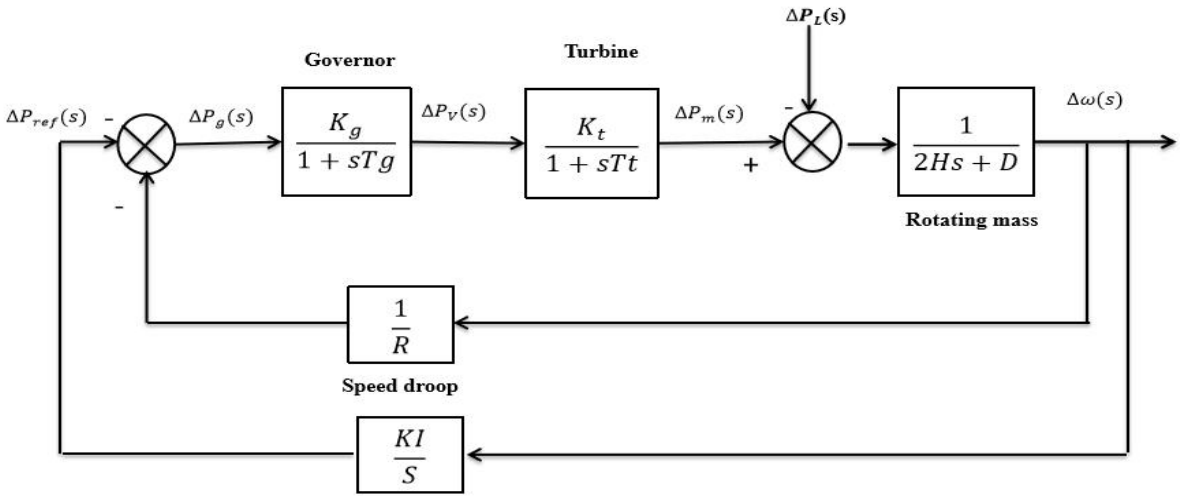

Fig. 3.11. Automatic generation control for isolated system

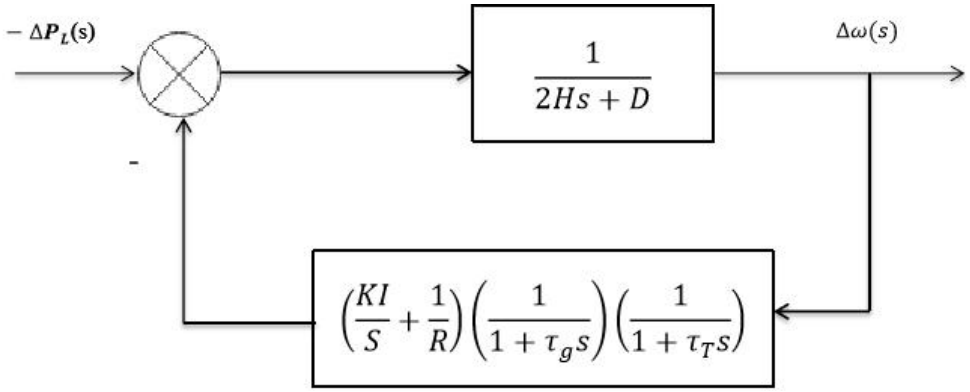

Fig. 3.12. An isolated power system's AGC block diagram.

Fig. 3.12 shows the system's closed-loop transfer function. With only $-\Delta P_L$ as inputs becomes

$$\frac{\Delta\omega(s)}{-\Delta P_L(s)} = \frac{s(1+\tau_g s)(1+\tau_T s)}{s(2H_S+D)(1+\tau_g s)(1+\tau_T s)+KI+\frac{s}{R}}$$

When system features and speed controls are entered into the aforementioned equation, R = 0.05 pu. Closed-loop transfer function. To find step response, use Appendix C.

$$T(s) = \frac{0.1s^3 + 0.7s^2 + s}{s^4 + 7.08s^3 + 10.56s^2 + 20.8 + 6}$$

3.3. Generator Voltage Control System

Flux and generator voltage are related. Excitation regulates voltage. AVR refers to the voltage control system. According to [2] Fig. 3.13 shows the AVR system.

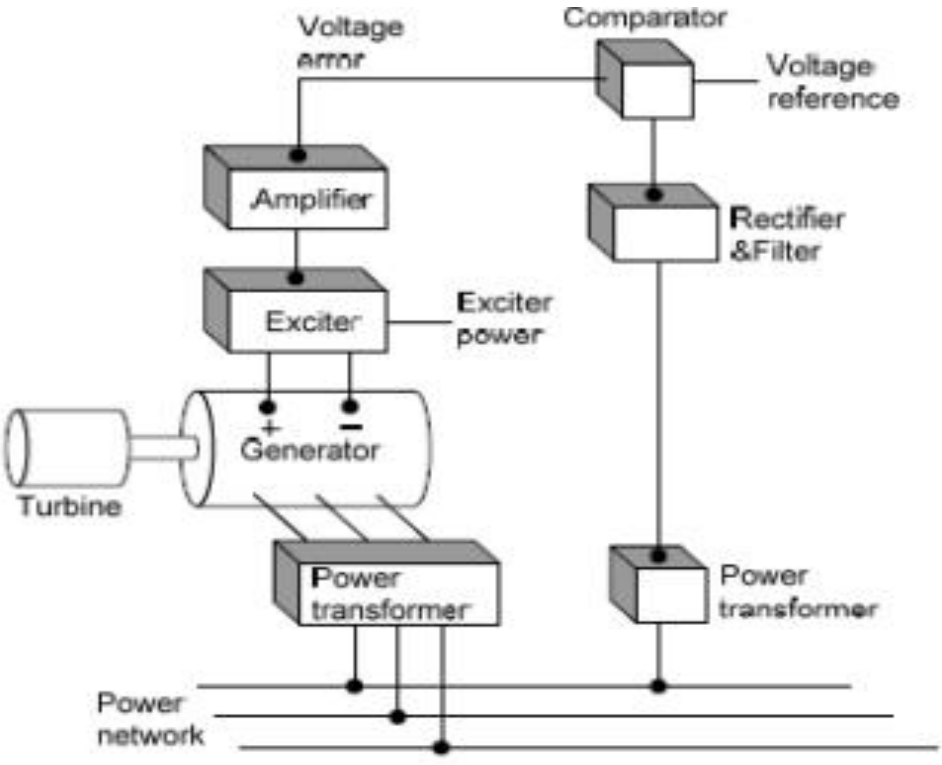

Fig. 3.13 AVR system representation

By referring to Fig. 3.13 which contains the different blocks of Automatic voltage regulator system, the model of each block can be obtained in following sections. Governor, prime mover, load, and inertia model are essential components.

3.3.1. Modeling of automatic voltage regulator

The bus voltage is maintained while the reactive power output is modified by the AVR loop, which controls the generator's terminal voltage. Continuous terminal voltage detection, rectification, smoothing, and evaluation using a DC reference are necessary for the procedure. The "error voltage" is used to control alternator field excitation after amplification and shaping.

AVR is required for synchronous generators. In the event of mishaps, malfunctions, or frequent load changes, the synchronous generator's terminal voltage is adjusted by the automatic voltage regulator (AVR). The AVR enhances the transient stability of the system [2].

3.3.1.1. Comparator

A comparator contrasts the reference DC signal $|V|$ with the measured signal $V_{(ref)}$. The difference between these two signals, "Ve," which is referred to as the error signal, produces an error voltage. This error signal is given by: $\Delta_e = \Delta|V_{ref}| - \Delta|V|$

Using the transform of Laplace for the equation

$$\Delta V_{ref} = \Delta V(s) - \Delta e(s)$$

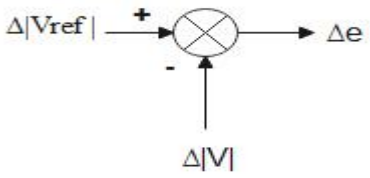

Fig. 3.14. The model of comparator

This comparator compares the reference voltage to the terminal voltage that has been stepped down, converted, and rectified [40]. In Equation (3.21), the difference between reference and operational voltages is (v_{ref}). And terminal voltage (v_t) is the error signal.

$$e(t) = v_{ref} - v_t \tag{3.21}$$

Fig. 3.15 shows AVR operation. One-phase potential transformer measures voltage. Inverted voltage is compared to a predetermined DC reference point. The exciter field is under the

control of the amplified error signal, which also raises the exciter terminal voltage. Consequently, the generator's field current increases, increasing the generator's electromagnetic field. As a result, there is an increase in the production of reactive power, which raises the voltage.

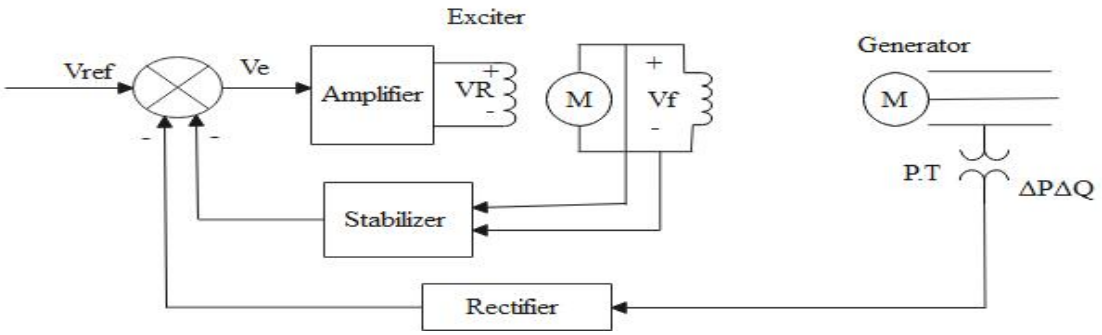

Fig. 3.15. Automatic voltage regulator block diagram [22]

3.3.1.2. Amplifier Model

The transfer function of amplifier model is

$$\frac{V_R(s)}{V_e(s)} = \frac{K_A}{1 + sT_A} \tag{3.22}$$

Where KA is a gain and TA is a time constant.

Depending on the amplification factor, the amplifier amplifies the erroneous signal. Excitation system uses many types of amplifiers. Examples include a tuned generator, amplidyne, and electronic amplifier.

$\Delta VR \infty \Delta e$

$$\Delta VR = KA\Delta e \tag{3.23}$$

Where, KA = Amplifier gain

ΔVR = Output voltage of an amplifier. Taking an equation's Laplace transform (3.22),

$$\Delta VR(s) = KA\Delta e(s)$$

Amplifier transfer function

$$\frac{\Delta VR(s)}{\Delta e(s)} = KA = GA$$

Where KA stands for instantaneous amplifier gain and GA stands for amplifier transfer function. In Fig. 3.16, an amplifier is shown. The letter KA designates the amplifier, which might be magnetic, rotating, or contemporary electrical. When, Ve is error voltage signal and VR is amplifier Voltage. The range of the average values of KA is between 10 and 400, while the range of its time constant, which is usually ignored, is between 0.02 and 0.1 seconds. The values of KA have fallen to the lowest range of 10 in this specific case. Because if we take it at a level higher than 10, its output signal will be higher than the desired value. Additionally, if we choose a number less than 10, the signal is below the desired level. The amplifier model's transfer function is made up of the following:

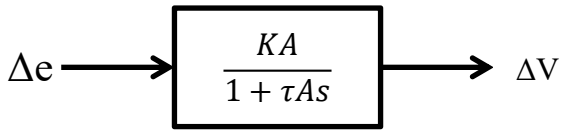

Fig. 3.16. Model of amplifier

3.3.1.3. Exciter Model

The exciter model's transfer function is

$$\frac{\mathrm{V_F(s)}}{\mathrm{V_R(s)}} = \frac{\mathrm{K_E}}{1 + \mathrm{sT_E}} \tag{3.24}$$

Where KE is a gain and TE is a time constant.

There are numerous types of excitation. However, contemporary excitation systems the letter KA designates the amplifier, which might be magnetic, rotating, or contemporary electrical, like silicon controlled rectifiers (SCR). The exciter's output voltage exhibits a nonlinear characteristic of voltage as a result of the saturation effects within the magnetic circuit. As a result, the terminal voltages and the exciter's field voltage do not directly correlate. The IEEE recommended papers contain a variety of models that have been built with differing levels of sophistication. A linearized model that disregards saturation and other nonlinearities while accounting for the fundamental time constant is a useful representation of a contemporary exciter. The linearized exciter model ignores saturation and other nonlinearities while accounting for the primary time constant [41].

Let R_e a resistor in the exciter field, and L_e constituting the exciter field inductance.

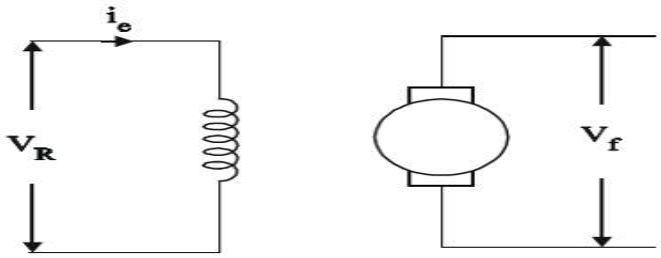

Fig. 3.17. Circuit of an exciter

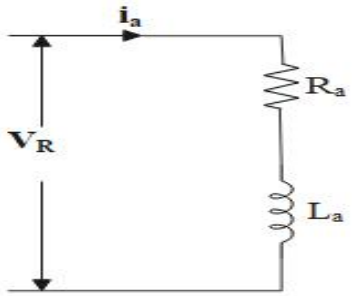

Fig. 3.18. Circuit for field winding of an exciter

From Fig 3.17, the input voltage

$$\Delta VR(s) = Re\Delta_{ie} + Le + \frac{d}{dt}\Delta_{ie} \tag{3.25}$$

Voltage of an exciter's output or generator's field voltage $\Delta V_f \infty \Delta_{ie}$

$$\Delta V_f = k_1\Delta_{ie} \tag{3.26}$$

Using the Laplace transform of equations (3.25) and (3.26)

$$\Delta VR(s) = [R_e + L_{es}]\Delta_{ie(s)}$$

$$\Delta V_f = k_1\Delta_{ie}$$

Then, transfer function of the exciter, $G_e = \frac{\Delta Vf_{(s)}}{\Delta VR_{(s)}} = \frac{K1}{Re+Les} = \frac{K1}{Re[1+Les+(\frac{Le}{Re})s]}$

Where; $G_e = \frac{K1/Re}{1+Les+\left(\frac{Le}{Re}\right)s} = \frac{Ke}{1+sTe}$

$$G_e = \frac{Ke}{1+Re} = \frac{KE}{1+\tau Es} and\ Te = \frac{Le}{Re}$$

When VF is used to represent the exciter voltage, the time constant $Te\,(\tau Es)$ of modern excitation is very small, and Ke (KE) is the exciter gain. Exciter time constant TE and gain are the two components that make up an exciter's transfer function.

$$\frac{\mathrm{V_F\,(S)}}{\mathrm{V_R\,(S)}} = \frac{\mathrm{K_E}}{1 + \mathrm{T_E\,S}} \tag{3.27}$$

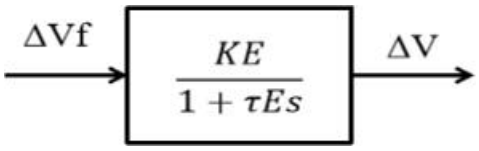

Fig. 3.19. Model of an exciter

3.3.1.4. Generator Model

The transfer function of generator model is

$$\frac{V_t(s)}{V_F(s)} = \frac{K_G}{1 + sT_G} \tag{3.28}$$

The generator load and machine magnetization curve both influence the terminal voltage of the e.m.f. produced by synchronous machines. The terminals of the machine produce three-phase AC power. Depending on the energy available at that specific location, it may be produced using a water turbine at a low speed or a steam turbine operating at a very high speed. The excitation system works to keep the generator's terminal voltage constant under varying load conditions. Gain may represent the linearized transfer function from the generator's terminal voltage to its field voltage $\mathrm{K_G}$ and a time constant $\mathrm{T_G}$ as follows [2]. The generator's terminal voltage is equal to the difference between the induced and emf (E) and drop across the armature ($\mathrm{V_{drop}}$)

$\Delta_{\mathrm{V}} = \Delta\mathrm{E} - \mathrm{V_{drop}}$: With no load, the drop can be neglected or ignored.

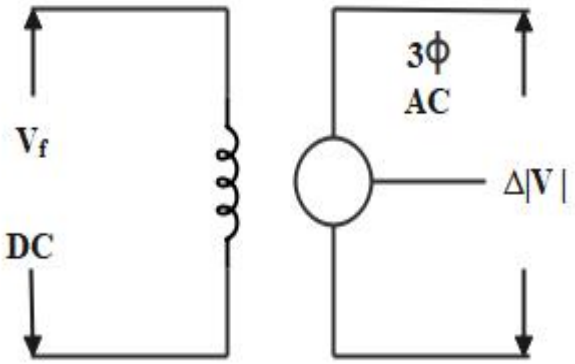

Fig. 3.20. A synchronous generator's circuit diagram

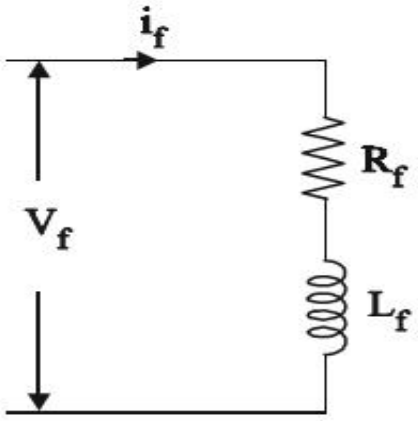

Fig. 3.21. Equivalent circuit for the synchronous generator's field winding

V = E (Ignored or neglected drop)

Taking transform $\Delta V(s) = \Delta E(s)$

Fig 3.21 applying KVL to the field winding

$$\Delta V_f = R_f \Delta_{if} + L_f \frac{d}{dt} \Delta_{if} \tag{3.29}$$

$$E_{max} = IfX_L = I_f \omega L_{fa}$$

$$E_{rms} = \left(\frac{I_f}{\sqrt{2}}\right) \omega L_{fa}$$

$$I_f = \frac{\sqrt{2}}{\omega L_{fa}} E_{rms} = \frac{\sqrt{2}E}{\omega_{Lfa}}$$

$$\Delta V_f = \frac{\sqrt{2}E}{\omega L_{fa}} [R_f VE] + L_f \frac{d}{dt} \Delta E$$

Taking Laplace transform

$$\Delta V_f = \frac{\sqrt{2}E}{\omega L_{fa}}\left[R_f + sLf\right] + \Delta Vf$$

The transfer function of the generator

$$\frac{\Delta V(s)}{\Delta Vf} = \frac{\Delta E(s)}{\Delta Vf(s)} = \frac{\Delta E(s)}{\frac{\sqrt{2E}}{\omega Lfa}[Rf + sLf]\Delta E(s)} = \frac{\omega Lfa}{\sqrt{2}Rf\,[1 + \frac{Lfs}{Rf}]} = \frac{Kf}{1 + \tau GS} = \frac{KG}{1 + \tau GS}$$

$$\frac{Lfs}{Rf} = \tau GS$$

$$Kf = \frac{\omega Lfa}{\sqrt{2}Rf} = KG$$

Where

Ţ: The direct axis time constant for an open circuit.

Lf: is field windings' self-inductance and R_f is field winding resistance

L_{fa} : Between the rotor field and the stator armature, called the mutual inductance coefficient.

The terminal voltage of an electromotive force produced by a synchronous machine is a function of the generator load and the magnetization curve. TG may range from 1.0 to 2.0 seconds from full load to no load and K_G may fluctuate between 0.7 and 1.0.

$$\frac{V_t(S)}{V_F(S)} = \frac{K_G}{I + T_G S} \tag{3.30}$$

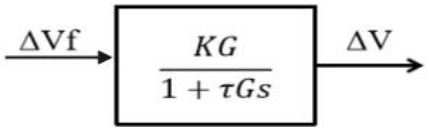

Fig. 3.22. Generator rotor model

3.3.1.5. Sensor Model

The sensor, which senses voltage via a potential transformer, is expected to have a time constant (T_R) that lies between 0.01 and 0.06 in range. The sensor model's transfer function is

$$\frac{V_s(s)}{V_t(s)} = \frac{K_R}{1 + sT_R} \tag{3.31}$$

Where K_R is a gain and T_R is a time constant.

In this approach, the potential transformer senses the generator's terminal voltage K_R and then bridge rectifies the output at this end. This model has a time constant τ and a gain of K [2]

$$\frac{V_S(S)}{V_t(S)} = \frac{K_R}{1 + \tau_R S} \tag{3.32}$$

The block diagram in Fig. 3.23 is built using the aforementioned Equations (3.20–3.32), as shown below. Where the gain K feedback path and time constant of the chosen component. τ_G range of 0.01 to 0.06 seconds is assumed. The AVR closed loop model is obtained by combining each of the component blocks, as shown below.

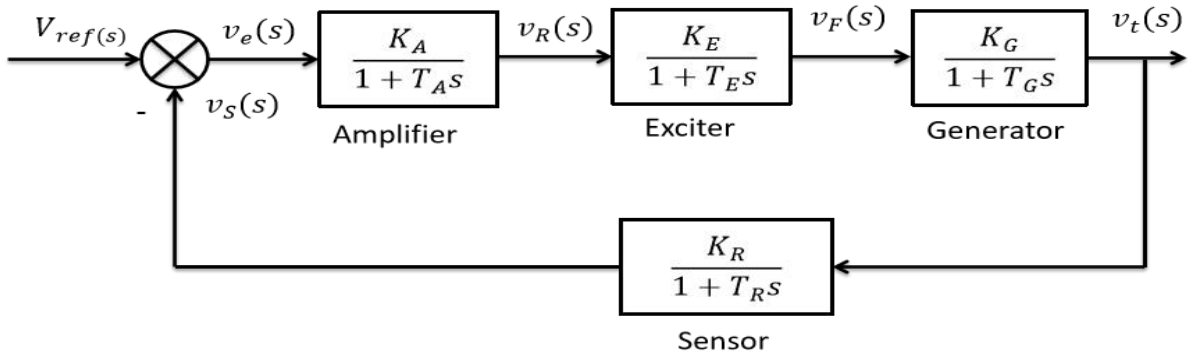

Fig. 3.23. Closed-loop block diagram of automated voltage regulator

According to the diagram, the voltage transducer's time constant is in the negative DC generator's field winding (sensor). An amplifier's gain and time constant are first building blocks. The second block represents a DC generator's field winding time constant, whereas the third block represents an AC generator's.

3.3.1.6. State Space Model of AVR

The dynamic Equations corresponding to the block diagram shown in Fig 3.23 can be written as:

Amplifier model

$$V_R = \frac{K_A}{1 + T_A s} V_{ref} - V_s$$

$$V_R(1 + T_A s) = K_A(V_{ref} - V_s)$$

$$V_R + T_A \frac{dV_R}{dt} = K_A(V_{ref} - V_s)$$

$$\frac{dV_R}{dt} = \frac{K_A}{T_A}V_{ref} - \frac{K_A}{T_A}V_s - \frac{1}{T_A}V_R \tag{3.33}$$

Exciter model

$$V_F = \frac{K_E}{1 + T_E s}V_R$$

$$V_F(1 + T_E s) = K_E V_R$$

$$\frac{dV_F}{dt} = \frac{K_E}{T_E}V_R - \frac{1}{T_E}V_F \tag{3.34}$$

Sensor model

$$V_s = \frac{K_R}{1 + T_R s}V_t$$

$$V_s(1 + T_R s) = K_R V_t$$

$$V_s + T_R\frac{dV_s}{dt} = K_R V_t$$

$$\frac{dV_s}{dt} = \frac{K_R}{T_R}V_t - \frac{1}{T_R}V_s \tag{3.35}$$

Generator model

$$V_t = \frac{K_G}{1 + T_G s}V_F$$

$$V_t(1 + T_G s) = K_G V_F$$

$$V_t + T_G\frac{dV_t}{dt} = K_G V_F$$

$$\frac{dV_t}{dt} = \frac{K_G}{T_G}V_F - \frac{1}{T_G}V_t \tag{3.36}$$

Equations (3.33) through (3.36) describe a model that may be rewritten in the state space form as

$$\frac{d}{dt}\begin{bmatrix} V_R \\ V_F \\ V_S \\ V_t \end{bmatrix} = \begin{bmatrix} -\frac{1}{T_A} & 0 & -\frac{K_A}{T_A} & 0 \\ \frac{K_E}{T_E} & -\frac{1}{T_E} & 0 & 0 \\ 0 & 0 & -\frac{1}{T_R} & \frac{K_A}{T_A} \\ 0 & \frac{K_G}{T_G} & 0 & -\frac{1}{T_G} \end{bmatrix}\begin{bmatrix} V_R \\ V_F \\ V_S \\ V_t \end{bmatrix} + \begin{bmatrix} K_A \\ 0 \\ 0 \\ 0 \end{bmatrix} V_{ref}$$

$$V_t = [0\ 0\ 0\ 0]\begin{bmatrix} V_R \\ V_F \\ V_S \\ V_t \end{bmatrix} Ma$$

Using Fig 3.23's block diagram, we can develop the below open-loop transfer function:

$$\mathrm{KG\ (s)H\ (s)} = \frac{\mathrm{K_A K_E K_G\, K_R}}{(1+\mathrm{T_A s})(1+\mathrm{T_E s})(1+\mathrm{T_G s})(1+\mathrm{T_R s})} \tag{3.37}$$

Additionally, the generator terminal-specific closed loop transfer function voltage $\mathrm{V_t(s)}$ to the reference voltage $\mathrm{V_{ref}(s)}$ is:

$$\frac{\mathrm{V_t(s)}}{\mathrm{V_{ref}\,(s)}} = \frac{\mathrm{K_A K_E K_R K_G\,(1+T_R s)}}{(1+\mathrm{T_A s})(1+\mathrm{T_E s})(1+\mathrm{T_G s})(1+\mathrm{T_R s}) + \mathrm{K_A K_E K_G\, K_R}} \tag{3.38}$$

With the automated voltage regulator system of SGE, the following parameters [2]

$$KE = 1, KG = 0.8, KR = 1, \tau A = 0.1, \tau E = 0.4, \tau G = 1.4\ and\ \tau R = 0.05 \tag{3.39}$$

The open-loop transfer function of the AVR system is presented next.

$$\mathrm{K_G(s)H(s)} = \frac{\mathrm{K_{A(1)(1)(0.8)(1)}}}{(1+0.1\mathrm{s})(1+0.4\mathrm{s})(1.4+\mathrm{s})(1+0.05\mathrm{s})}$$

$$\frac{0.8\mathrm{K_A}}{(1+0.05\mathrm{s})+(1+0.5\mathrm{s})+(1+\mathrm{s})}$$

$$\frac{32\mathrm{K_A}}{(\mathrm{s}+20)(\mathrm{s}+2)(\mathrm{s}+1)}$$

$$= \frac{32\mathrm{K_A}}{\mathrm{s^3}+23\mathrm{s^2}+62\mathrm{s}+40} \tag{3.40}$$

Additionally, the system's steady-state response is

$$V_{tss} = \frac{\lim}{s \to 0} sVt(s) = \frac{K_A}{1 + K_A} \tag{3.41}$$

$$1 + K_G(s) = 0$$

$$1 + \frac{32K_A}{s^3 + 23s^2 + 62s + 40} = 0$$

The characteristic polynomial equation becomes

$$s^3 + 23s^2 + 62s + 40 + 32K_A = 0 \tag{3.42}$$

Stability Test

The K_A range for control stability is calculated using the Routh-Hurwitz array [2]

$$\begin{array}{c|cc} S^3 & 1 & 62 \\ S^2 & 23 & 40 + 32K_A \\ S^1 & \frac{1386 - 32KA}{23} & 0 \\ S^0 & 40 + 32K_A & 0 \end{array}$$

According to the S^1 row, K_A must be less than 43.3125 in order for the control system to be stable, and according to the S^0 row, K_A must be more than -1.35. As a result, the amplifier gain needs to be $K_A < 43.3125$ for control stability when K_A is positive. Use Appendix D to find the root-locus plot.

3.4. LFC-AVR System Model

If the effect of voltage on real power is considered, the following linearized equation is obtained:

$$P_e = P_s * \Delta\delta + K_1 E' \tag{3.43}$$

Where

K_1 : is there a slight change in stator emf that causes a change in electrical power.

P_s : The synchronizing power coefficient.

Also including the small effect of rotor angle upon generator terminal voltage is considered as follows.

$$V_t = K_2 \Delta\delta + K_3 E' \tag{3.44}$$

Where

K2: is the terminal voltage difference generated by a minor rotational angle change..

K3: the minor change in stator emf is caused by a change in terminal voltage.

Finally, modifying the generator field transfer function to include effect of rotor angle, the stator emf can be expressed as

$$E^{'} = \frac{K_G}{1 + TG_s}(V_f - K_4\Delta\delta \qquad (3.45)$$

The aforementioned constants are determined by the operational conditions and network settings [16].

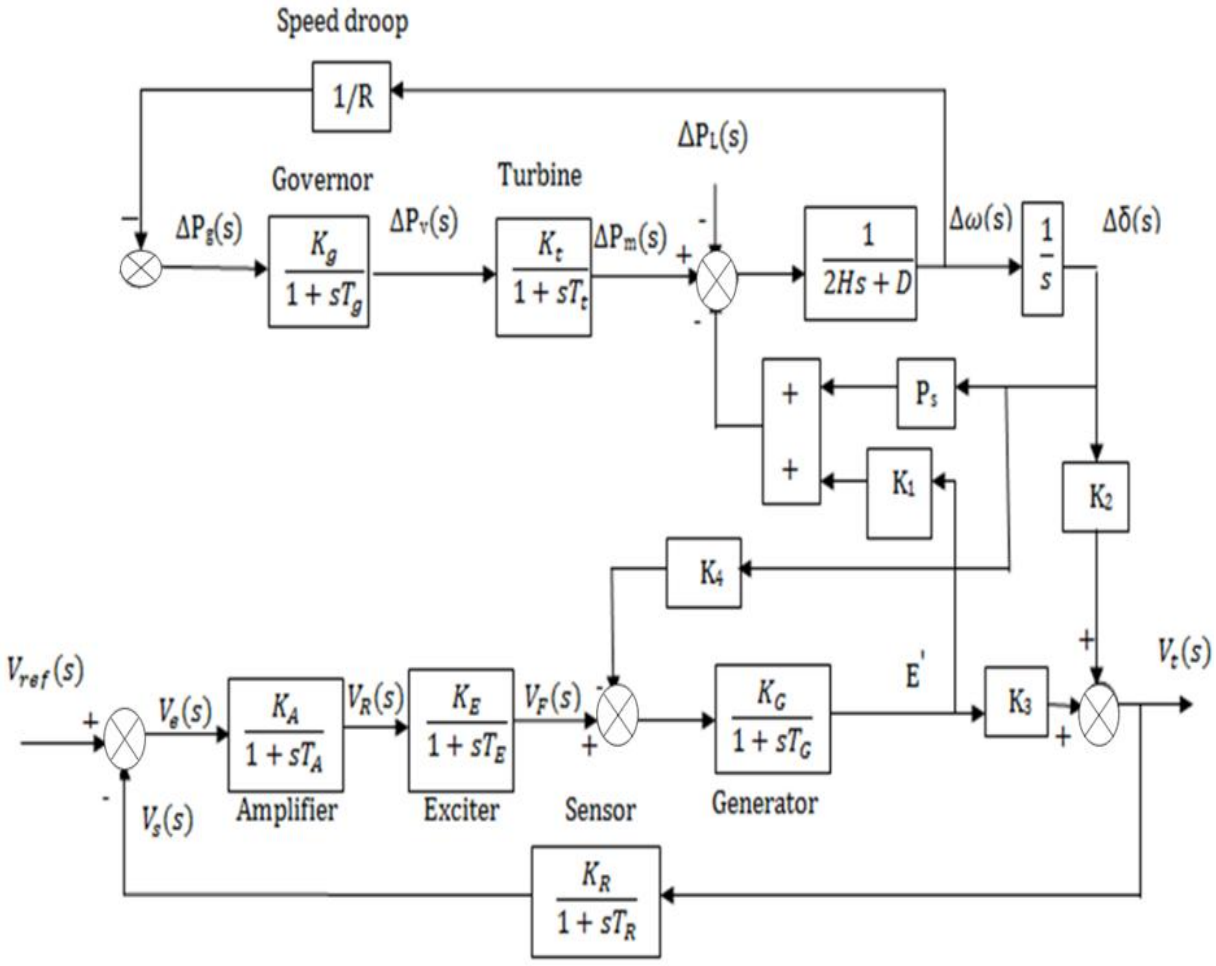

Fig. 3.24. The block schematic of an LFC-AVR single area power system [2].

The dynamic Equations corresponding to the block diagram shown in Fig 3.24 can be written as

$$\Delta\dot{P}_V = \frac{K_g}{T_g}\Delta P_{ref} - \frac{1}{RT_g}\Delta\omega - \frac{1}{T_g}\Delta P_V \tag{3.46}$$

$$\Delta\dot{P}_m = \frac{K_t}{T_t}\Delta P_v - \frac{1}{T_t}\Delta P_m \tag{3.47}$$

$$\Delta\dot{\omega} = \frac{1}{2H}\Delta P_m - \frac{1}{2H}\Delta P_L - \frac{D}{2H}\Delta\omega - \frac{P_s}{2H}\Delta\delta - K_1 E' \tag{3.48}$$

$$\Delta\dot{\delta} = \Delta\omega \tag{3.49}$$

$$\dot{V_R} = \frac{K_A}{T_A}V_{ref} - \frac{K_A}{T_A}V_S - \frac{1}{T_A}V_R \tag{3.50}$$

$$\dot{V_F} = \frac{K_E}{T_E}V_R - \frac{1}{T_E}V_F \tag{3.51}$$

$$\dot{E}' = \frac{K_G}{T_G}V_F - \frac{K_4 K_G}{T_G}\Delta\delta - \frac{K_G}{T_G}E' \tag{3.52}$$

$$\dot{V_S} = \frac{K_R K_3}{T_R}E' + \frac{K_R K_2}{T_R}\Delta\delta - \frac{1}{T_R}V_S \tag{3.53}$$

CHAPTER FOUR

CONTROLLER DESIGN

4.1. INTRODUCTION

An automated system should have little variation in both the load frequency control loop and the voltage regulator. As a result, loops can be described with linear differential equations and linear transfer functions [42].

Controllers in a power system are programmed for a working environment. They adjust to slight changes in load demand to keep frequency and terminal voltage constant. Every generator has a number of loops. LFC regulates real power and frequency while AVR monitors reactive power and voltage [43].

Earlier, researchers had independently done a study on LFC. The two loops aren't conversing literally. Frequency and voltage might change based on end-user needs. The AVR loop controls the generator's output voltage, which determines the true power output. Recently, LFC-AVR control has received greater attention from researchers [44]. Fig 4.1 depicts an AGC machine with an LFC and AVR loop.

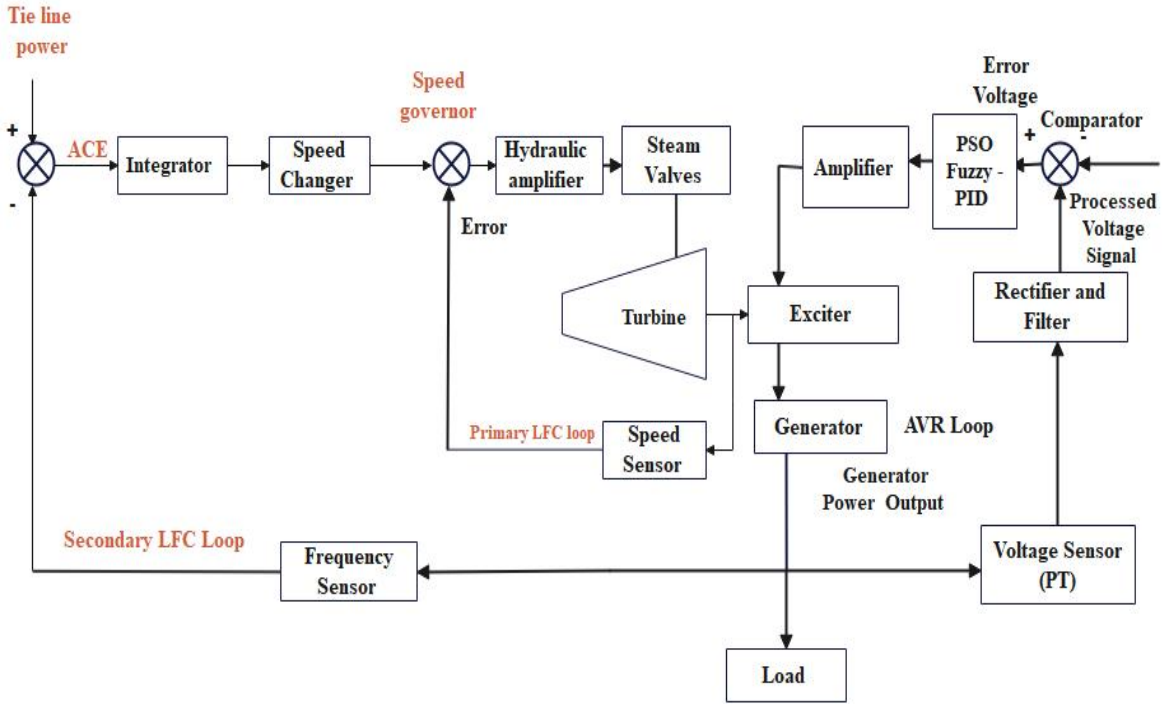

Fig. 4.1. Generator's combined LFC and AVR loops

4.2. Design of Conventional Controller

4.2.1. Proportional-Integral-Derivative PID controller

Integral controllers reduce steady-state error, proportional controllers enhance oscillation, and derivative controllers attenuate oscillation to improve transient performance and stability [45]. Commercial settings use PI and PID controllers. PI controllers increase dynamic responsiveness and steady-state error. PID means proportional, integral, and derivative [46].

a) The proportional term: The gain term modifies the output proportionally to the current error value.

b) The Integral term: The integral term, also called reset, has a magnitude and duration proportional to the mistake. When instantaneous inaccuracy is compounded over time, the accumulated offset before the change can be calculated (integrating the error).

c) The Derivative term: To calculate process error rate of change, use derivative gain and slope. The process error slope is its first order time derivative. The proportional PID controller component limits incorrect disturbance responses. Integral term eliminates steady state error, whereas derivative term reduces dynamic response, increasing system stability [15].

The equation of PID controller is given as

The transfer function $G_C(s)$for the corresponding PID controller is given as

$$G_C(s) = \left(K_p + \frac{K_i}{s} + K_d s\right) E(s) \tag{4.1}$$

$$K_P \left[1 + \frac{1}{T_P\, s} + \ T_d s\right] \tag{4.2}$$

Where K_P is a gain for controller and T_P and T_d are the time constant.

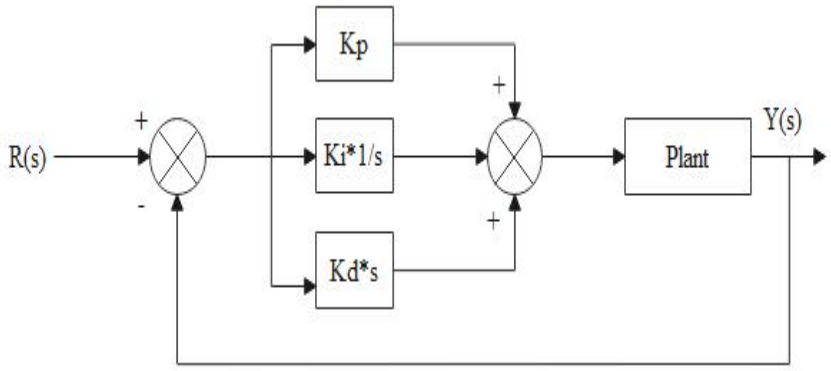

Fig. 4.2. General Block diagram of PID controller

The PID Controller equation is as Follows:

$$G_{PID}(s) = K_P\left(1 + \frac{1}{T_I s} + T_D s\right) = T_P + \frac{K_I}{s} + K_D s$$

PID controller parameter tuning using Ziegler-Nichols method

$$K_{PO} = \frac{1.2T}{KL}, T_{IO} = 2L, T_{DO} = 0.5L$$

4.2.2. Controller structure fuzzy logic

Fuzzy logic controllers help to reduce system instability. Components of a fuzzy logic controller include:

1. Fuzzification module (Fuzzifier).
2. Rule base and Inference engine.
3. Defuzzification module (Defuzzifier).

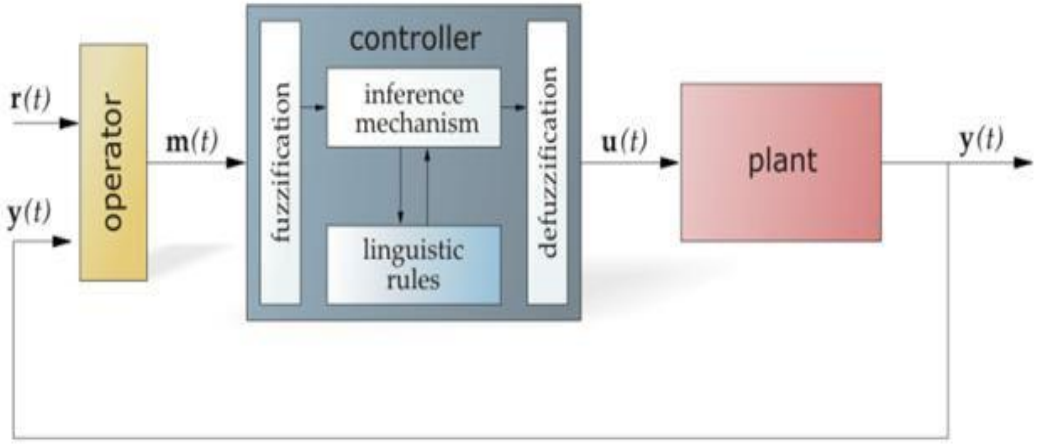

Fig. 4.3. Basic Configuration of a Fuzzy Logic Controller [47]

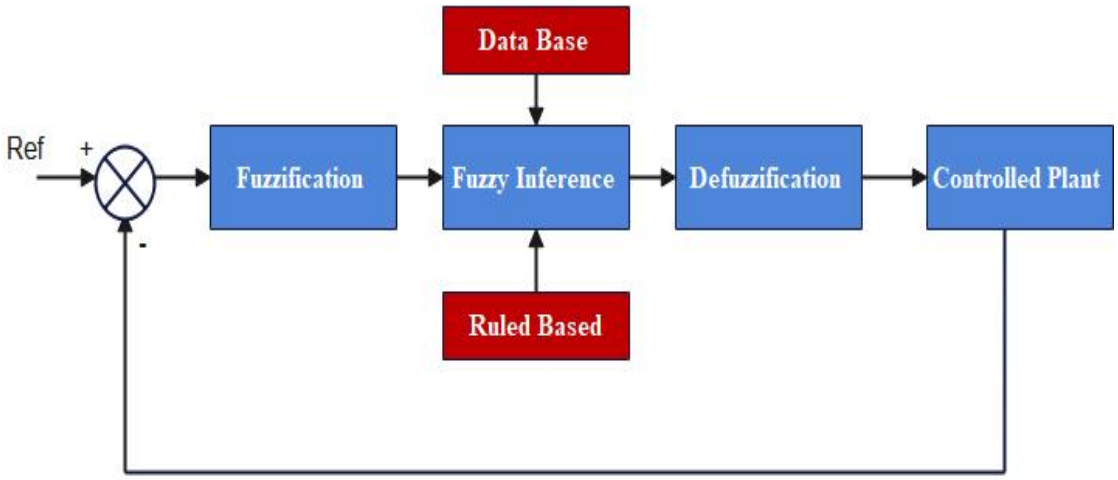

Fig. 4.4. Block diagram structure of FLC

4.2.3. Fuzzy controller design

Lotfi A. Zadeh, a Berkeley computer science professor in 1965, introduced fuzzy logic. A multivalued logic that defines values between yes or no, true or false, high or low, etc. is fuzzy logic (FL). When ideas like "relatively tall" and "extremely fast" are encoded with instructions that simulate human thought, computers can manage them. Fuzzy systems are a Greek alternative to traditional set membership and logic. Fuzzy logic describes fuzzy systems.

Fuzzy logic is popular because it reduces the complexity of problem-solving models. Fuzzy logic uses linguistic concepts to describe the causal link between input and output constraints [7].

This study used an If-Then rule and a Mamdani fuzzy controller. The rule base's language variables are as follows:

Five fuzzy sets set the input variables in the fuzzy block's selected triangle membership functions. Fuzzy sets include:

- $\mathrm{ET} = \{\mathrm{NB}, \mathrm{NM}, \mathrm{Z}, \mathrm{PM}, \mathrm{PB}\}$
- $\mathrm{DET} = \{\mathrm{NB}, \mathrm{NM}, \mathrm{Z}, \mathrm{PM}, \mathrm{PB}\}$
- $\mathrm{KP} = \{\mathrm{NB}, \mathrm{NM}, \mathrm{Z}, \mathrm{PM}, \mathrm{PB}\}$
- $\mathrm{KI} = \{\mathrm{NB}, \mathrm{NM}, \mathrm{Z}, \mathrm{PM}, \mathrm{PB}\}$
- $\mathrm{KD} = \{\mathrm{NB}, \mathrm{NM}, \mathrm{Z}, \mathrm{PM}, \mathrm{PB}\}$

NB stands for Negative Big, NM is Negative Medium, Z is Zero, PM is Positive Medium, and PB is Positive Big. Fig 4.13 shows the linguistic If-Then rules. These rules apply to the input error (ET) and change of error membership functions (DET). Given the 25 If-Then combinations for the two inputs, there are only 25 rules (5 x 5). In fuzzy controller design, the rule base is commonly built with a priori data.

1. The physical law that governs the system dynamics
2. Data from existing (PID) controller
3. Expert knowledge about the plant

Here's how to become system-savvy. Formula for generic conventional control error: $e(t) = r(t) - c(t)$, and assuming a constant set point one can arrive at $\frac{de(t)}{dt} = \frac{dc(t)}{dt}$

Where $r(t)$= reference/ desired output signal

$e(t)$ = error signal

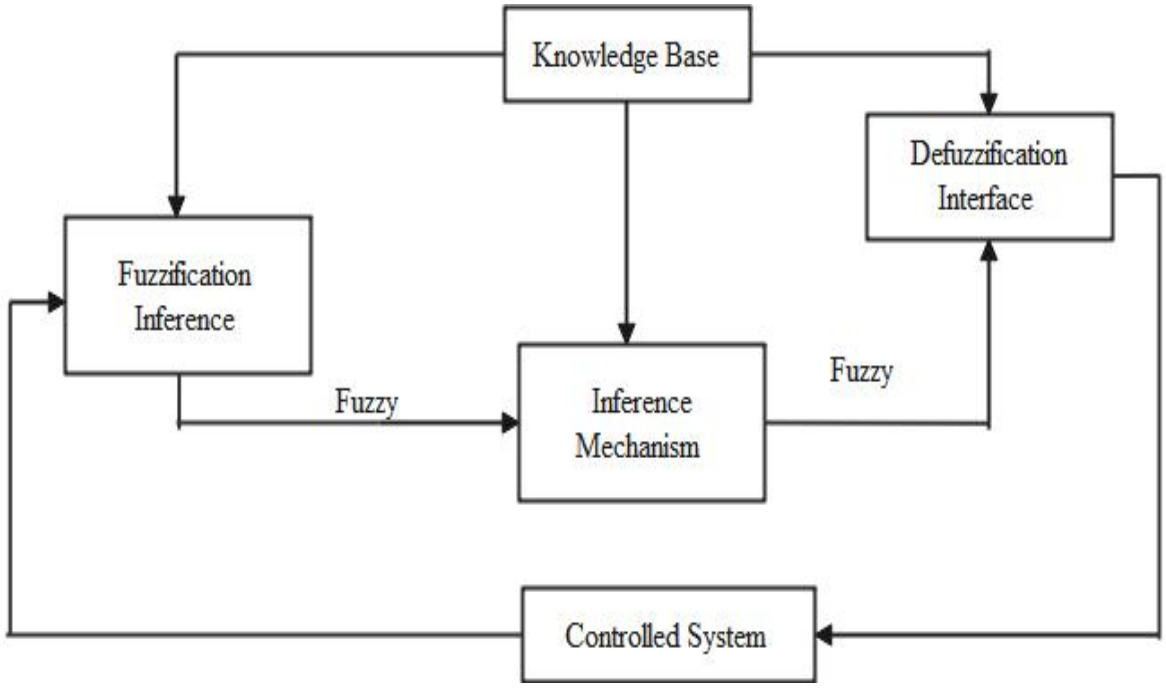

Fig. 4.5. Block diagram of the FLC building blocks

The development of the control system based on fuzzy logic involves the following steps:

- Selection of the control variables
- Membership function definition
- Rule formation
- Defuzzification strategy

Matlab Simulink helped the fuzzy controller traverse the input/output universe [-1, 1][48]. The FLC controller was utilized to dynamically respond, minimize or eliminate the steady-state error, and regulate the generator excitation systems.

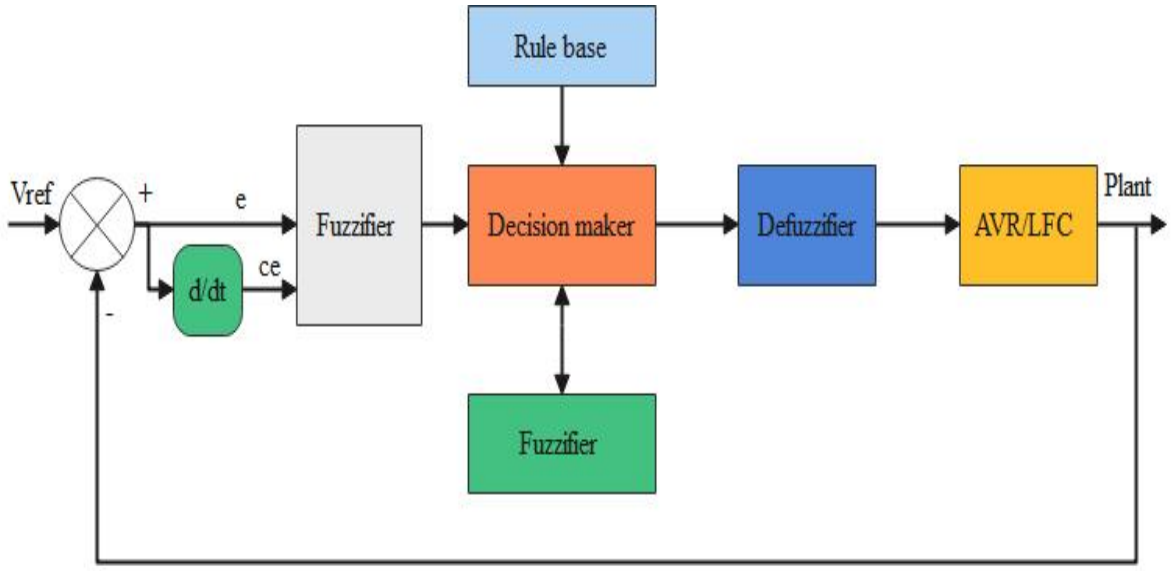

Fig. 4.6. Basic configuration of the fuzzy logic controller

The input variables below are measured based on expert knowledge or the knowledge of the plant operator and quantified linguistically. The first block inside the controller is fuzzification, which converts each piece of input data to degrees of membership by a lookup or several membership functions. The fuzzification block thus matches the input data with the conditions of rulers to determine how well the condition of each matches the particular input. In this controller, five fuzzy subsets are selected. Those are; -Negative big (NB), Negative small (NS), Zero (Z), Positive small (PS), and Positive big (PB). Inputs to the fuzzy logic controller are error (ET) and error change (DET). The inputs are:

$$ET = V_o - V_{ref} \tag{4.3}$$

$$DET = E_k - V_{k-1} \tag{4.4}$$

V_0 : is the current output voltage, while V_{ref} is the reference input voltage and k denotes the values taken at the starting of voltage. Rule Editor is used to modify the system's rules. The Fuzzy Controller's Rule Editor encodes Table 4.1's 25 rules.

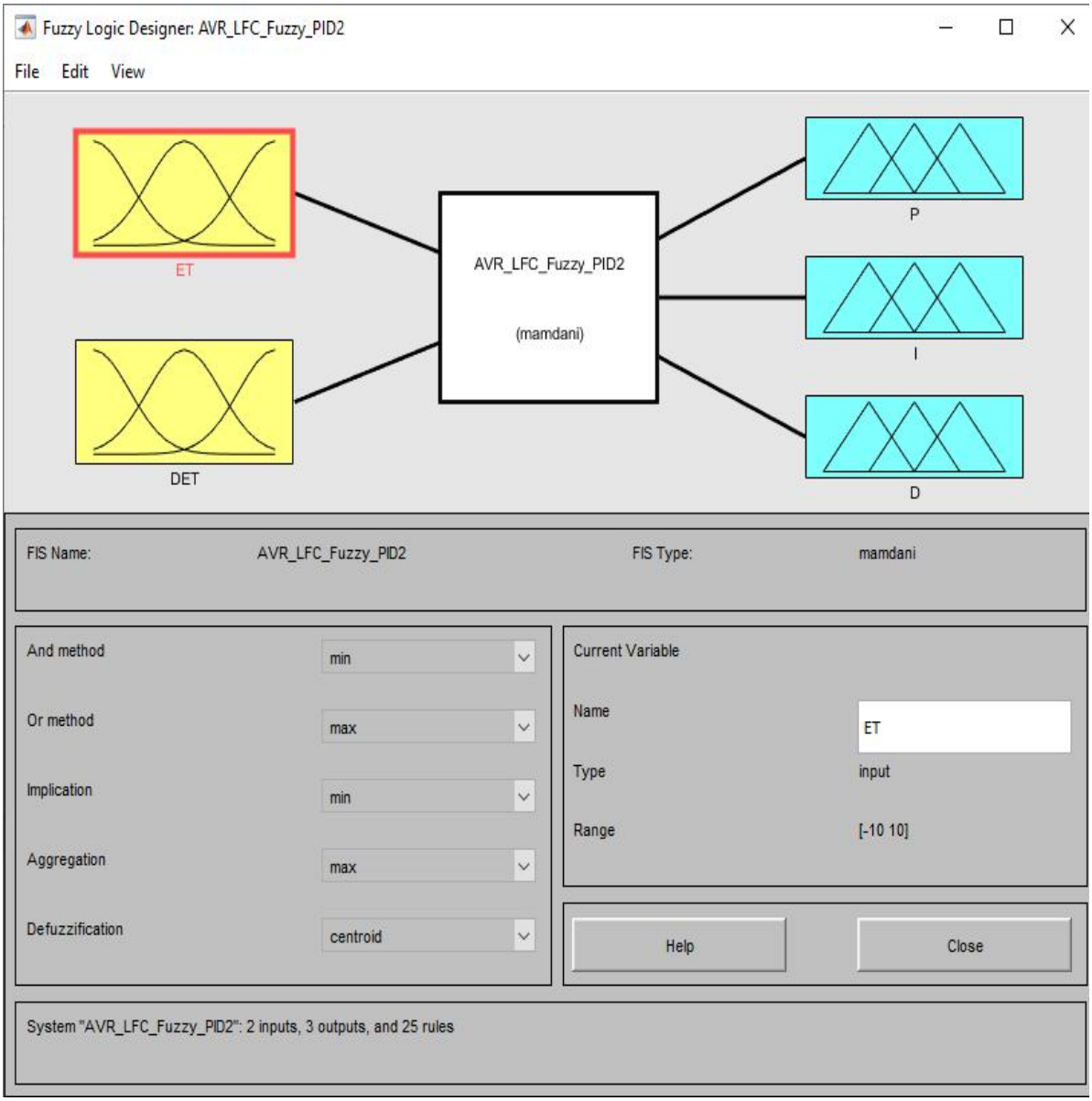

Fig. 4.7. The MAT LAB's Fuzzy Inference System Editor and Programmer

Error (ET) and change of error (DET) are controller inputs, while P, I, and D are outputs. Fig 4.7 shows the controller's two inputs and three outputs. Each control variable has five partitions. Five fuzzily defined subsets of these partitions, known as membership functions, are created: ET (NB, NM, Z, PM, PB) and DET (NB, NM, Z, PM, PB), Fig (4.8-4.9) display the membership function (input variables) and fuzzy subsets (changing of error variable) and Fig (4.10-4.11) demonstrate the membership feature (output variable). Each input in this configuration has a single dominating fuzzy subset, according to the triangle membership function.

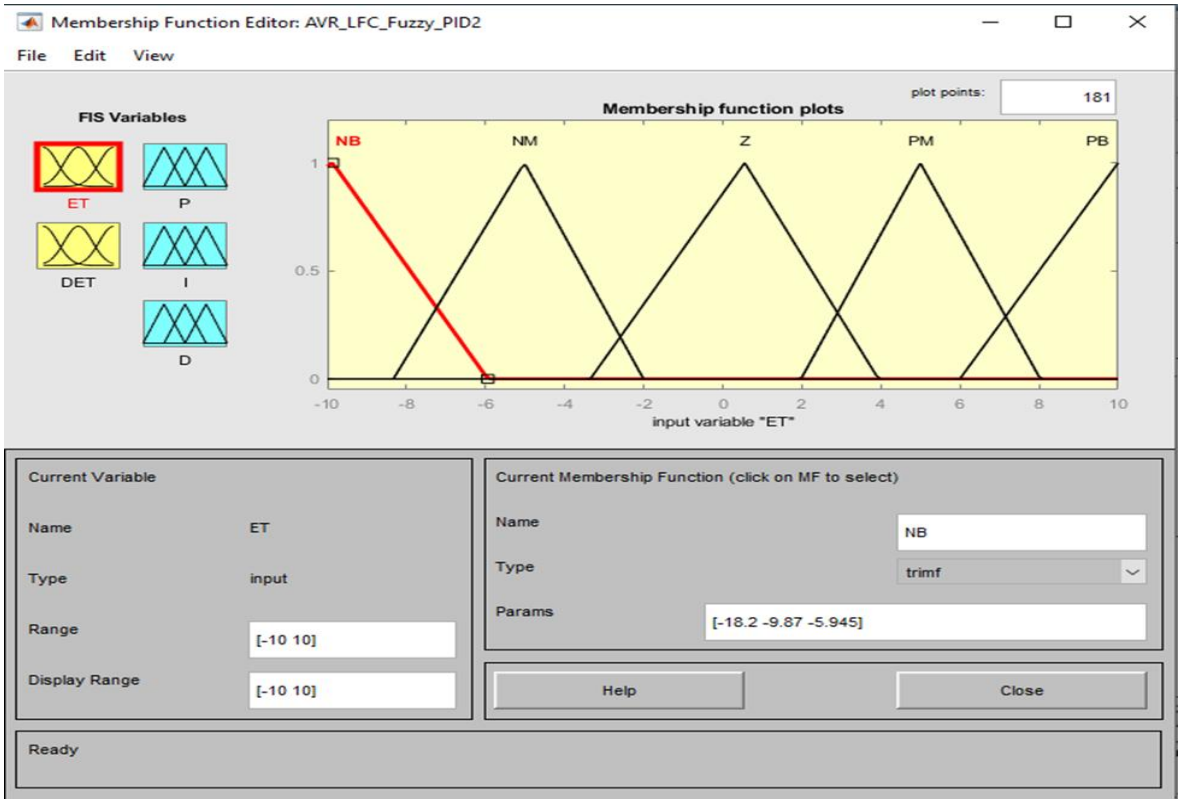

Fig. 4.8. Membership function error (ET)

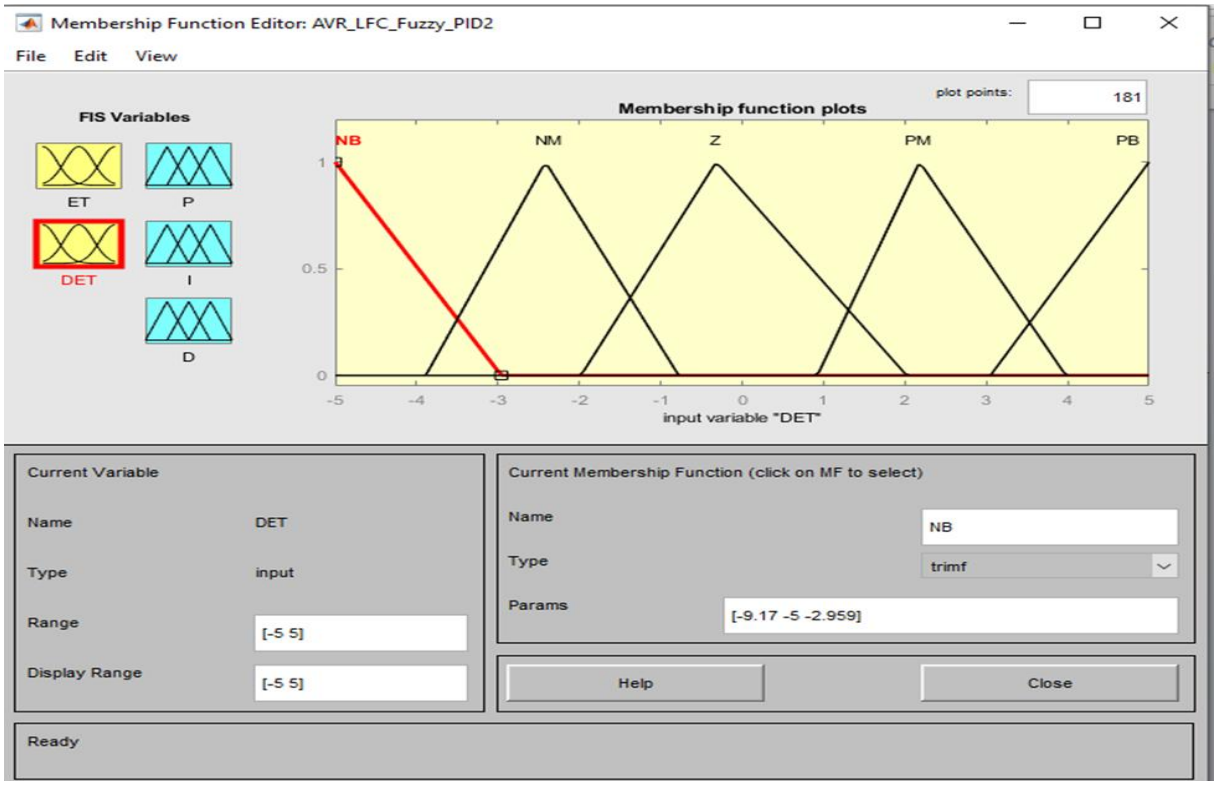

Fig. 4.9. The membership function for the variable "change of error (DET)" as an input.

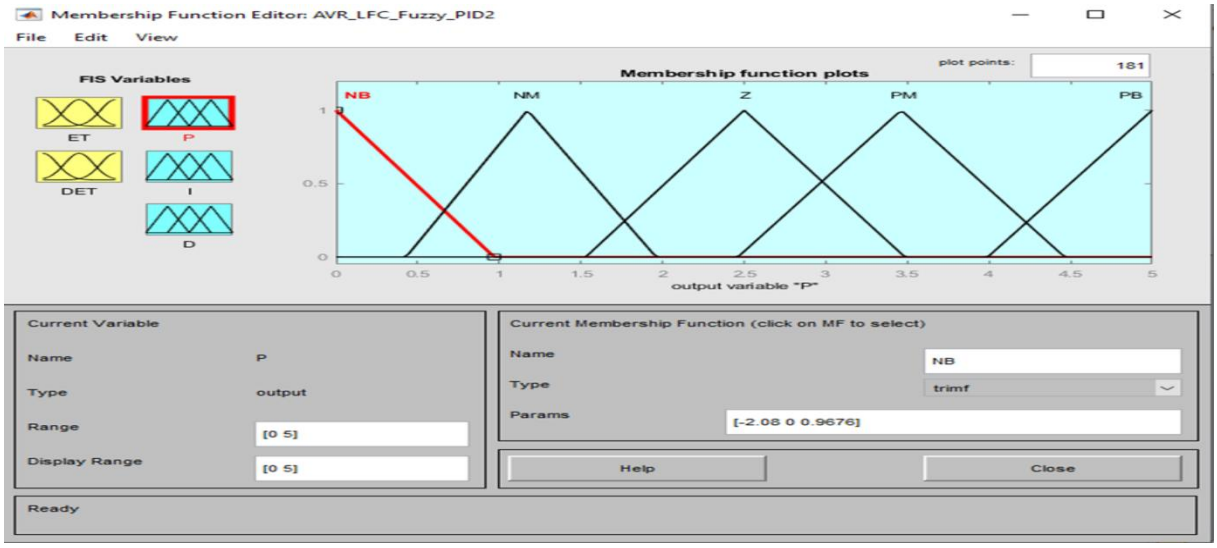

Fig. 4.10. Output variable membership function P

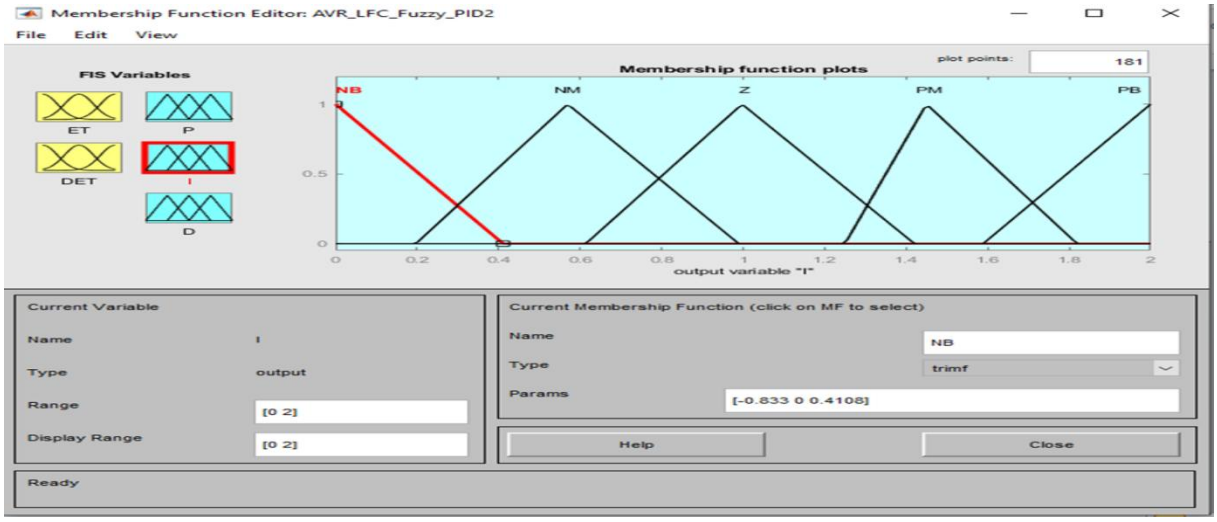

Fig. 4.11. Membership function for the variable that is output I

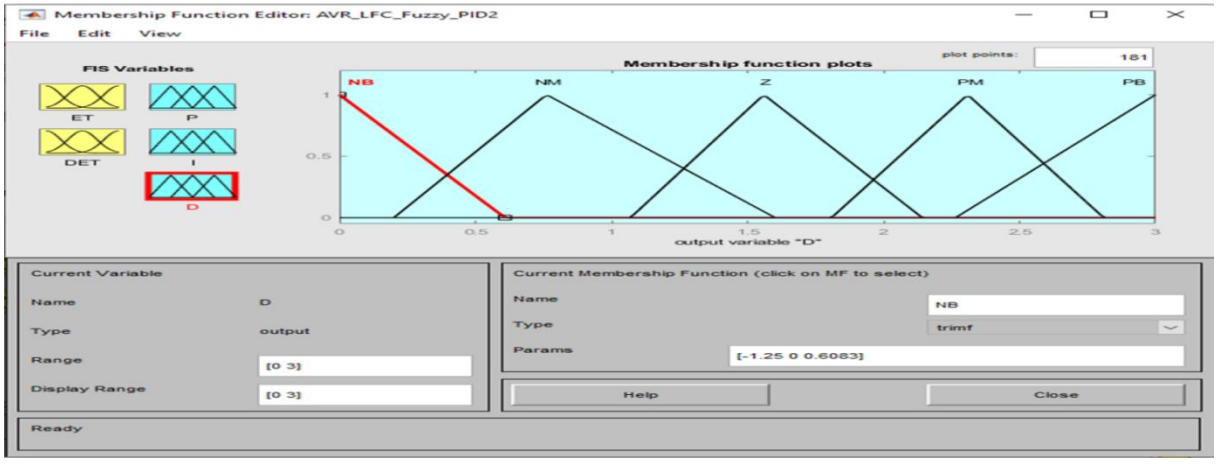

Fig. 4.12. D output variable membership function

A typical controller's design includes control laws that govern its operation. Fuzzy logic controllers use language principles to give the operator a more natural control option in a human setting.

$X = YM$ Summarizes combinatorial study. Total output variables are marked by M, while rules with the same number of linguistic values as input variables are denoted by X.
In this paper $Y = 5$, and$m = 2$, hence the number of rule for AVR $X = 25$ rule base can be written as if (ET is NB) and (DET is NB) then (P is NB) (I is NB) (D is NB), if (ET is NB) and (DET is NM) then (P is NB) (I is NB) (D is NB) …etc. as shown in Fig 4.13.

Table 4.1 Rule Base for AGC and AVR

P I D		Error Signal				ET
		NB	NM	Z	PM	PB
DET	NB	NB	NB	NM	NM	Z
	NM	NB	NM	NM	Z	PM
	Z	NM	NM	Z	PM	PM
	PM	NM	Z	PM	PM	PB
	PB	Z	PM	PM	PB	PB

These PID fuzzy calculation blocks in this study use Max-Min inferential law and defuzzification according to the centroid point method. The inference method will combine rule recommendations into a single set of criteria. There are two types of fuzzy inference systems in the fuzzy MATLAB toolbox: Mamdani-type and Sugeno-type. The most popular technique for determining rule output is Mamdani. Mamdani's method includes the Membership Function Editor, Rule Editor, Rule Viewer, and Surface Viewer (FIS). In addition to inputs and outputs, the Fuzzy inference system (FIS) handles high-level concerns. The defuzzification technique is also set at the Fuzzy inference system. The membership function editor is used to outline the shapes of all the membership functions related to every variable, as shown in Fig 4.8–4.12, which explain how to design each variable's membership function using the editor.

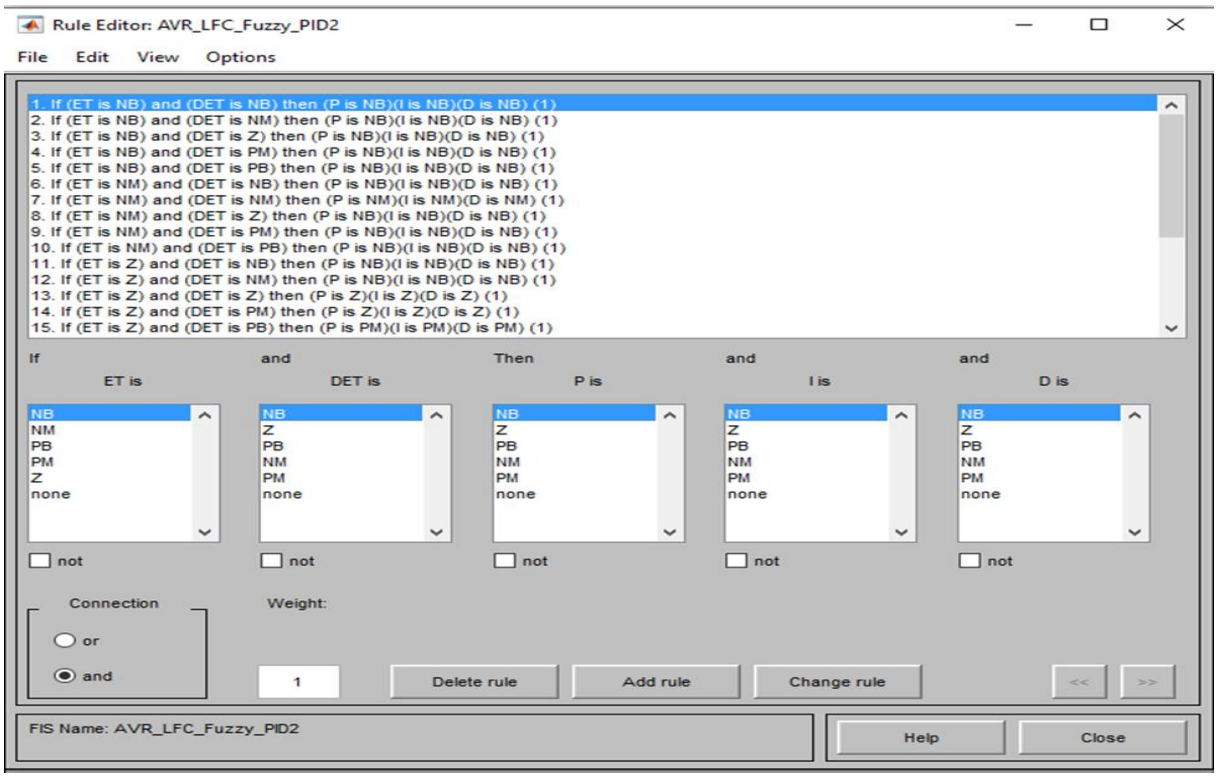

Fig. 4.13. The rule editor

The fuzzy inference system is searched, altered, and replaced using Rule Viewer and Surface Viewer. They are the tools that are the simplest to read. The rule viewer is a FI diagram built in MATLAB. As seen in Fig 4.14.

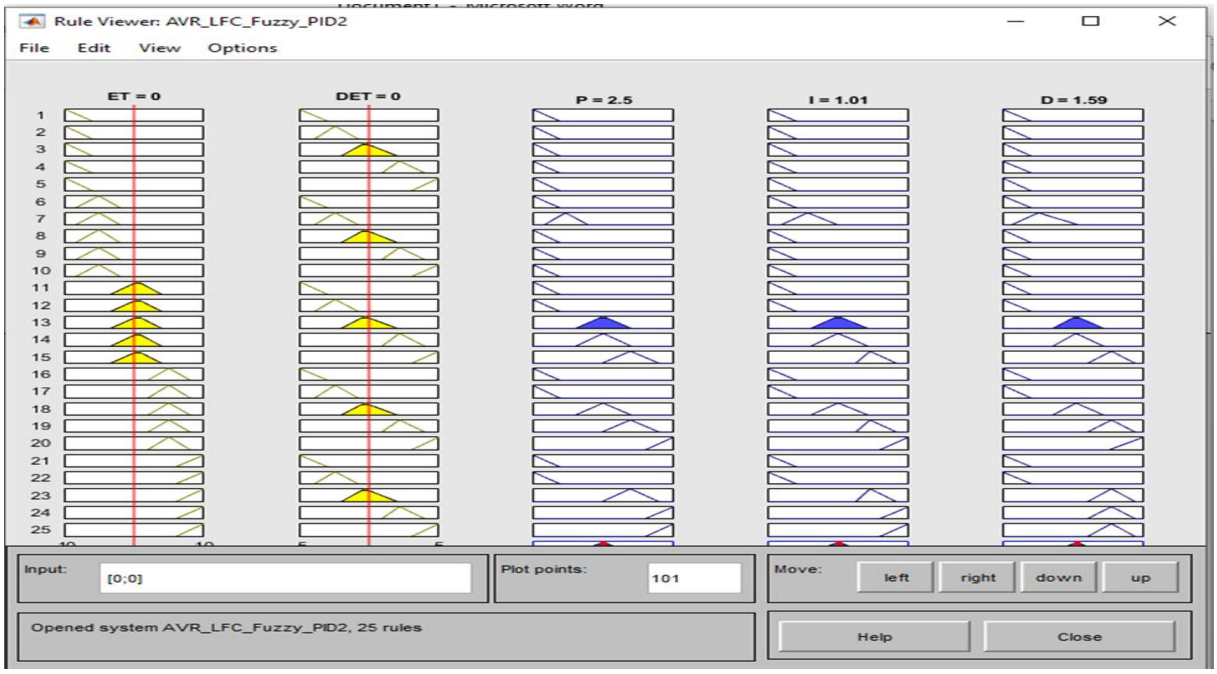

Fig. 4.14. Rule viewer

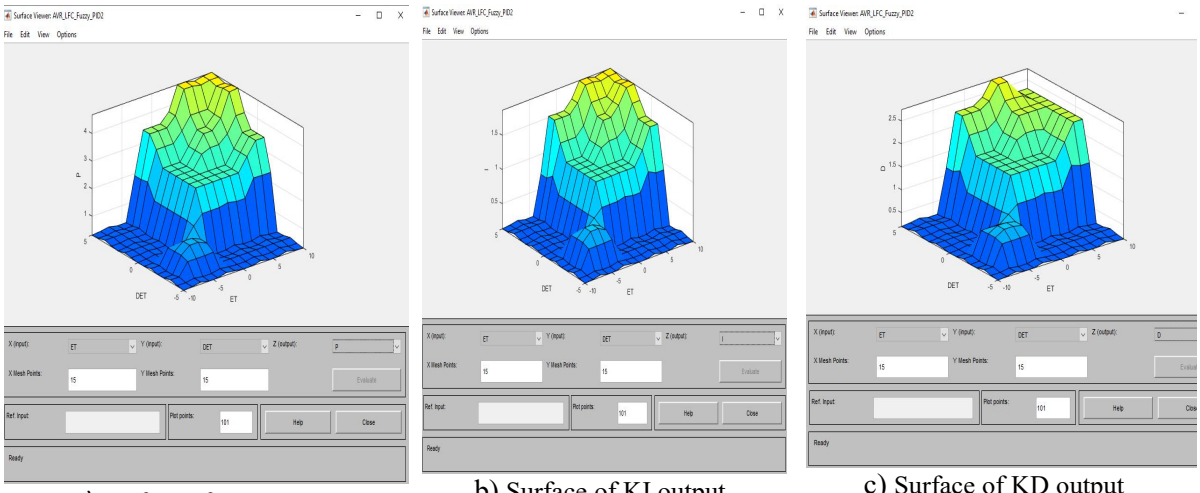

a) Surface of KP output b) Surface of KI output c) Surface of KD output

Fig. 4.15. Surface of fuzzy controller output

4.2.4. Fuzzy-Proportional-integral-derivatives (FPID) control design

Fuzzy-PID controllers are fuzzy logic-based with proportional-integral-derivative topologies. The fuzzy logic controller uses many-valued logic and reasoning instead of fixed and exact values that have the truth function varying from one point to another. This is particularly useful for controlling systems, especially when the exact model of the system is unavailable.

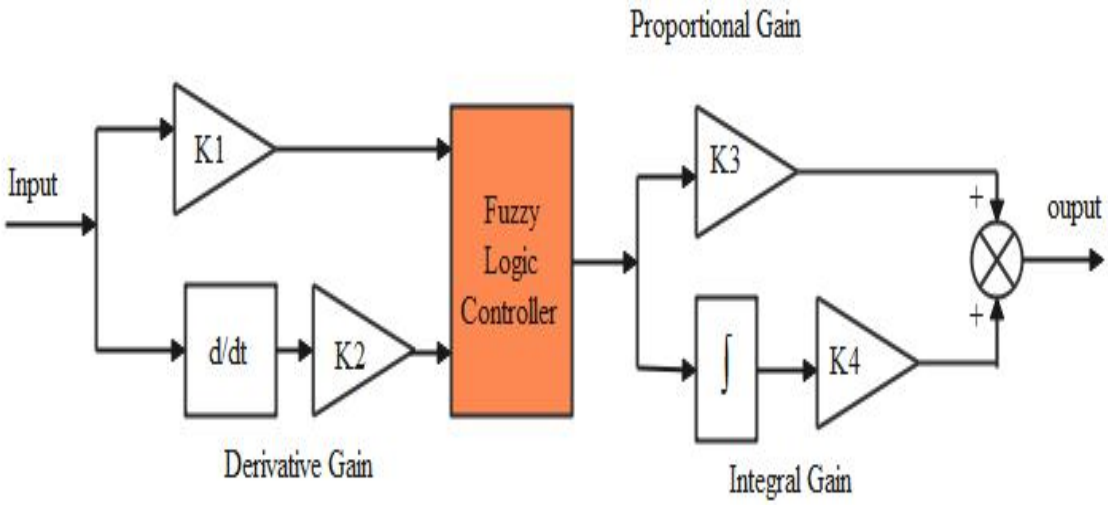

Fig. 4.16. A fuzzy PID controller diagram [49]

It uses a Mamdani-type fuzzy logic controller. It has two inputs labeled "error (ET)" and "change of error (DET)," three output variables (PID controller parameters), and three input variables labeled (K_P, K_I, K_D). Here's a list of input and output physical values for the variables.

- $ET = [-10 \text{ to } 10]$
- $DET = [-5 \text{ to } 5]$
- $K_P = [0 \text{ to } 5]$
- $K_I = [0 \text{ to } 2]$
- $K_D = [0 \text{ to } 3]$

System and input value define input ranges. Error input is the difference between estimated and set point power, and error change equals current minus prior power. Fig (4.17) shows how to transform a fuzzy logic controller into a PID controller. To regulate the system, generate, tweak, and implement a set of rules governing the input-output link's membership function. First, control the membership function.

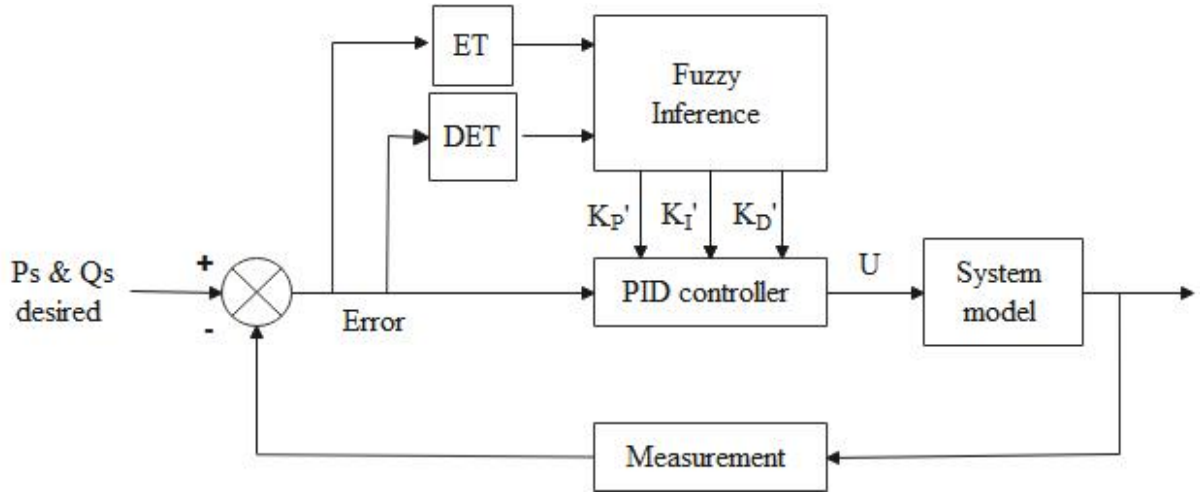

Fig. 4.17. The fuzzy PID controller structure and system model

The following is a description of the mathematical equation for the parameters of an online-tuned PID controller:

$$K_P = K_P' + K_P 0$$
$$K_I = K_I' + K_I 0 \quad (4.5)$$
$$K_D = K_D' + K_D 0$$

Where, $K_P^{'}$, $K_I^{'}$ and $K_D^{'}$ are the fuzzy logic results from Fig 4.16. K_P0 , K_I0 and K_D0 establish the PID controller's initial value. The PID parameters K_P, K_I and K_D will be modified to offer online and self-tuned values under fluctuating system conditions.

4.3. Particle swarm optimization algorithm (PSO)

Eberhart and Kennedy developed it as a population-based stochastic optimization method (1995). It's encouraged by replicating social behavior like fish schooling or birds flocking. When all the "particles" are joined, the outcome is a "set" or "swarm." The vectors X I and V I represent the particle's area and velocity. When solving a problem, it's crucial to consider the role of each particle. After then, the particles will traverse across the search zone, altering their speed and position to locate the perfect spot at every instant. These vectors reflect a particle's position and velocity in a d-dimensional space [50].

$$[X_i = x_i{}^1, x_i{}^2, \ldots x_i{}^d]$$
$$[V_i = v_i{}^1, v_i{}^2, \ldots v_i{}^d] \tag{4.6}$$

The best location of a particle is the position which provides the lowest objective value (J) to that particle.

Let $pbest_i = \left[pbest_i{}^1, pbest_i{}^2 \ldots pbest_i{}^d\right]$ be the best position yielding the high-quality fitness value for the i^{th} particle; and $gbest_i = \left[gbest_i{}^1, gbest_i{}^2 \ldots gbest_i{}^d\right]$ is the global best position in the whole swarm population. The PSO algorithm updates its velocity and population using the following equation [35][50].

$$V_i{}^{d(k+1)} = W(v_i{}^{d(k)}) + c_1(rand\ 1)\left(pbest_i{}^{d(k)} - X_i{}^{d(k)}\right) + c_2(rand2)(gbest_i{}^{d(k)} - X_i{}^{d(k)}) \tag{4.7}$$

Particle Swarm Optimization technique to choice an appropriate controller parameter set K (K_P, K_D, K_I) of the PID controller. Particle swarm optimization (PSO) is used in a PID controller to develop an AVR generator's step transient response. The PSO rules were created to change three optimal controller parameters so the managed system could produce a superb step response.

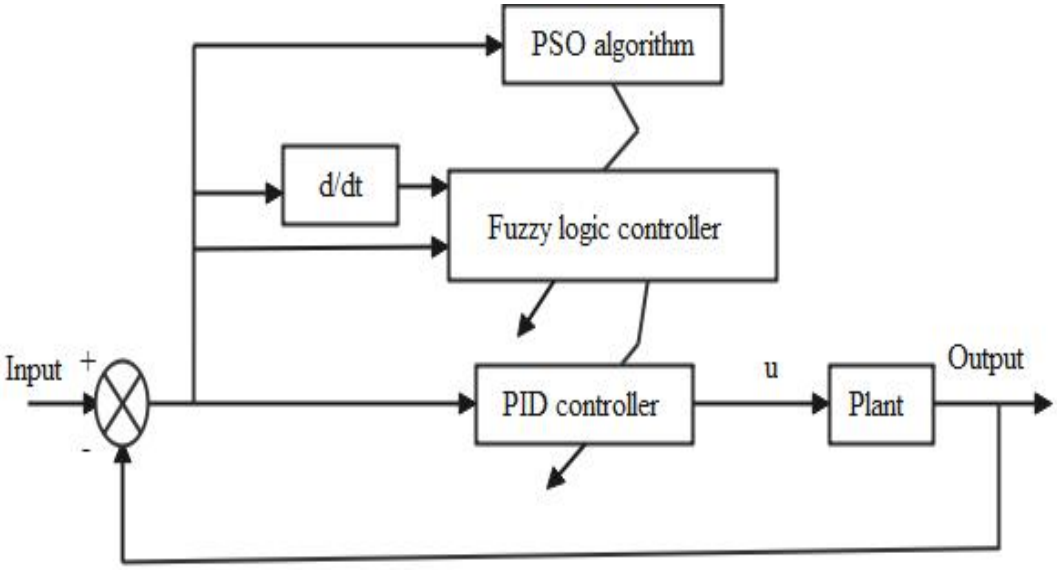

Fig. 4.18. Block Diagram of PSO-Fuzzy-PID

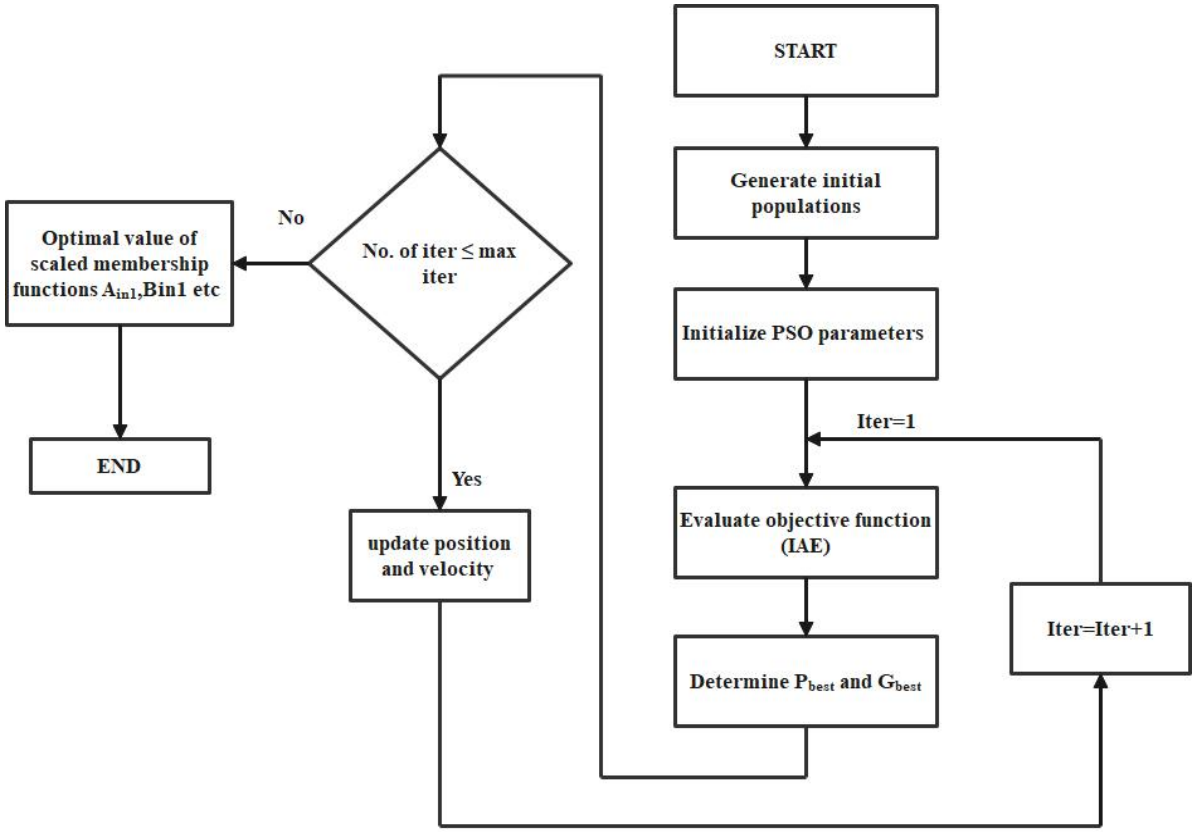

Fig. 4.19. Flowchart of PSO algorithm

One of the best and most efficient optimization methods is particle swarm optimization. First, initial values for velocity and position are assigned to each particle. Position and velocity updates are based on the fitness function's optimal value. Pbest and gbest are fitness values needed for particle updating (global best). The Pbest value is tracked throughout each particle iteration, and the gbest value is based on the best solutions. The PSO method updates particle position and velocity using the following equations.

$$V_{i,d}^{j+1} = \alpha v_{i,d}^{j} + C_1 r_1 \left(P_{best} - x_{i,d}\right) + C_2 r_2 \left(\mathrm{g}_{best} - x_{i,d}\right) \tag{4.8}$$

$$V_{i,d}^{j+1} = \alpha v_{i,d}^{j} + v_{i,d}^{j+1} \tag{4.9}$$

Where 1, j id v + - new updated velocity of i-particle in (j+1) iteration, j id v - i-velocity particle's in j-iteration; 1, j id x + - new updated position of i-particle in (j+1) iteration, j id x - i particle's last position in j-iteration; C_1 and C_2 Update velocity is the most critical characteristic affecting particle position. Important factors include acceleration and inertial weight. During updating, particle velocity and position must meet the parameters below.

$$V_{d\_min} \leq v_{i,d}^{j+1} \leq V_{d\_max}$$

$$X_{d\_min} \leq x_{i,d}^{j+1} \leq X_{d\_max}$$

The three scaling weights of the fuzzy-PID controller in this study, $\mathrm{K_P}$, $\mathrm{K_I}$ and $\mathrm{K_D}$ are determined using the PSO algorithm.

The Following Fitness function integral of Absolute Error (IAE) is used

$$J(\theta) = \int |e(t)|\, dt$$

The following is the search limit for the FPID controller's scaling weight:

$$\begin{cases} 0 \leq \mathrm{K_P}^* \leq 2 \\ 0 \leq \mathrm{K_I}^* \leq 2 \\ 0 \leq \mathrm{K_D}^* \leq 2 \end{cases}$$

The following equation shows how Particle Swarm Optimization modifies Fuzzy-PID controller parameters to minimize J min.

The PSO algorithm must be built in phases to change a fuzzy PID controller.

- **Step 1.** Size of particles $N = 10$, search space $D = 3$, K_a, K_b, K_c maximum iteration $M = 100M$, inertial weight $\alpha = 0.5$, and acceleration factors $C1 = 1,\ C2 = 1$ are recommended.
- **Step 2**. After initializing velocity and position, compute the initial fitness P_{best} vector for each particle.
- **Step 3.** Following the formulas, reduce g_{best} from P_{best} as much as possible.
- **Step 4.** Step 3: Update the velocity and position vectors of the particles using the formulas.
- **Step 5.** Compute P_{best} and P_{best} for the new update position. Replace the old fitness values with the new ones if they've risen (less than the previous fitness values).
- **Step 6.** Repeat steps 3, 4, and 5 until final iteration or desired fitness function value.

4.4. Design of PSO- based fuzzy- PID

The fuzzy-PID controller is synthesized based on the structure of the PID with K_P, T_I and T_D, parameters, determined according to the fuzzy logic calculated blocks $P, I,$ and D corresponding to defuzzied output values K_{Pf} or T_{If} or T_{Df} and then multiplied with the corresponding scaling weights,, i.e. K_a, K_b, K_c, following the formula as below:

$$K_P = K_{Pf}K_a;\ T_I = T_{If}K_b;\ \ T_D = T_{Df}K_c \tag{4.10}$$

The Particle swarm optimization algorithm is used to optimize 3 scaling weights, i.e. $K_a \rightarrow K_a^*,\ K_b \rightarrow K_b^*,\ K_c \rightarrow K_c^*$.

For this proposed PSO-based fuzzy-PID controller, the parameters of the fuzzy-PID are continuously adjusted in a specified range. However, the scaling weights' fuzzy-PID is optimized by PSO algorithm. So that after applying the PSO algorithms, the parameters' Fuzzy-PID is optimized as follows:

$$K_P^* = K_{Pf}K_a^*;\ T_I^* = T_{If}K_b^*; K_D^* = T_{Df}K_c^* \tag{4.11}$$

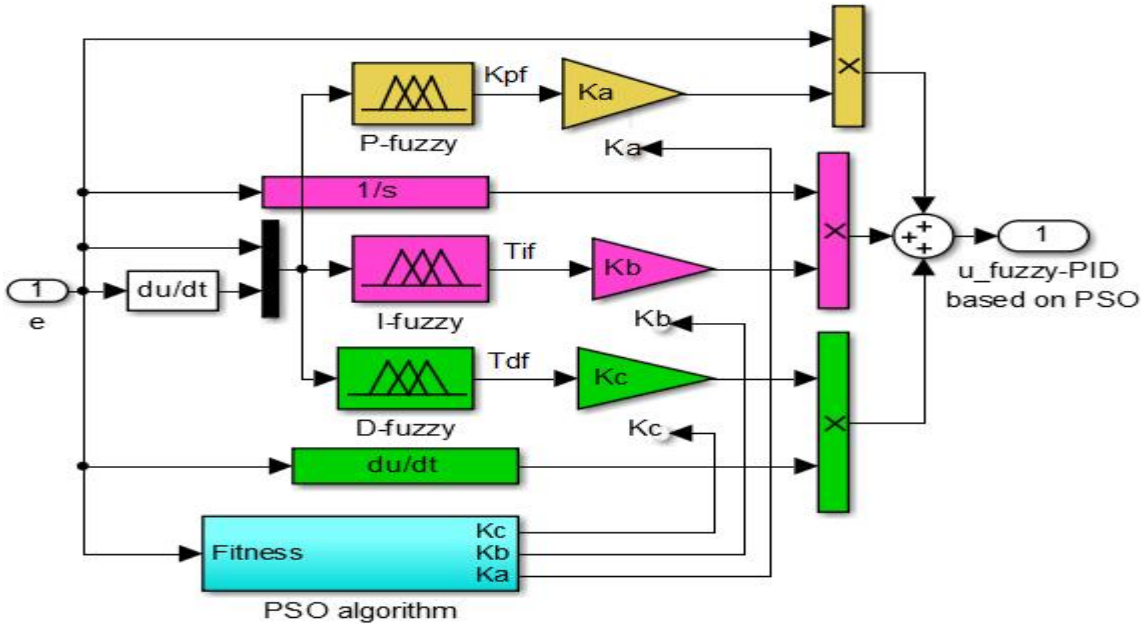

Fig. 4.20. Structure diagram of a PSO-based Fuzzy-PID [51]

Fig. 4.20 shows the structure diagram describing the incorporate between the fuzzy-PID controller and PSO algorithms.

The P, I, D - fuzzy logic calculated blocks, corresponding to K_{Pf} , T_{If} , T_{Df} are presented in Fig.4.20.

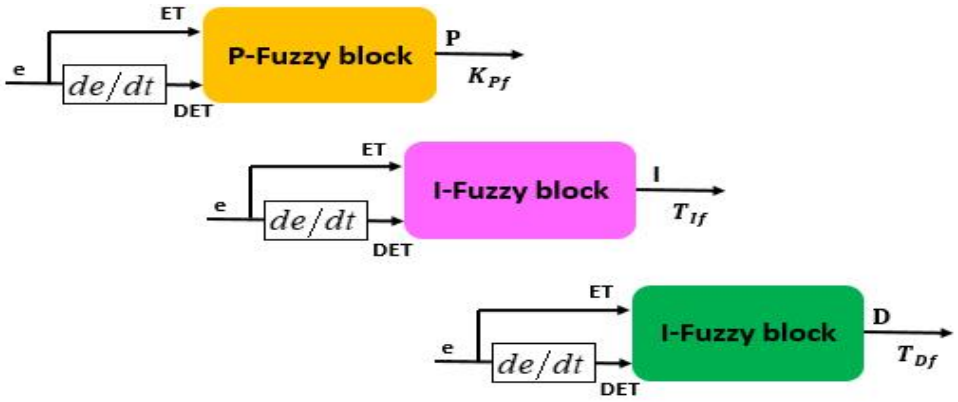

Fig. 4. 21. Structure diagram of the fuzzy calculated blocks [51]

Two input fuzzy variables of each P-fuzzy, I-fuzzy, D-fuzzy are ET and DET, corresponding to e and $\frac{de}{dt}$. The output fuzzy variables of the P-fuzzy, I-fuzzy, D-fuzzy blocks are P, I, D, corresponding to parameters K_{Pf} , T_{If} , T_{Df}. The physical value range of the input variables and the output variables are as follows: $\mathrm{ET} = [-10\ \ 10]$, $\mathrm{DET} = [-5\ \ 5]$, $\mathrm{P} = [0\ 5]$, $\mathrm{I} = [0\ 2]$, $\mathrm{D} = [0\ 3]$

CHAPTER FIVE

SIMULATION RESULT AND DISCUSSION

When simulating the control of a synchronous generator system, numerous situations were employed to compare and monitor the output results:

1. With PID controller
2. With PSO-Fuzzy PID controller
3. Comparison of the output simulation Results

5.1. Automatic voltage controller (AVR) excitation system

The table below shows the specs for a synchronous generator with AVR (from Hadi Sadat's power system study)[2]

Table 5.1 Required variable for the AVR simulation [2].

Parameters	K_A	K_E	K_G	K_R	τ_A	τ_E	τ_G	τ_R
Value	10	1.0	1.0	1.0	0.1	0.4	1.0	0.05

1. AVR loop without a controller

The simulation of SG using AVR without a control loop is represented in Fig. 5.1.

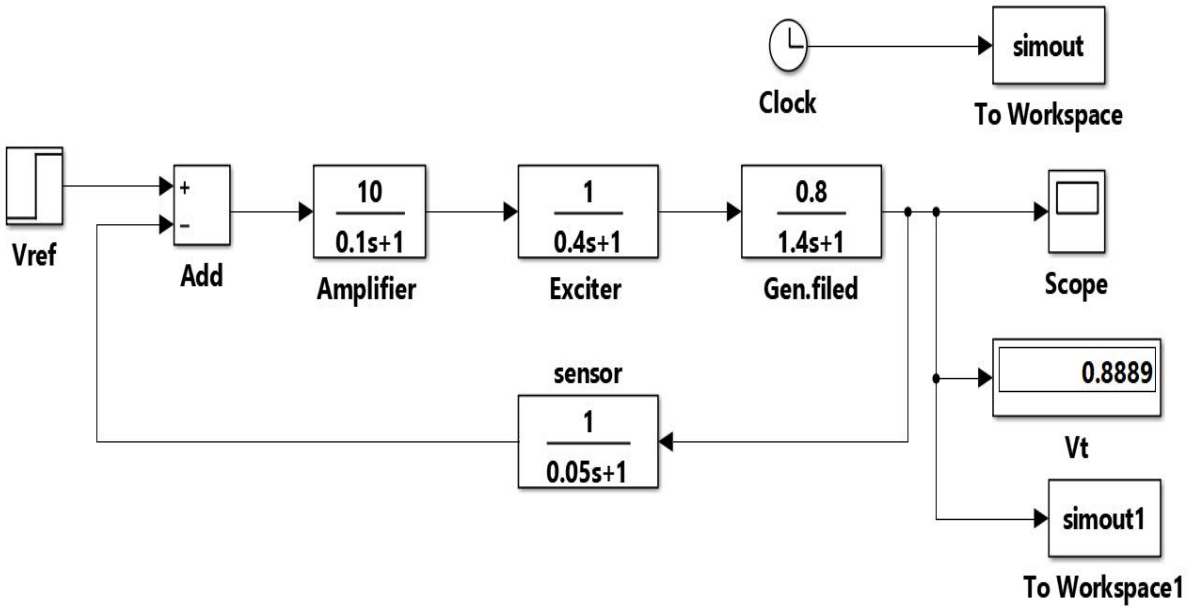

Fig. 5.1. Simulink diagram for AVR loop

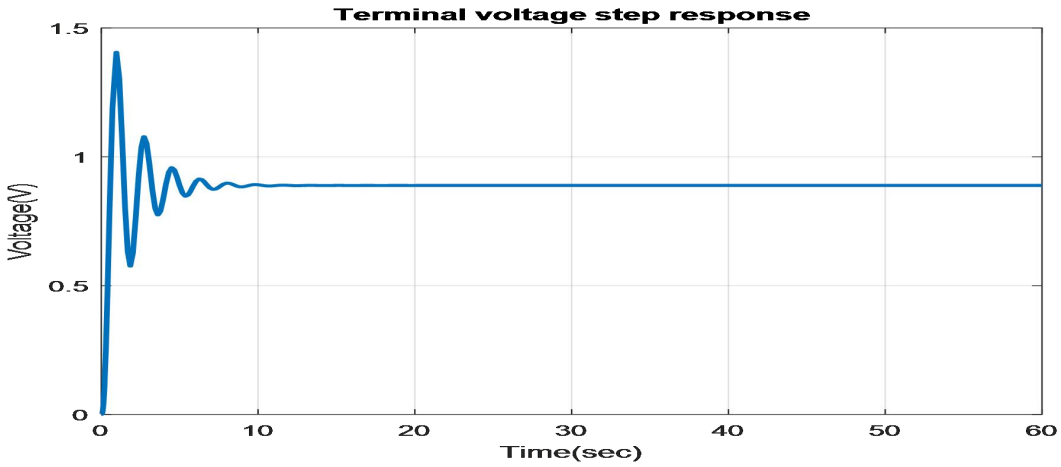

Fig. 5.2. AVR Loop Response to Step Voltage in the Absence of a Controller

Table 5.2 Results of the AVR's terminal voltage response without a controller

Results	Settling time	Overshoot (Voltage)	Steady state (Voltage)	Steady state error
Value	6	0.58	0.8889	0.1111

Terminal voltage response shows a substantial overshoot, delayed settling time, oscillatory response, and steady state error more than 0.09.

5.2. Load Frequency Controller (LFC)

Any control system must have a stable control loop that responds to transient frequency faults and has no steady-state frequency error. When system demand increases, the governor must reduce turbine speed before regulating steam supply. The nominal LFC system parameters studied for this work are similar to those in most research articles[3], [22], [25].

5.2.1. Load Frequency Control without control loop

The Table below lists the parameters for the synchronous generator with load frequency controller (LFC). (Adapted from Hadi Sadat's Power System Analysis)[2].

Table 5.3 The variables needed for the simulation of (LFC)

Parameters	τ_g	τ_T	H	D	R	ΔP_L
Value	0.2	0.5	5	0.8	0.05	0.2

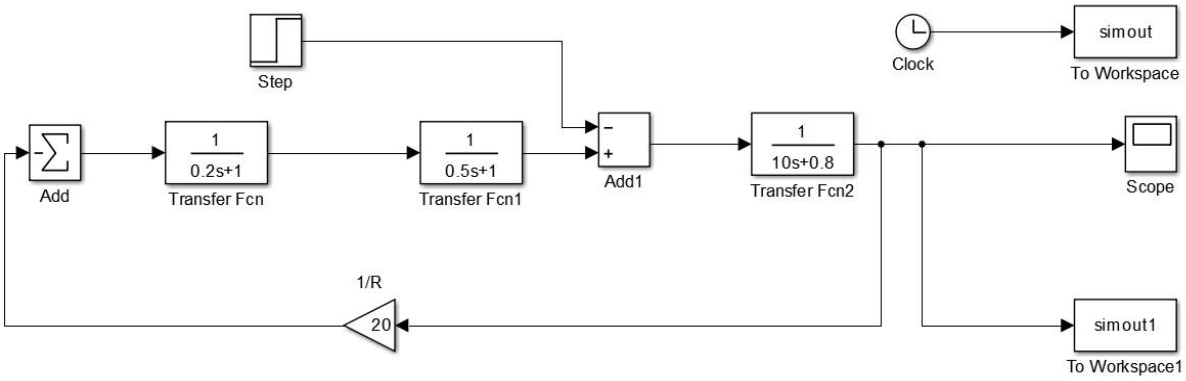

Fig. 5.3. Simulation block diagram of load frequency control without a control loop

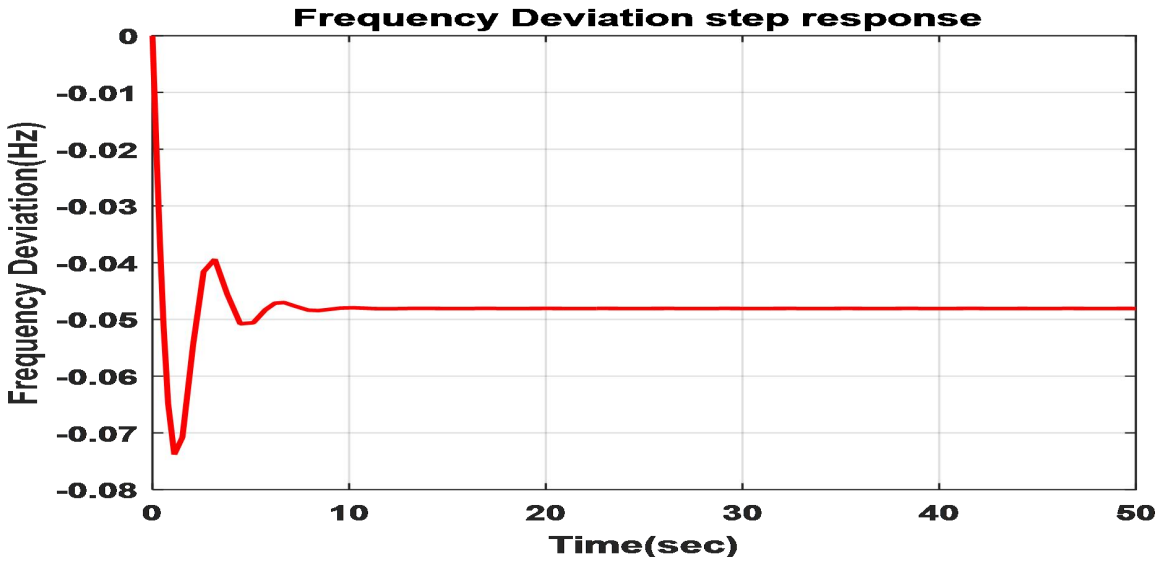

Fig. 5.4. LFC's response to frequency deviations without a control loop

Table 5.4 The results of LFC and PID frequency deviation response

Results	Settling time (sec)	undershoot (Hz)
Value	10(sec)	0.075(sec)

The frequency deviation response in Fig. 5.4 illustrates the system's substantial overshoot and lengthy settling period.

5.3. AGC including LFC and Voltage control model

In the AGC topic, it was discovered that the synchronizing power coefficient is the product of a slight change in the real power P_S as well as the shift in the power angle $\Delta\delta$. The linearized equation below shows the effect of voltage on real power.

$$\Delta P_e = P_s * \Delta\delta + K_2 E$$

K2 represents the variation in electric output for a modest stator emf adjustment. The slight effect of rotor angle on generating terminal voltage can now be added as shown in the following formula.

$$\Delta V_t = K_5 * \Delta\delta + K_6 E$$

K5 is the terminal voltage change caused by a moderate rotor angle movement under constant stator emf.

K6 Terminal voltage variation when rotor angle remains the same despite a stator emf shift. To account for rotor angle, the generator field transfer function must be adjusted to explain the stator emf:

$$E = \frac{K_G}{1 + T_G} * (V_f - K_4 * \Delta\delta)$$

The network settings and the operational environment have an impact on the aforementioned constant. The aforementioned equations in the AGC system and the AVR system are used to create a linearized model for the combined LFC and AVR.

1. **LFC loop with integrator**

Combining the LFC and AVR feedback loops and taking into account the combining effect results in the following simulation diagram. Integrators speed up procedures (rest action). Adding the integrator (delay) to Fig. 5.5's blocks creates the LFC simulation diagram.

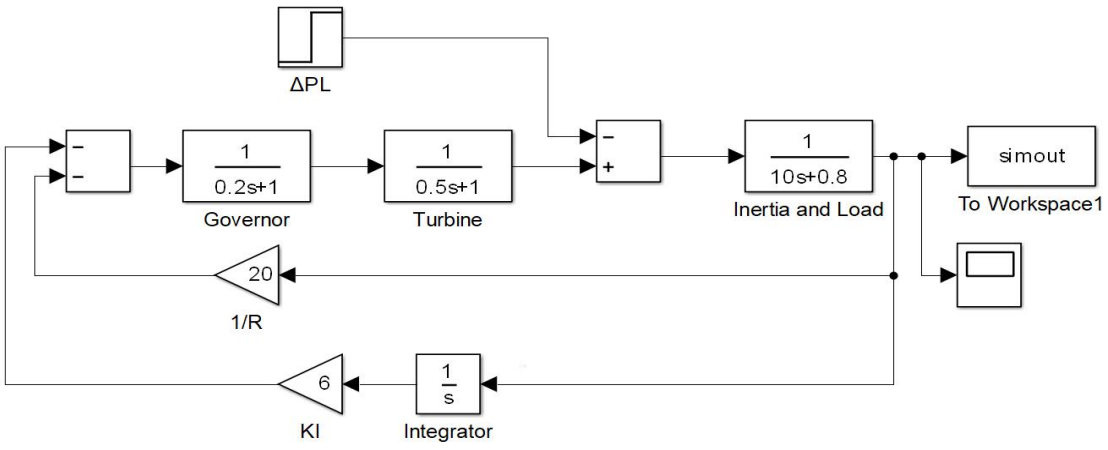

Fig. 5.5. LFC loop Simulink diagram with integrator (reset) action

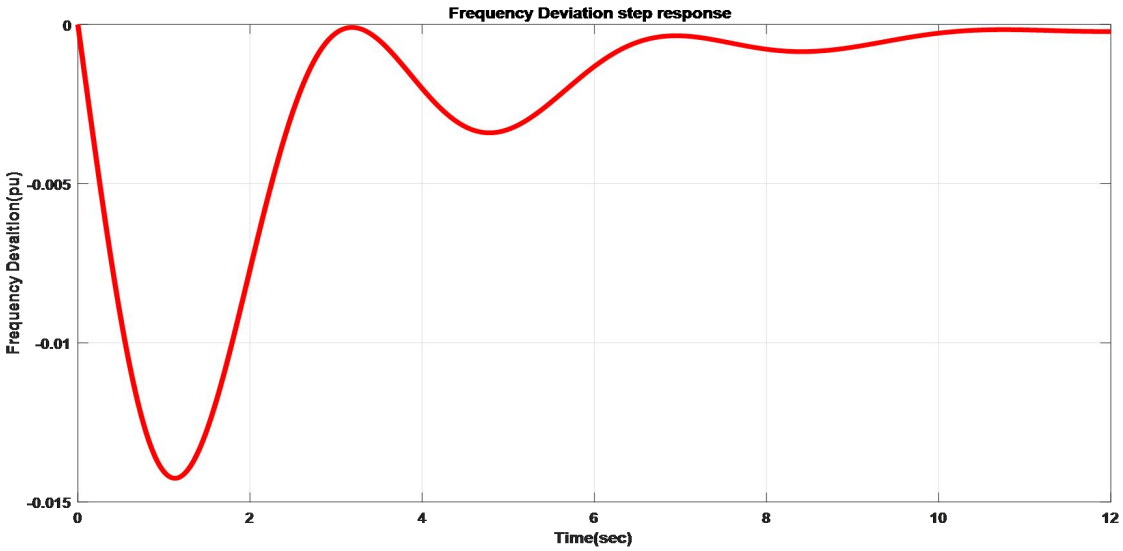

Fig. 5.6. Step response to frequency variation of the LFC using an integrator

The steady state frequency deviation is based on a zero step-response, and after 10 seconds, the frequency returns to normal.

Table 5.5 Results comparison for the LFC loop

Case	KI	Overshoot (Hz)	Undershoot (Hz)	Settling time
1	2	0.022	0	33
2	4	0.09	0	16
3	6	0.0153	0	10
4	8	0.09	2.3	9
5	10	0.04	1.3	11
6	12	0.054	2.3	14

According to Table 5.5, the LFC loop performs best when KI = 6. According to this, scenario three (3) provides the best balance of overshoot, undershoot, and settling time. Below, both occurrences of Case 3 of the LFC loop were simulated with PID and PSO-Fuzzy-PID.

2. Automatic generation control with excitation system without control loop

Automated voltage regulation and load frequency control don't work well together. As seen in Fig. 5.7, a simulation of AGC with an excitation mechanism without control loops.

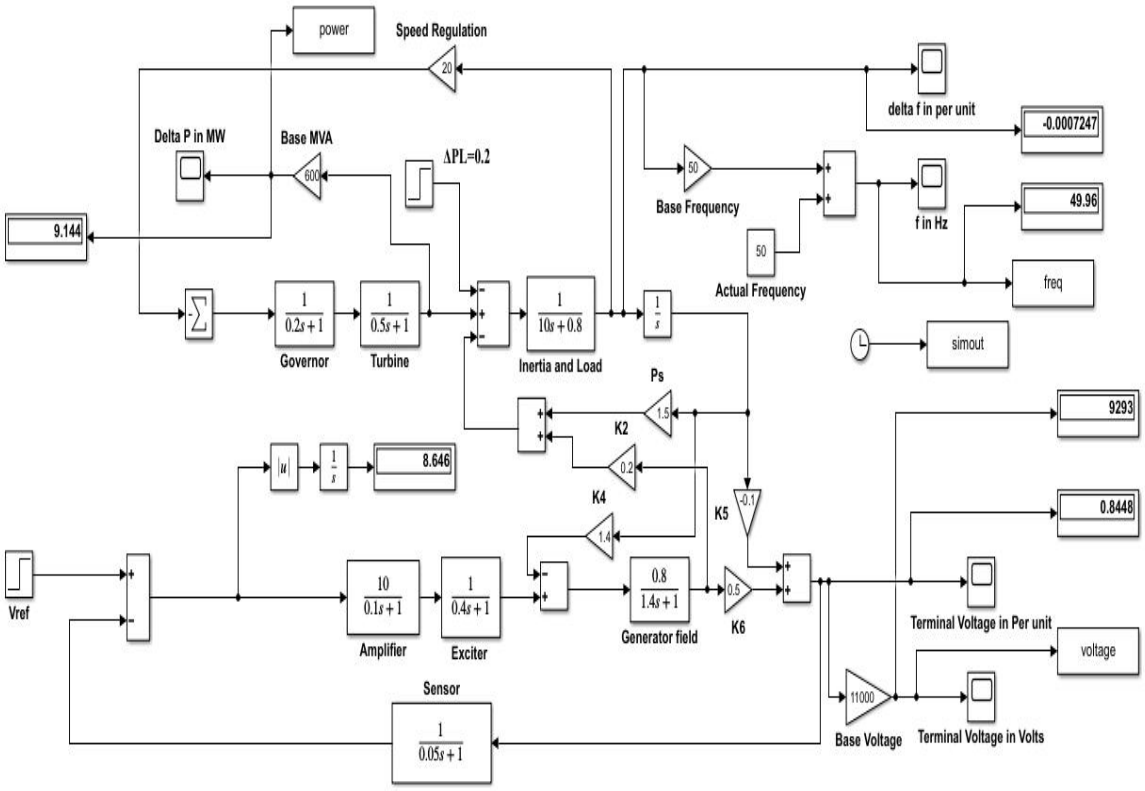

Fig. 5.7. AGC simulation block diagram without a controller

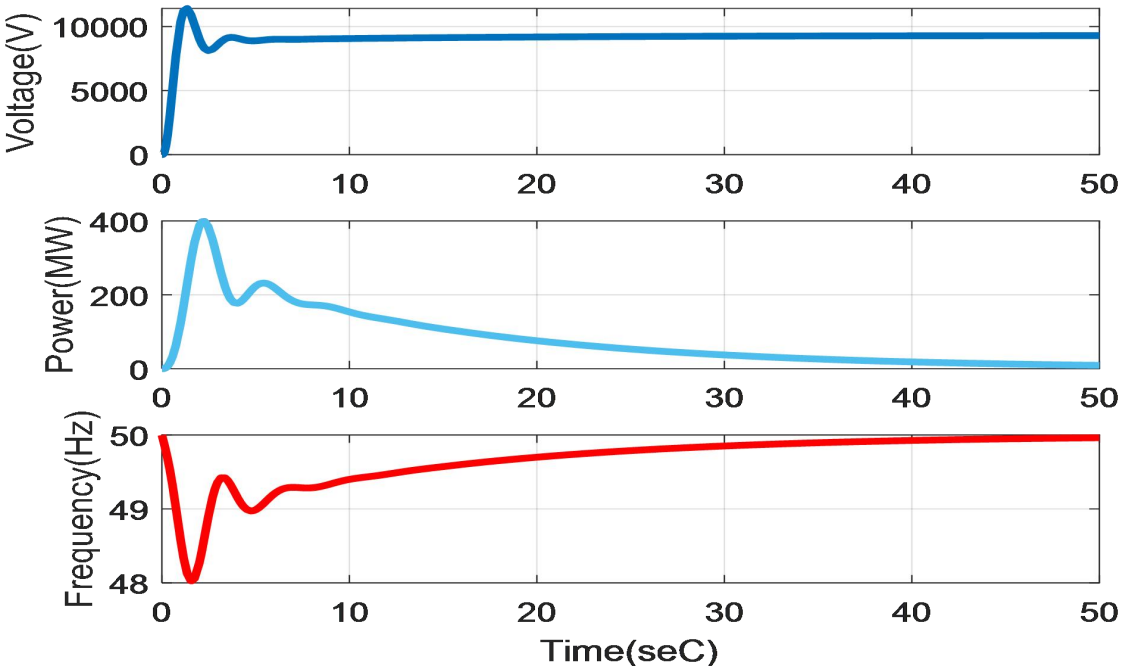

Fig. 5.8. Step response of the AGC without a controller

Table 5.6 Results of AGC with excitation system but no controller for terminal voltage and frequency deviation.

Results	Settling time	Percentage overshoot	Steady-state response	Steady state error
$\Delta\omega$	39(sec)	0.0725(Hz)	-	-
V_t	41(sec)	0.22(V)	0.8448	0.1552

The system is unstable with steady state error more than 0.091 for K_A=10.

3. Simulation of AVR and LFC with PID controller

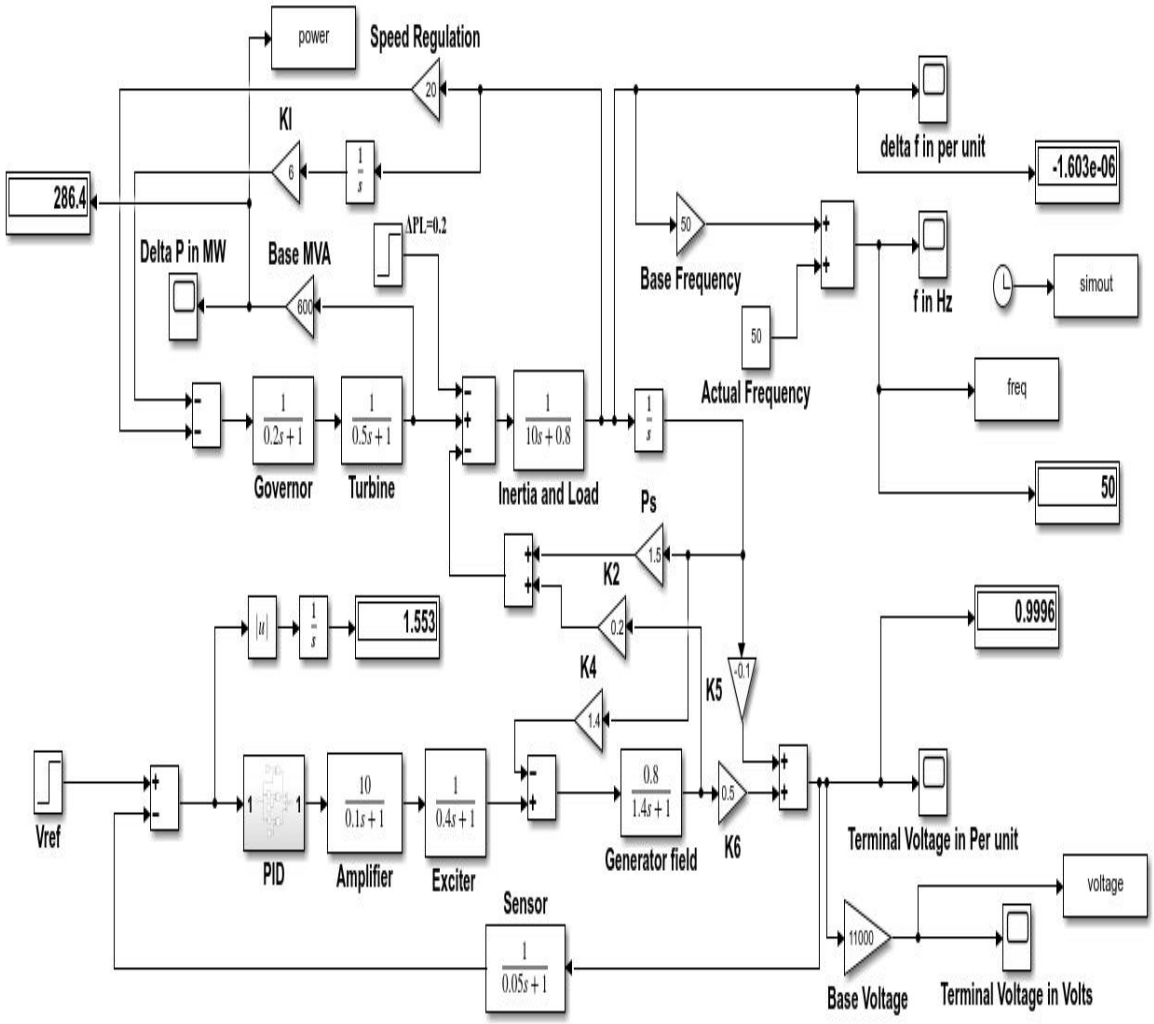

Fig. 5.9. AVR and LFC simulation block schematic with PID controller

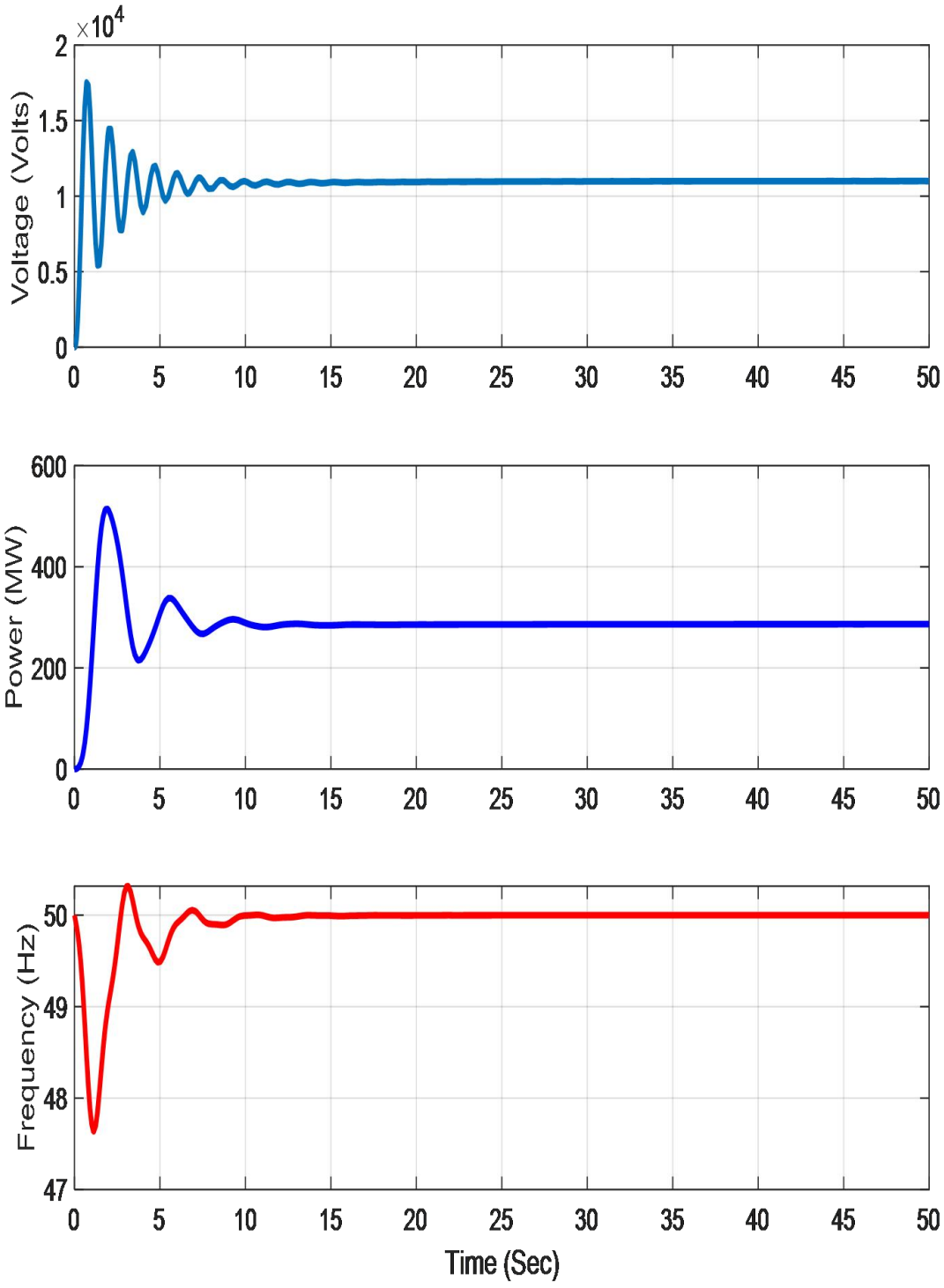

Fig. 5.10. PID controller response

4. Simulation of AVR and LFC with PSO fuzzy PID controller

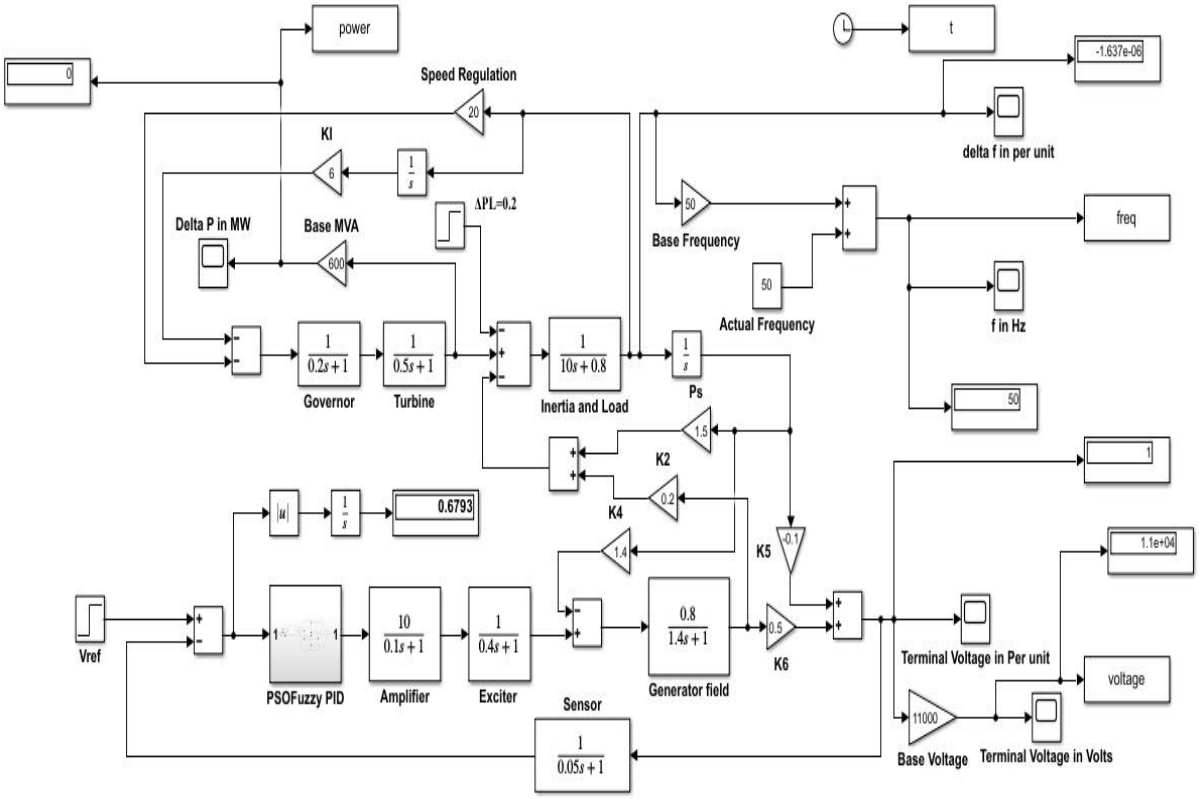

Fig. 5.11. AVR and LFC simulation block diagram with a PSO-fuzzy-PID controller

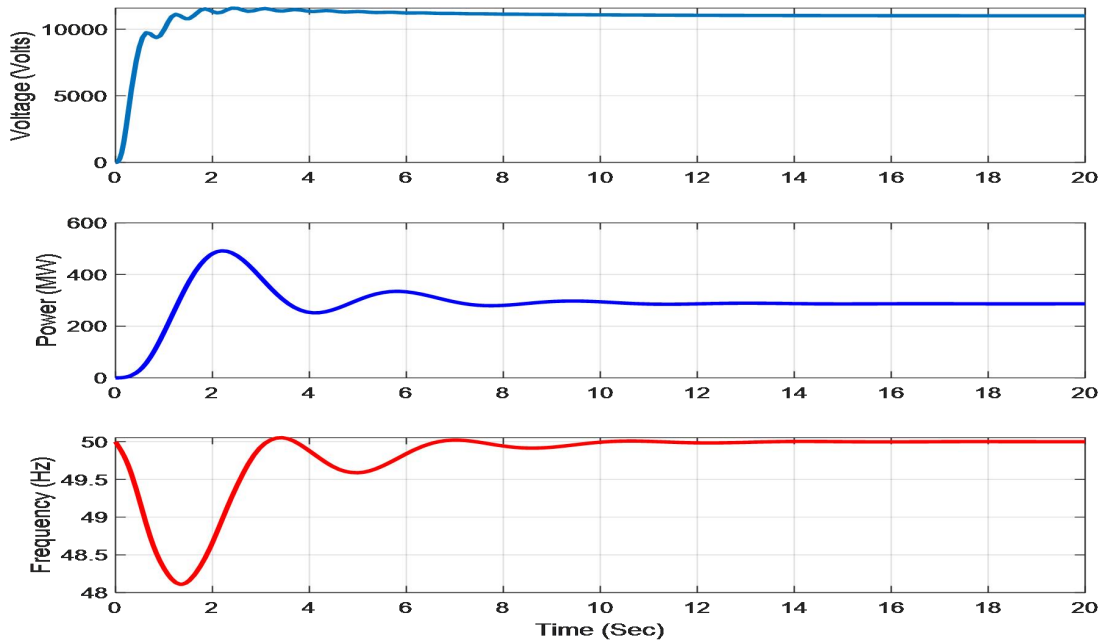

Fig. 5.12. PSO Fuzzy PID Response

5 Performance evaluation of PID controller and PSO-Fuzzy-PID controller responses

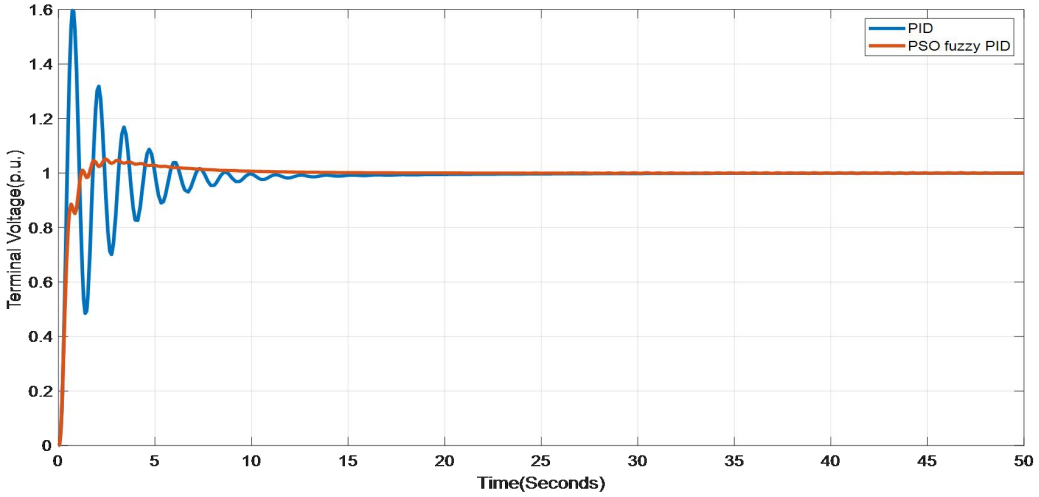

Fig. 5.13. Terminal Voltage Response per Unit Comparison

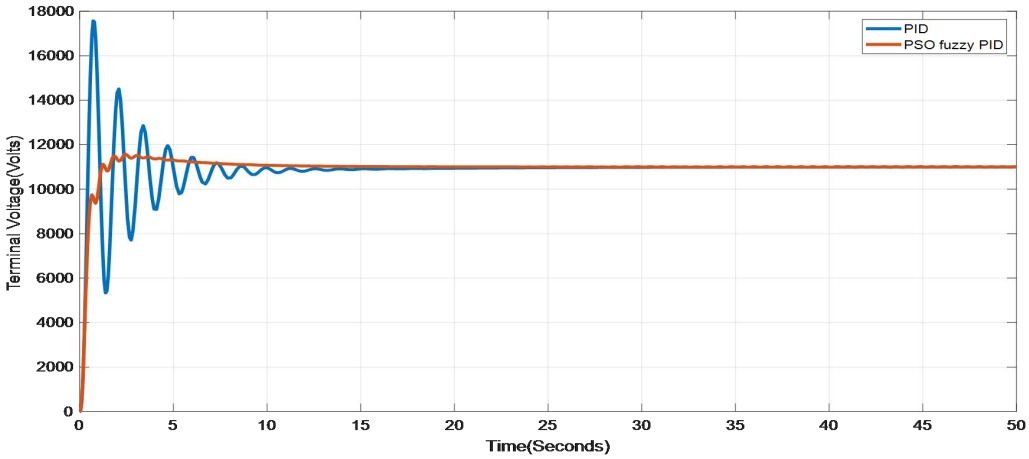

Fig. 5.14. Volts of terminal voltage response comparison

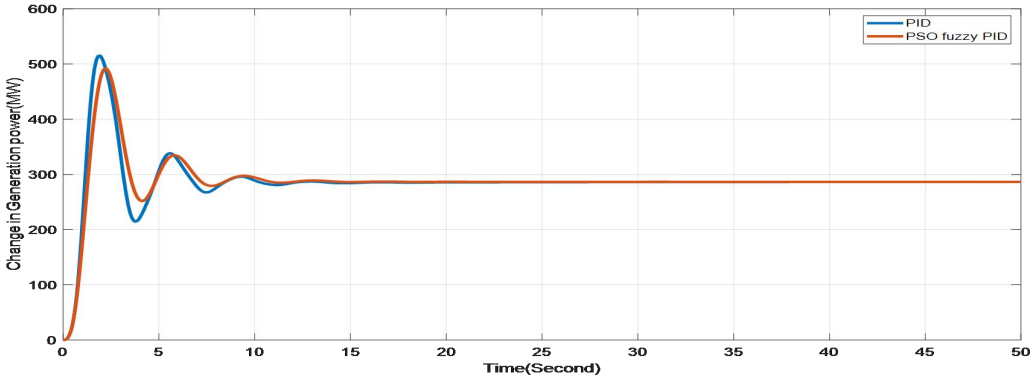

Fig. 5.15. Comparison of generation power response to change in MW

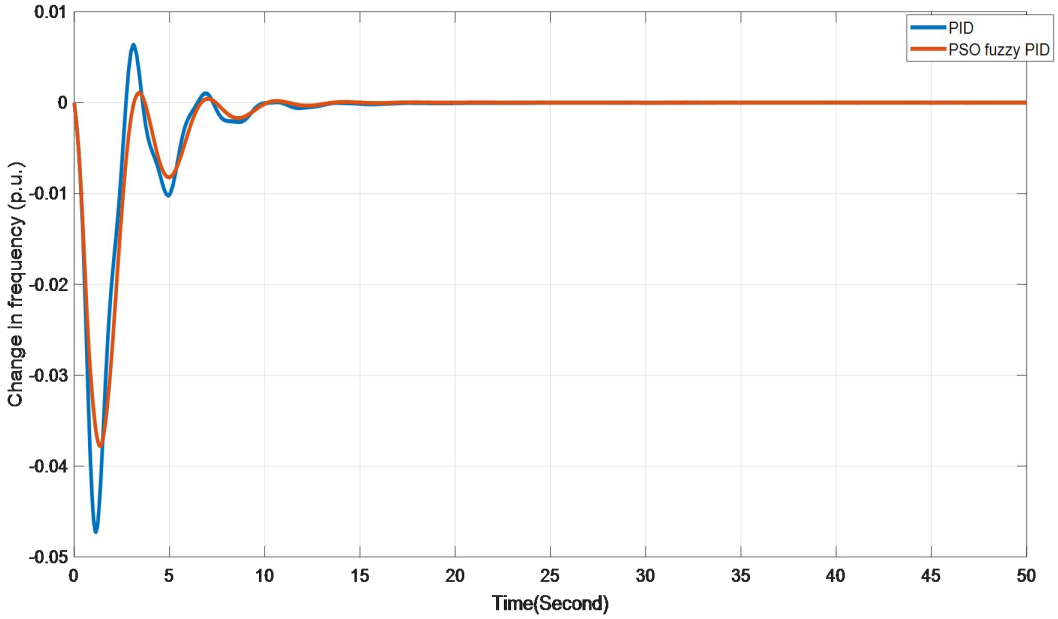

Fig. 5.16. The frequency response change in each unit is compared.

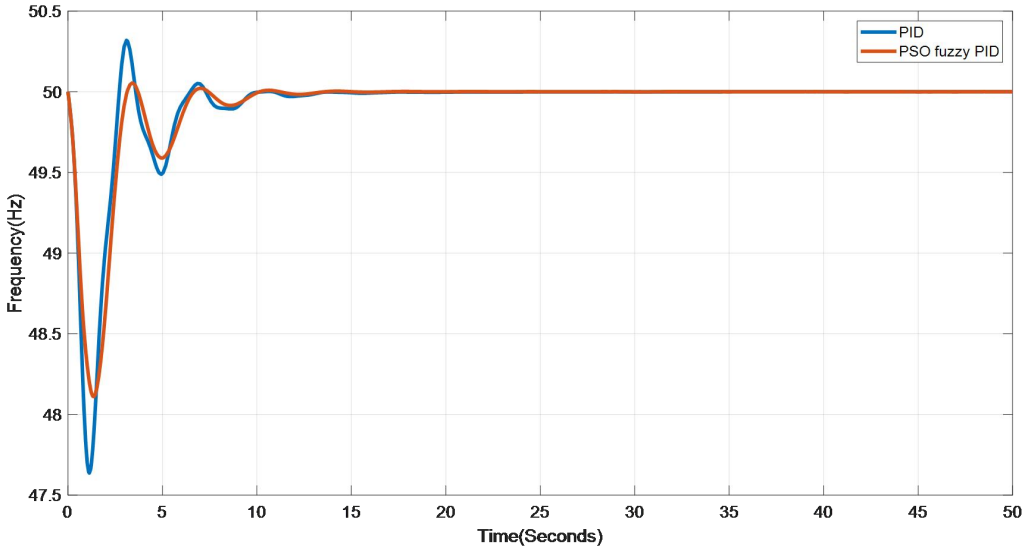

Fig. 5.17. A comparison of the difference in Hz caused by the frequency response

Table 5.7 Terminal voltage Time response result

Controllers	Settling time in second	Percentage overshoot (V)	steady state response	steady state error
PID	10(second)	0.59(V)	0.9996	0.0004
PSO-Fuzzy PID	6(second)	0.05(V)	1	0

Table 5.8 Power Time response result

Controllers	Settling time in sec	Percentage overshoot	Steady state(p.u)	steady state error (p.u)
PID	10(seconds)	0.79	0.2684	0.0761
PSO-Fuzzy PID	10(seconds)	0.71	1	0

Table 5.9 Frequency Time response result

Controllers	Settling time in sec	Overshoot in Percentage (Hz)
PID	9(seconds)	0.6342
PSO-Fuzzy PID	9(seconds)	0.1067

Table 5.10 Performance Comparison of PID and PSO-Fuzzy PID

Controllers	KP	KI	KD	IAE
PID	3.6	0.4	0.2	1.553
PSO-Fuzzy PID	1.63	1	1.27	0.6793

According to the Table 5.10, PID is more expensive than PSO-based Fuzzy PID IAE Values. As a result, Fuzzy PID based on PSO performs better than PID controller.

5.4. Discussion

This thesis introduced a novel control strategy that combines the advantages of classic PID control and fuzzy logic control by using the PSO algorithm to fine-tune the scaling weights coefficients of the fuzzy-PID controller. The fuzzy-PID controller is created using standard fuzzy rules and paired with PID control, but the PSO method is used to fine-tune the fuzzy-three PID's scaling weights. And then the simulation model of the combined load frequency and voltage control of synchronous generator system without/with disturbance using the proposed controller was built on MATLAB. The two proposed controllers, the fuzzy-PID controller and the PSO-based fuzzy-PID controller, have been shown to be effective in the simulation results for the combined load frequency and voltage control of synchronous generator systems. The simulation outcomes demonstrated that the suggested fuzzy-PID

algorithm, based on PSO, offered superior control quality compared to the conventional PID algorithm. The proposed fuzzy-PID controller based on PSO is also thought to be an effective control approach for a class of complex nonlinear uncertain control objects. The results from PID-and PSO-based fuzzy PID controllers are described in more detail below. It is necessary for the PI controller in the load frequency control loop to quickly return the frequency deviation caused by the applied step load or disturbance to zero. According to Fig. 5.13, the AVR's PID settling time is 10 seconds. Additionally, based on Fig.5.13, the AVR with a PSO-Fuzzy- PID controller's settling time is six-second. PSOFPID improved the AVR model's dynamic responsiveness. Table 5.7 compares terminal voltage response per volt and p.u. (Fig. 5.13-5.14). PSO-Fuzzy-PID controller model settled faster and overshot less after a load shift (perturbation or disturbance).

Table 5.10 shows that the PSO-based fuzzy PID controller's IAE is much lower than the conventional PID controller's 1.533. The PID-controlled LFC finds equilibrium in 9 seconds and overshoots by 0.6342. It overshoots by 0.6342. Table 5.9 shows that the PSOFPID LFC has a 9-second settling time and 0.1067 overshoot. Compared to PID, PSOFPID improves the dynamic responsiveness of the LFC model. Table 5.9 and Fig 5.16 and 5.17 show the frequency response per unit and in Hz. Table 5.9 lists improvements. PSOFPID controllers produce less overshoot than typical PID controllers. KI represents the LFC integrator gain, which is six. In load frequency control, the PI controller's settling time and overshoot are commonly desirable, as too quick of controller action might easily accelerate the synchronous generator's deterioration. Table 5.7–5.10 and Fig 5.13–5.17 in Automatic Generation Control, a controller model's quick settling time and small/negligible overshoot are highly required.

CHAPTER SIX

CONCLUSION, RECOMMENDATION AND FUTURE SCOPE

6.1. CONCLUSION

Voltage and frequency are both affected by variations in load in the power system. AVR controls voltage and reactive power, while LFC controls frequency and real power.

This study explores MATLAB/SIMULINK's AGC using PID and PSOFPID. This inquiry seeks synchronous machine input/output data. PSO based fuzzy-PID control (PSOFPID) and PID controllers are utilized to control the synchronous generator's LFC and AVR. This determines how much the AGC's dynamic response may be improved.

First, create a mathematical model to analyze and develop a control system. The transfer function (TF) method and the state variable approach (SVA) methods are often employed techniques. The work presented in this thesis created a mathematical model of a synchronous generator to study its stability. This model used transfer function (TF). The system was further characterized using a state space model with linear differential equations. LFC has a governor, load, prime mover, and turbine; AVR has simply an exciter, synchronous machine, and transmission line. They're the system's bulk. If the state variables are recognized, first-order differential equations can be generated for every state equation.

Second, Simulink is used to create mathematically accurate simulations of the power system's stability. This strategy complements the first. It was vital to investigate the connection between LFC and AVR to better understand automated generation control (AGC). Both the LFC and AVR loops underwent separate study and trials. The standard PID controller's and PSO based Fuzzy-PID's results were compared. This study demonstrates the potential benefits of these relatively new approaches for adaptive controller design and simulation while demonstrating certain limitations and potential implementation difficulties. A fuzzy PID controller model based on PSO provided less Integral Absolute Error (IAE), a shorter settling period, and a reduced overshoot after a specific load variation, research found. This was noticed when a standard PID controller was used. The dynamic responsiveness of mixed LFC

and AVR loops was also examined. This research was conducted to explore integrated LFC and AVR loops.

6.2. RECOMMENDATION

In this thesis, single-area power system models are considered for analysis. The responses like change in frequency, power deviation and terminal voltages are observed. The system response with proposed PSO based Fuzzy-PID controller is compared to the conventional controller and found that the intelligent controller is better than the conventional controller..

6.3. FUTURE WORK

For improved dynamic responsiveness of the synchronous generator control system in the future, new control approaches for combined AVR and LFC single areas, such as Neuro Fuzzy Control (NFLC), are advised.

REFERENCE

[1] S. J. Balser and H. K. Clark, “Long-Term Disturbance Monitoring for Improved System Analysis,” IEEE Comput. Appl. Power, vol. 2, no. 2, pp. 33–36, 1989, doi: 10.1109/67.24939.

[2] H. Saadat, “Hadi Saadat ." power system analysis" , Ch: 12.,” Tata Mcgraw hill, pp. 527–566, Jan. 2002.

[3] G. Singh and J. K. Dhami, “Load Frequency and Voltage Control of Two Area Interconnected Power,” Int. J. Eng. Res. Technol., vol. 8, no. 15, pp. 1–4, 2016.

[4] A. Ikhe, “Load Frequency Control for Interconnected Power System Using Different Controllers,” Autom. Control Intell. Syst., vol. 1, no. 4, p. 85, 2013, doi: 10.11648/j.acis.20130104.11.

[5] T. Gupta and D. K. Sambariya, “Optimal design of fuzzy logic controller for automatic voltage regulator,” IEEE Int. Conf. Information, Commun. Instrum. Control. ICICIC 2017, vol. 2018-Janua, pp. 1–6, 2018, doi: 10.1109/ICOMICON.2017.8279140.

[6] A. Soundarrajan, S. Sumathi, and C. Sundar, “Particle swarm optimization based LFC and AVR of autonomous power generating system,” IAENG Int. J. Comput. Sci., vol. 37, no. 1, 2010.

[7] D. Devaraj and B. Selvabala, “Real-coded genetic algorithm and fuzzy logic approach for real-time tuning of proportional-integral-derivative controller in automatic voltage regulator system,” IET Gener. Transm. Distrib., vol. 3, no. 7, pp. 641–649, 2009, doi: 10.1049/iet-gtd.2008.0287.

[8] A. Usman and B. P. Divakar, “Simulation Study of Load Frequency Control of Single and Two Area Systems,” 2012 IEEE Glob. Humanit. Technol. Conf., pp. 214–219, 2012.

[9] M. Michalczuk, B. Ufnalski, and L. M. Grzesiak, “Fuzzy logic based power management strategy using topographic data for an electric vehicle with a battery-ultracapacitor energy storage,” COMPEL - Int. J. Comput. Math. Electr. Electron. Eng.,

vol. 34, no. 1, pp. 173–188, 2015, doi: 10.1108/COMPEL-11-2013-0388.

[10] G. Singh and R. Bala, “Automatic Generation \& Voltage Control of Interconnected Thermal Power System Including Load Scheduling Strategy,” 2011.

[11] E. Rakhshani and J. Sadeh, “Application of power system stabilizer in a combined model of LFC and AVR loops to enhance system stability,” in 2010 International Conference on Power System Technology, 2010, pp. 1–5, doi: 10.1109/POWERCON.2010.5666038.

[12] V. Bandal, S. Member, B. Bandyopadhyay, and A. M. Kulkarni, “Design of power system stabilizer using power rate reaching law based sliding mode control technique,” no. January 2006, 2015, doi: 10.1109/IPEC.2005.207040.

[13] S. Kumari, G. Shankar, S. Gupta, and K. Kumari, “Study of load frequency control by using differential evolution algorithm,” 1st IEEE Int. Conf. Power Electron. Intell. Control Energy Syst. ICPEICES 2016, pp. 1–5, 2017, doi: 10.1109/ICPEICES.2016.7853508.

[14] T. Hussein, “A Genetic Algorithm for Optimum Design of PID Controller in Load Frequency Control,” vol. 6, no. 10, pp. 1205–1208, 2012.

[15] H. E. Patoding, “Modeling Control of Automatic Voltage Regulator With Proportional Integral Derivative,” Int. J. Res. Eng. Technol., vol. 04, no. 09, pp. 241–245, 2015, doi: 10.15623/ijret.2015.0409044.

[16] E. Rakhshani, K. Rouzbehi, and S. Sadeh, “A new combined model for simulation of mutual effects between LFC and avr loops,” Asia-Pacific Power Energy Eng. Conf. APPEEC, vol. 2009, no. Appeec, 2009, doi: 10.1109/APPEEC.2009.4918066.

[17] N. Thapa, N. Murmu, A. Narayan, and B. Besra, “Automatic voltage regulator and automatic load frequency control in two area power system,” Int. J. Res. Eng. Technol. Sci., vol. VII, pp. 1–7, 2017.

[18] Y. Oğuz, “Fuzzy PI Control with parallel fuzzy PD control for automatic generation control of a two-area power systems,” Gazi Univ. J. Sci., vol. 24, no. 4, pp. 805–816, 2011.

[19] P. Dabur, N. Yadav, and V. Tayal, “Matlab Design and Simulation of AGC and AVR for Multi Area Power System and Demand Side Management,” Int. J. Comput. Electr. Eng., pp. 259–264, 2011, doi: 10.7763/IJCEE.2011.V3.324.

[20] T. R. Shyama, R. S. Kumar, and V. Shanmugasundaram, “Design of FGSPI Controller Based Combined LFC and AVR of Two Area Interconnected Power Generating System,” Int. J. Eng. Adv. Technol., vol. 1, no. 4, pp. 135–139, 2012, [Online]. Available: https://www.researchgate.net/publication/288351312_Design_of_FGSPI_controller_based_combined_LFC_and_AVR_of_two_area_interconnected_power_generating_system.

[21] V. K. Thotan, “Multi-area power system using fuzzy logic based LFC and AVR,” Int. J. Emerg. Trends Eng. Dev., vol. 6, no. 4, pp. 48–59, 2014.

[22] V. Nath and D. K. Sambariya, “Analysis of AGC and AVR for Single Area and Double Area Power System Using Fuzzy Logic Control,” Int. J. Adv. Res. Electr. Electron. Instrum. Eng., vol. 4, no. 7, pp. 6501–6511, 2015, doi: 10.15662/ijareeie.2015.0407075.

[23] A. Singh, R. Singh, and R. Kushwah, “Automatic Voltage Regulator and Automatic Load Frequency Control of Electrical Power Plant with Optimal Tuning Controller PID,” Int. J. Res. Appl. Sci. Eng. Technol., vol. 3, no. X, pp. 274–279, 2015.

[24] C. M. J and D. R. Jayapal, “Performance analysis of FL, PI and PID controller for AGC and AVR of a Two-Area Power System,” Int. J. Sci. Res. Publ., vol. 5, no. 1, pp. 1–7, 2015.

[25] M. Orosun, R. Orosun, and S. S. Adamu, “Modeling and Simulation of Automatic Generation Control System for Synchronous Generator with Model Predictive Controller,” Zimbabwe J. Sci. Technol., vol. 11, pp. 142–157, 2016.

[26] P. Andhare and N. Asati, “PID Controlled Automatic Voltage Regulator with Load Frequency Control,” Int. J. Electr. Electron. Comput. Eng., pp. 05–10, 2016.

[27] A. Sharifian, “Assess the Modeling Effects of PSS and Governor on Voltage Stability of Power System,” J. Electr. Electron. Syst., vol. 5, no. 3, 2016, doi: 10.4172/2332-

0796.1000199.

[28] G. Shahgholian, “Power System Stabilizer Application for Load Frequency Control in Hydro-Electric Power Plant,” Int. J. Theor. Appl. Math., vol. 3, no. 4, p. 148, 2017, doi: 10.11648/j.ijtam.20170304.14.

[29] R. Fagna, “Load Frequency Control of Single Area Thermal Power Plant Using Type 1 Fuzzy Logic Controller,” Sci. J. Circuits, Syst. Signal Process., vol. 6, no. 6, p. 50, 2017, doi: 10.11648/j.cssp.20170606.11.

[30] M. M. Ibrahim, J. D. Jiya, and I. O. Harrison, “Modelling and Simulation of Automatic Voltage Regulator System,” Int. J. Comput. Appl., vol. 178, no. 1, pp. 24–28, 2017, doi: 10.5120/ijca2017915715.

[31] M. B. Singh, M. K. Debnath, S. Choudhury, and S. K. Kar, “Design and application of PID-PID dual loop controller for load frequency control,” Int. J. Recent Technol. Eng., vol. 8, no. 1, pp. 266–271, 2019.

[32] P. K. Mohanty, B. K. Sahu, T. K. Pati, S. Panda, and S. K. Kar, “Design and analysis of fuzzy PID controller with derivative filter for AGC in multi-area interconnected power system,” IET Gener. Transm. Distrib., vol. 10, no. 15, pp. 1–23, 2016, doi: 10.1049/iet-gtd.2016.0106.

[33] D. K. Lal and A. K. Barisal, “Combined load frequency and terminal voltage control of power systems using moth flame optimization algorithm,” J. Electr. Syst. Inf. Technol., vol. 6, no. 1, pp. 1–24, 2019, doi: 10.1186/s43067-019-0010-3.

[34] D. K. S. Krishna, S, R.Ramya, “A Simple Fuzzy Excitation Control System for Synchronous Generator,” pp. 1–43, 2011, doi: 10.1007/978-81-322-1847-0_1.

[35] S. Bouallègue, J. Haggège, M. Ayadi, and M. Benrejeb, “PID-type fuzzy logic controller tuning based on particle swarm optimization,” Eng. Appl. Artif. Intell., vol. 25, no. 3, pp. 484–493, 2012, doi: 10.1016/j.engappai.2011.09.018.

[36] Y. del Valle, “Particle Swarm Optimization: Basic Concepts, Variants and Applications in Power Systems,” EEE Trans. Evol. Comput., vol. 12, no. 2/2002, pp. 21–23, 2008, [Online]. Available: http://orgprints.org/1358/.

[37] S. K. Sinha and R. Prasad, “PSO Tuned Combined Optimal Fuzzy Controller for AGC of Two Area Interconnected Power System,” pp. 537–542, 2009.

[38] M. T. Bina and A. Kashefi, “Three-phase unbalance of distribution systems: Complementary analysis and experimental case study,” Int. J. Electr. Power Energy Syst., vol. 33, no. 4, pp. 817–826, 2011, doi: https://doi.org/10.1016/j.ijepes.2010.12.003.

[39] N. E. Y. Kouba, M. Menaa, M. Hasni, and M. Boudour, “Optimal control of frequency and voltage variations using PID controller based on particle swarm optimization,” 2015 4th Int. Conf. Syst. Control. ICSC 2015, pp. 424–429, 2015, doi: 10.1109/ICoSC.2015.7152777.

[40] M. R. I. Sheikh, S. M. Muyeen, R. Takahashi, T. Murata, and J. Tamura, “Application of self-tuning FPIC to AGC for load frequency control in multi-area power system,” 2009 IEEE Bucharest PowerTech Innov. Ideas Towar. Electr. Grid Futur., no. August, 2009, doi: 10.1109/PTC.2009.5282221.

[41] G. Yan and C. Li, “An Effective Refinement Artificial Bee Colony Optimization Algorithm Based On Chaotic Search and Application for PID Control Tuning,” vol. 7, Nov. 2010.

[42] A. Chakrabarti and S. Halder, Power System Analysis: Operation And Control 3Rd Ed. PHI Learning Pvt. Ltd., 2010.

[43] N. Y. OI, Elgerd McGraw-Hill, “Electric energy systems theory: an introduction,” vol. 2nd edn., 1982.

[44] K. R. M. V. Chandrakala and S. Balamurugan, “Simulated annealing based optimal frequency and terminal voltage control of multi source multi area system,” Int. J. Electr. Power Energy Syst., vol. 78, pp. 823–829, 2016.

[45] T. Chaiyatham, I. Ngamroo, S. Pothiya, and S. Vachirasricirikul, “Design of optimal fuzzy logic-PID controller using bee colony optimization for frequency control in an isolated wind-diesel system,” Transm. Distrib. Conf. Expo. Asia Pacific, T D Asia 2009, vol. 1, pp. 1–4, 2009, doi: 10.1109/TD-ASIA.2009.5356804.

[46] A. O'Dwyer, Handbook of PI and PID controller tuning rules World Scientific., vol. 70, no. 5. 1998.

[47] R. Latha, S. Kanthalakshmi, and J. Kanagaraj, "Design of Power System Stabilizer using Fuzzy Based Sliding Mode Control Technique," p. 16, 2014.

[48] D. K. Chaturvedi, Modeling and simulation of systems using MATLAB® and Simulink®. CRC press, 2017.

[49] A. Delassi, S. Arif, and L. Mokrani, "Comparison between PID , Fractional PID and Fuzzy PID for Load Frequency Control Problem," 2014.

[50] J. J. Liang, A. K. Qin, S. Member, P. N. Suganthan, S. Member, and S. Baskar, "Comprehensive learning PSO for global optimization of multimodal functions," IEEE Trans. Evol. Comput., vol. 10, no. 3, pp. 281–295, 2006.

[51] T. L. Mien, V. Van An, and B. T. Tam, "A Fuzzy-PID controller combined with PSO algorithm for the resistance furnace," Adv. Sci. Technol. Eng. Syst., vol. 5, no. 3, pp. 568–575, 2020, doi: 10.25046/aj050371.

APPENDIX

APPENDIX A:- root locus plot for frequency stability check,

- KA=10; num=1;
- den= [1 7.08 10.56 0.8];
- Fig (1), rlocus (num, den)

APPENDIX B: Frequency Deviation Step Response:

- PL=0.2; numc=[0.1 0.7 1]; denc=[1 7.08 10.56 20.8]; t=0:0.02:10;
- c=-PL*step(numc,denc,t); figure(2),plot(t,c) 'xlable(t,sec),ylable(p.u)';
- title('Frequency Deviation step response') (num,den)

Frequency deviation step response, Appendix C In the following equation:

- PL=0.2; KI=6; numc=[0.1 0.7 1 0];
- denc=[1 7.08 10.56 20.8 KI]; t=0:0.02:12;
- c= -PL*step(numc,denc,t); plot(t,c),grid 'xlable(t,sec),ylable(p.u)';
- title('Frequency Deviation step response')

Appendix C Root-locus plot for appendix Cwith the following parameters:

- KI=6; num=[0.1 0.7 1 0];
- den=[1 7.08 10.56 20.8 KA];
- Fig (4),rlocus(num,den);grid on

APPENDIX D: The Automated voltage regulation step responseswas not sufficient even with a smaller amplifier gain of $KA = 10$, as shown by the analysis in Figs. 5.1 and 5.2 above. Therefore, it is required to include controller's that might add a zero to the AVR open loop transfer function in order to boost the relative stability of the excitation system. This may be accomplished by including a stabilizer feedback system in the control. The stabilizer gain KF and time constant TF can be properly adjusted to get a better or adequate response from AVR.

To determine the range of KA required for control system stability, use the Routh-Hurwitz array. The gain of the amplifier is set at KA=40. Utilize MATLAB to find the system close loop transfer function and get the results. The AVR system now includes a stabilizer for rate (speed) feedback. The derivative gain is changed to K F=0.1, and the stabilizer time constant is T F=0.04 seconds.

To get the root-locus plot, use the commands below.

- num=32,
- den=[1 23 62 40];
- Fig (5), rlocus(num, den);

Below, we have a closed transfer function.

$$T(s) = \frac{1280(s+25)}{s^4 + 48s^3 + 637s^2 + 6870s + 37{,}000}$$

Then use a Matlab command to get the result.

- KA = 40, numc = KA*[1280 25],
- denc = [1 48 637 6870 37000], t = 0:0.05:20,
- c = step(numc,denc,t),
- Fig (6), plot (t,c), grid on

APPENDIX E: Initialize the Matlab Simulink code for the fuzzy controller's parameters.

[System]
Name='AVR_ LFC_ Fuzzy_ PID2'
Type='mamdani'
Version=2.0 \sNumInputs=2 NumOutputs=3
NumRules=25
AndMethod='min'
OrMethod='max'
ImpMethod='min'
AggMethod='max'
DefuzzMethod='centroid'

[Input1]
Name='ET'
Range=[-10 10]
NumMFs=5
MF1='HQ':'trimf',[-18.2 -9.87 -5.9445178335535]
MF2='HD':'trimf',[-8.33 -5.02 -2.00792602377808]
MF3='HL':'trimf',[5.99735799207397 10 18.3]
MF4='HV':'trimf',[1.98 4.99339498018493 8.03]
MF5='HI':'trimf',[-3.35 0.555 3.93659180977542]

[Input2]
Name='DET'

[Output2]
Name='I'
Range=[0 2]
NumMFs=5
MF1='VD':'trimf',[-0.833 0 0.410832232496697]
MF2='VI':'trimf',[0.614 0.997357992073976 1.42]
MF3='VL':'trimf',[1.5891677675033 2 2.83]
MF4='VG':'trimf',[0.197 0.569352708058124 0.989]
MF5='VV':'trimf',[1.25 1.45 1.81902245706737]

[Output3]
Name='D'
Range=[0 3]
NumMFs=5
MF1='VD':'trimf',[-1.25 0 0 .608322324966975]
MF2='VI':'trimf',[1.07 1.562.14200792602378]
MF3='VL':'trimf',[2.26486129458388 3 4.25]
MF4='VG':'trimf',[0.200254953764861

```
Range=[-5 5]
NumMFs=5
MF1='TA':'trimf',[-9.17 -5 -2.95904887714663]
MF2='TI':'trimf',[-1.98 -0.317 2.02113606340819]
MF3='TL':'trimf',[3.05151915455746 5 9.17]
MF4='TZ':'trimf',[-3.88667107001321 -
2.41667107001321 -0.779671070013209]
MF5='TV':'trimf',[0.925 2.18 3.97622192866578]
[Output1]
Name='P'
Range=[0 5]
NumMFs=5
MF1='VD':'trimf',[-2.08 0 0.967635402906208]
MF2='VI':'trimf',[1.53 2.5 3.48414795244386]
MF3='VL':'trimf',[3.99273447820343 5 7.08]
MF4='VG':'trimf',[0.429 1.17239101717305 1.96]
MF5='VV':'trimf',[2.46235138705416
3.46235138705416 4.46235138705416]
0.761254953764861 1.60125495376486]
MF5='VV':'trimf',[1.80911492734478
2.30911492734478 2.80911492734478]

[Rules]
1 1, 1 1 1 (1) : 1
1 4, 1 1 1 (1) : 1
1 2, 1 1 1 (1) : 1
1 5, 1 1 1 (1) : 1
1 3, 1 1 1 (1) : 1
2 1, 1 1 1 (1) : 1
2 4, 4 4 4 (1) : 1
2 2, 1 1 1 (1) : 1
2 5, 1 1 1 (1) : 1
2 3, 1 1 1 (1) : 1
5 1, 1 1 1 (1) : 1
5 4, 1 1 1 (1) : 1
5 2, 2 2 2 (1) : 1
5 5, 2 2 2 (1) : 1
5 3, 5 5 5 (1) : 1
4 1, 1 1 1 (1) : 1
4 4, 1 1 1 (1) : 1
4 2, 2 2 2 (1) : 1
4 5, 5 5 5 (1) : 1
4 3, 3 3 3 (1) : 1
3 1, 1 1 1 (1) : 1
3 4, 1 1 1 (1) : 1
3 2, 5 5 5 (1) : 1
3 5, 3 3 5 (1) : 1
3 3, 3 3 5 (1) : 1
```

APPENDIX G: AVR Fitness function

```
function [fit, err]=avr_fitness(x)
ka=x(1);kb=x(2);kc=x(3);
sim('combined_LFC_AVR_PSOFuzzy_PID')
```

```
[mxnx]=size(iae_avr);
fit=iae_avr(mx,:);err=0;end
```

APPENDIX H: PSO calling function

```
Clc
warning off
t=cputime;
global  xl xun_con n np ka kb kc
ka=1;kb=1;kc=1;
 %global kc ti td tn;
fname='avr_fitness';% fitness function
n=3;
n_con=0;
  xl=[0 0 0];xu=[2 2 2];
np=2; %population size
feval_max=100;
maxgen=round(feval_max/np);% max. number of
generations
VMAX=0.25;
c1=1;c2=1;
No_runs=2;
trace_all=zeros(maxgen,n+2,No_runs);
final_pop_all=zeros(np,n+2,No_runs);
for iter=1:No_runs
iter
%calling PSO for obtining Optimum Parameters
[gbest,gbest_val,trace,gencount, funcount,
final_pop]=PSO_PFLESS(fname,n,np,xl,xu,maxge
n,feval_max,c1,c2,VMAX);
%to get actual x
xoptimal(iter,:)=gbest;
foptimal(iter)=gbest_val;
[row,col]=size(trace);
trace_all(1:row,:,iter)=trace;
gen_count(iter)=gencount;
fun_count(iter)=funcount;
final_pop_all(:,:,iter)=final_pop;
%cons_violations=res(maxgen,n+2)
% plot(trace);
end
[Best_val,Best_id]=min(foptimal);
Best_foptimal=Best_val
Best_optimal_parameter=xoptimal(Best_id,:)
trace_out=trace_all(1:gen_count(Best_id),n+1
,Best_id);
% Worst_foptimal=max(foptimal)
Mean_foptimal=mean(foptimal)
Std_foptimal=std(foptimal)
Worst_foptimal=max(foptimal)
final_pop_sol=final_pop_all(:,:,Best_id)
computation_time=(cputime-t)/No_runs
```